THE UNIVERSITY OF OKLAHOMA
GRADUATE COLLEGE

# ASSESSING THE INFLUENCE OF ELECTRON DONOR AND CELL-CELL INTERACTIONS ON *IN SITU* MICROBIAL SULFATE AND HYDROGEN CONSUMPTION USING FIELD AND LABORATORY APPROACHES

A DISSERTATION SUBMITTED TO
THE GRADUATE FACULTY
in partial fulfillment for the degree of
Doctor of Philosophy

By
STEVE H. HARRIS, JR.
Norman, Oklahoma
2004

Downloaded from SHAREOK. Persistent Handle URL: https://hdl.handle.net/11244/699

UMI Number: 3120038

INFORMATION TO USERS

The quality of this reproduction is dependent upon the quality of the copy submitted. Broken or indistinct print, colored or poor quality illustrations and photographs, print bleed-through, substandard margins, and improper alignment can adversely affect reproduction.

In the unlikely event that the author did not send a complete manuscript and there are missing pages, these will be noted. Also, if unauthorized copyright material had to be removed, a note will indicate the deletion.

UMI®

UMI Microform 3120038

Copyright 2004 by ProQuest Information and Learning Company.

All rights reserved. This microform edition is protected against unauthorized copying under Title 17, United States Code.

ProQuest Information and Learning Company
300 North Zeeb Road
P.O. Box 1346
Ann Arbor, MI 48106-1346

**ASSESSING THE INFLUENCE OF ELECTRON DONOR AND CELL-CELL INTERACTIONS ON *IN SITU* MICROBIAL SULFATE AND HYDROGEN CONSUMPTION USING FIELD AND LABORATORY APPROACHES**

**A DISSERTATION APPROVED BY THE DEPARTMENT OF BOTANY AND MICROBIOLOGY**

**BY**

**Joseph M. Suflita, Ph.D.**

**Michael J. McInerney, Ph.D.**

**Richard L. Smith, Ph.D.**

**Ralph S. Tanner, Ph.D.**

**Luther White, Ph.D.**

© Copyright by Steve H. Harris, Jr. 2004
All Rights Reserved

## Acknowledgments

I would like to recognize some of the many individuals who in different ways helped me realize my goal of completing this thesis. First, I thank my parents for instilling in me the value of an education as well as the importance doing that which is right. Secondly, I am grateful to Doug and Kathy Law for teaching me the skill of independent thinking as well as being my friends. In addition, I extend my gratitude to Dr. Joseph M. Suflita for allowing me the opportunity to become what I want to be and for insisting that I do my best by always pushing me to 'take it to the next level'. I have learned lessons from him that extend beyond the walls of the laboratory, and I am in debt to him for the rest of my life.

I would also like to thank the members of my committee Dr. Michael J. McInerney, Dr. Richard L. Smith, Dr. Ralph S. Tanner, and Dr. Luther White for their teaching and guidance through this process. I wish to express my thanks to the past and present members of our laboratory as well as to my fellow members of the CRAP family for engaging and inspirational conversations.

I am also grateful to my daughters, Madison, Molly Beth, and Maly for the many lessons they have taught me, not the least of which is the necessity to occasionally take some time out to wrestle. Finally, I would like to acknowledge my wife Kristen Harris for her loyalty and perserverance during this journey. Thank you for embarking on this adventure with me, I look forward to continuing it together.

## Table of Contents


| | Page |
|---|---|
| Acknowledgments | iv |
| List of Tables | vii |
| List of Figures | x |
| Preface | xiv |
| Abstract | xvii |

Chapter 1. Changes in organic matter biodegradability influencing sulfate reduction in an aquifer contaminated by landfill leachate

| | |
|---|---|
| Abstract | 1 |
| Introduction | 2 |
| Materials and Methods | 3 |
| Results | 10 |
| Discussion | 21 |
| References | 26 |

Chapter 2. *In situ* hydrogen consumption kinetics as a potential measure of subsurface microbial activity

| | |
|---|---|
| Abstract | 29 |
| Introduction | 30 |
| Materials and Methods | 33 |
| Results | 37 |

Discussion..... 44

References..... 53

Chapter 3. Examination of the rate, fate and threshold associated with hydrogen consumption by anaerobic bacteria: a basis for an amensalism between acetogens and methanogens

Abstract..... 58

Introduction..... 59

Materials and Methods..... 61

Results..... 65

Discussion..... 81

References..... 88

Appendix 1. Progress Curve Analysis for Enzyme and Microbial Kinetic Reactions using Explicit Solutions based on the Lambert *W* Function

Abstract..... 93

Introduction..... 94

Materials and Methods..... 98

Results..... 101

Discussion..... 113

References..... 116

Appendix 2. The use of a nonlinear regression routine for estimating kinetic parameters from progress curves

Steps in using nonlinear regression analysis..... 119

Installation of programs for kinetic analysis of progress curve data..... 127

Obtaining initial estimates of $S_0$, $K_m$, and $V_{max}$ via linear transformations..... 127

Estimating kinetic parameters via nonlinear regression..... 128

Suggested readings and references..... 133

## List of Tables

Chapter 1 Page

Table 1. Values of selected chemical and physical parameters from the well adjacent to the landfill and the well located 90 meters downgradient..... 8

Chapter 2

Table 1. Summary of hydrogen consumption rates, geochemical parameters and thermodynamics as a function of the electron-accepting regimes investigated in the present study..... 41

Chapter 3

Table 1. Hydrogen kinetic and threshold estimates in whole cells and cell free extracts of selected hydrogenotrophs..... 67

Table 2. Time final ($T_f$) determinations of undissociated acetic acid concentrations and in situ $\Delta G'$ values calculated as a function of acetate concentrations once resting cells of *A. woodii* reached the hydrogen threshold..... 69

Table 3. Fate of hydrogen in a typical competition experiment between resting cells of *A. woodii* and *M. hungatei*..... 76

Table 4. Hydrogen consumption rate in *M. hungatei* as a function of various amendments..... 80

## List of Illustrations

Chapter 1

Figure 1. Map of the study area. Site characteristics can be found at http://csdokokl.cr.usgs.gov/norlan/ ..... 5

Figure 2. Microbial sulfate consumption at site 35 in push-pull tests amended with sulfate only and in the presence of added sulfate and formate ..... 12

Figure 3. Comparison of sulfate reduction rates in intact cores determined from a previous study to those estimated from push-pull tests ..... 13

Figure 4. Breakthrough curves of sulfate, bromide, and formate in an unamended (A) and formate-amended (B) push pull test at the downgradient location (site 47) ..... 15

Figure 5. Sulfate reduction activity distributions in a core segment incubated with $^{35}$S-sulfate and amendments of lactate and *Desulfovibrio* preparations ..... 18

Figure 6. Sulfate reduction rates in sediment slurries at saturating (5mM) sulfate concentrations and in the presence of different groundwaters as potential electron donor sources ..... 20

Chapter 2

Figure 1. *In situ* microbial hydrogen consumption as determined from field tests under sulfate reducing conditions at the Norman landfil site ..... 38

Figure 2. *In situ* microbial hydrogen consumption as determined from field tests under various electron accepting conditions at Cape Cod ..... 40

Figure 3. Hydrogen consumption in a sediment slurry from the Norman landfill site. The inset shows the corresponding semi-logarithmic plot ..... 43

Figure 4. Theoretical energy yield as a function of hydrogen concentration for selected fermentation intermediates ..... 47

Chapter3

Figure 1. Hydrogen thresholds in resting cells of *A. woodii* as a function of gallate and acetate concentration ..... 70

Figure 2. Hydrogen consumption and resulting thresholds in resting cells of *A. woodii* receiving hydrogen reamendment or a washed preparation of *M. hungatei*..... 71

Figure 3. Hydrogen oxidation rate as a function of dissolved hydrogen concentration in cell free extracts of $H_2$/syringate-grown and fructose-grown *A. woodii*..... 73

Figure 4. Hydrogen decay in competition experiments. A. Replicate coculture incubations containing *A. woodii* and *M. hungatei* and model prediction. B. Monococulture incubations containing *A. woodii* and *M. hungatei* and model prediction..... 75

Figure 5. Hydrogen $V_{max}$ estimates in *M. hungatei* as a function of cell density... 78

Appendix 1

Figure 1. The three real branches of the Lambert function..... 103

Figure 2. Model predictions, and best fit kinetic parameters from equation (8) based on substrate depletion data with normally distributed noise..... 105

Figure 3. Contour plots showing dependence of the RSSE on $V_{max}$ and $K_m$ estimates from four simulated data sets..... 106

Figure 4. Comparison of initial estimates of $K_m$ and $V_{max}$ from the three linearization approaches..... 109

Figure 5. Hydrogen depletion by microorganisms in activated sludge and model predictions based on the $V_{max}$ and $K_m$ estimated from equation 8..... 110

Figure 6. Two-dimensional contour plot of the error function associated with $K_m$ and $V_{max}$ estimates from hydrogen depletion in activated sludge..... 112

Appendix 2

Figure 1. Hydrogen depletion by *Eubacterium limosum* illustrating fit of the Michaelis-Menten model with a threshold term ..... 122

Figure 2. Two-dimensional depiction of a hypothetical error function illustrating the presence of multiple minima..... 126

Figure 3. Simulation of hydrogen decay by two organisms in monocultures and coculture..... 131

Figure 4. Hydrogen consumption in a coculture of *Acetobacterium woodii* and *Methanospirillum hungatei* and model prediction..... 132

## Preface

The activity of microorganisms exerts a substantial influence on the ever-changing conditions of the biosphere. Their small size, ubiquitous distribution, and potential enzymatic diversity impart an enormous collective ability for the recycling of elements and energy on the planet. Since the founding work of Winogradsky and Beijerinck, microbial ecologists have been concerned with describing the interactions of microorganisms with their biotic and abiotic surroundings. Often these investigations have taken the form of *in situ* approaches such as field studies as well as examination of complex microbial assemblages. In addition, microorganisms isolated from such environments have been subjected to intense laboratory analyses that are often used as a basis for predicting their ecological roles. However, the complexity of natural systems as well as limitations associated with laboratory studies place interpretational constraints on the information garnered by such endeavors.

The first two chapters of this dissertation address the quantitation of microbially catalyzed sulfate and hydrogen consumption occurring *in situ*. In Chapter 1, I examine the *in situ* rate of sulfate reduction at various locations downgradient from the Norman landfill and investigate the factors that control the rate of this process. I propose that the decreased rate of sulfate reduction downgradient from the landfill is not due to the lack of a suitable inoculum, electron acceptor or donor availability, or the presence of an unknown inhibitory substance. Rather it was the diminishing quality of electron donor along the flowpath that negatively impacts the *in situ* rate of sulfate reduction. In sediments from the downgradient location, the addition of a heat-killed suspension of a

sulfate reducing bacterium stimulated sulfate reduction by the same proportion as live cells. This result suggests that microbial inoculants can serve as a form of labile electron donor driving the very reaction the inoculant was intended to produce. This chapter was written in the format required by the journal *Microbial Ecology*.

Another process that is central to the global cycling of carbon and energy in nature is the ability of microorganisms to process the metabolic intermediate hydrogen. Hydrogen is a critical intermediate that is both produced and consumed by a variety of microorganisms during the oxidation of organic matter. In anaerobic environments, the continued oxidation of organic matter is contingent on the rapid consumption of hydrogen and subsequent maintenance at low levels. Thus, the rate of hydrogen turnover in aquifers reflects the metabolism of the total microbial community. Furthermore, intense competition for this electron donor exists among different trophic groups of microorganisms, necessitating an understanding of the factors that control the fate of hydrogen and the interactions among different hydrogenotrophic bacteria in anaerobic environments.

In Chapter 2, I examine *in situ* hydrogen consumption kinetics in two contaminated aquifers, one at Cape Cod, Massachusetts, and the other at Norman, OK. Apparent first order constants were obtained from field tests and combined with steady state hydrogen determinations to calculate *in situ* rates of hydrogen turnover. Hydrogen consumption rates were proportional to the electron accepting regime as well as the level of contamination. This is the first report of *in situ* measures of hydrogen turnover. Given the central nature of hydrogen in microbial foodwebs, I propose that such measurements are useful to gauge how fast the food chain is functioning as well as assess the impact of

stressors, such as a contamination episode, on microbial activities. In addition, hydrogen consumption in the laboratory exhibited kinetics that were very different from that determined in the field. Thus, laboratory assessments may be influenced by factors not present in the microoganisms' natural environment, suggesting the results from such investigations should be interpreted with caution. This manuscript was written in the format required by the journal *FEMS Microbiology Ecology.*

Chapter 3 investigates the factors influencing the fate of hydrogen and the interactions between acetogens and methanogens in pure culture. Acetogenic bacteria coexist with other hydrogen consumers in many environments, often in comparable numbers, although hydrogen consumption by acetogens is thought to be relatively ineffecient. In this chapter I describe a study of the factors influencing the outcome of hydrogen competition between these microorganisms as well as variables controlling the hydrogen threshold exhibited by the acetogen, *Acetobacterium woodii*. The hydrogen threshold could not be explained by a thermodynamic limitation as previously hypothesized. Rather the organisms simply were unable to consume hydrogen below the threshold concentration suggesting strict regulatory control measures as a function of hydrogen concentration. I further hypothesized that increasing the biomass level of *A. woodii* would confer a competitive advantage for this organism in coculture with a model methanogen, *Methanospirillium hungatei* JF1 and kinetic simulations supported this contention. Hydrogen consumption rates were consistent with model predictions, but the fate of hydrogen in cocultures was not. Surprisingly, the presence of the acetogen stimulated hydrogen oxidation by the methanogen suggesting an amensalistic interaction exists between organisms belonging to different kingdoms (*Archaea* and *Eubacteria*).

The factor responsible for the stimulation was heat-labile, and associated with the whole cells of *A. woodii* as well as membrane and cytoplasmic fractions but was not found in culture fluids. This manuscript was written for the journal *Applied and Environmental Microbiology.*

Appendix 1 was the result of a collaborative effort with my colleague Chetan Goudar who was responsible for the mathematical contribution and deveopment of the model. My contribution was to supply experimental hydrogen depletion data. I included this contribution in the appendix because it was this model that I used to analyze progress the curve data presented in chapters 1 and 3. This work details the implementation of an improved algorithm for obtaining solutions to differential rate expressions such as the Michaelis-Menten equation. This strategy represents a simplification of previous approaches that use a differential or nonlinear equation to solve the Michaelis-Menten equation via iterative estimation of $V_{max}$ and $K_m$. This contribution describes the evaluation of a simple algebraic expression that provides relatively accurate estimations of kinetic parameters from progress curve data. Appendix 1 was written for the *Journal of Microbiological Methods*. Appendix 2 includes an essay that describes the salient theory associated with nonlinear regression analysis as well as detailed instructions for preparing and analyzing progress curve data. A compact disc is included that contains the files required for kinetic parameter analysis as well as simulating the outcome of simple competition for a single substrate between two microorganisms. Thus, a researcher who desires to estimate $K_m$ and $V_{max}$ from substrate depletion data is provided with the necessary tools and background for making the best possible estimations. Software licensing aggreements do not allow me to include the MATLAB software

package on the disc. The researcher is responsible for purchasing this software, which is readily available from The MathWorks, Inc., Natick, Massachusettes. A fully compatible, 30-day evaluation version is offered by The MathWorks, Inc. on their website, www.mathworks.com.

**Abstract**

Information on *in situ* microbially-catalyzed reactions and the factors that influence those activities is required to accurately describe the transport and fate of both naturally occurring and contaminant forms of organic matter. While pure culture microbiological studies have provided insight on many phenomena, they are often difficult to extrapolate to more complex field settings. A combination of field and laboratory approaches proved useful for assessing differences in sulfate reduction rates at two locations in an aquifer contaminated by landfill leachate. The lack of activity in a downgradient location was not due to a deficiency in metabolic potential, sulfate availability, or quantity of dissolved organic matter (DOC). Rather, the quality of the DOC was such that it limited sulfate reduction at the distal site.

Given the importance of rate processes and the central role of hydrogen in anaerobic metabolism, comparable field methods were used to examine hydrogen turnover as an indicator of total community metabolism. Apparent first order rates in a number of redox zones in two aquifers differed by over three orders of magnitude and were negatively impacted by several environmental insults. Thus, such determinations have a necessary degree of sensitivity and may be an integrating gauge of *in situ* microbial activity.

Field determinations of the disposition of energy and materials ultimately depend on the interactions amongst microorganisms. The rate of hydrogen consumption by cocultures of *Acetobacterium woodii* and *Methanospirillum hungatei* could be described by a two-term Michaelis-Menten kinetic model, but the fate was consistently in favor of

the methanogen. A heat-labile factor associated with whole cells, membranes, and cytoplasmic preparations of the acetogen was responsible for an amensalism between the organisms. This interaction allowed the methanogen to successfully compete for hydrogen even at cell densities that would normally preclude such activity. At low hydrogen concentrations, the threshold exhibited by *A. woodii* was independent of reaction thermodynamics as well as endproduct inhibition. Thus, hydrogen metabolism must be regulated by a mechanism different than previously hypothesized. Clearly, if such interactions are manifest in defined cocultures, it is reasonable to expect similar processes influence hydrogen metabolism *in situ*.

# Chapter 1

## Changes in organic matter biodegradability influencing sulfate reduction in an aquifer contaminated by landfill leachate


### Abstract

*In situ* experiments were conducted to measure sulfate reduction rates and identify rate-limiting factors in a shallow, alluvial aquifer contaminated with municipal landfill leachate. Single-well, push-pull tests conducted in a well adjacent to the landfill with > 8 mM dissolved organic carbon (DOC) exhibited a sulfate reduction rate of 3.2 μmole $SO_4^{-2}$*L sediment$^{-1}$*day$^{-1}$, a value in close agreement with laboratory-derived estimates. Identical tests conducted in wells located 90 meters downgradient where DOC remained elevated (> 3 mM) showed no detectable sulfate consumption and laboratory assays confirmed this observation. However, the rate of sulfate reduction in sediment samples obtained from this site were three times larger when they were amended with filter-sterilized groundwater from the upgradient location. The effect of various amendments on sulfate reduction rates was further examined in laboratory incubations using sediment collected from the downgradient site amended with $^{35}$S-sulfate. Unamended sediments showed only weak conversion of the tracer to $^{35}$S-sulfide (5 to 7 cpm/cm$^2$), while the addition of *Desulfovibrio* cells increased $^{35}$S-sulfide production to 44 cpm/cm$^2$. However, the application of heat-killed *Desulfovibrio* had a similar stimulatory effect, as did a lactate amendment. Collectively, these findings indicate that the lack of measurable sulfate reduction at the downgradient site was not due to the absence of the necessary

metabolic potential, the presence of lower sulfate concentration, or the quantity of electron donor, but by its biodegradability. The findings also indicate that field bioaugmentation attempts should be interpreted with caution.

**Introduction**

The microbial decomposition of organic matter coupled with the reduction of sulfate is an important mechanism governing carbon and energy disposition in many anaerobic environments. In anoxic marine sediments up to half of the total organic carbon is mineralized by sulfate reducing microorganisms [11,15]. Freshwater environments also harbor active populations of sulfate reducers that dominate carbon and energy metabolism even when sulfate concentrations are low [20,32]. Sulfate reducing bacteria utilize an impressive array of organic molecules and hydrogen to support their metabolic activity [1,10,18,28,33]. Often, electron acceptor availability is considered as a dominant factor controlling the activity of this group of organisms [12,16,19,29]. However, the distribution and supply of suitable electron donors can also be a critical variable affecting sulfate reduction. Indeed, electron donor supply exerts a powerful influence on microbial activities in a variety of environments [14,17,23,26]. In turn, microbial activities play a prominent role influencing physical and geochemical processes in aquifers [6]. Thus, organic matter degradation in contaminant plumes both depends on and contributes to the evolution of groundwater quality along aquifer flowpaths. Landfill leachate plumes typically demonstrate decreasing dissolved organic carbon (DOC) concentrations with increasing distance from the source [4,5,8]. Nevertheless, the distal portions of these plumes typically retain DOC levels that are diminished by only one-half to one-third of the concentration measured at the landfill source. For example, at

the Grindsted landfill, organic carbon concentrations were >6mM near the source and remained elevated at 60 m distance [27]. Thus, it is not unusual for elevated DOC levels to persist along aquifer flowpaths despite geochemical evidence of extensive microbial degradation.

We examined the influence of organic matter degradability on sulfate reduction along an aquifer flowpath. At an upgradient location near the landfill, *in situ* rates of sulfate reduction in the aquifer could be measured and even stimulated with formate in the presence of high (>8 mM) DOC levels in the groundwater. In contrast, sulfate reduction was not measurable in comparable assays conducted at a downgradient location, although DOC levels were still relatively high (~3 mM). Our results indicate that sulfate reduction rates in the more distal location are restricted by the biodegradability rather than the concentration of dissolved organic carbon in the groundwater.

**Materials and Methods**

**Field Site.** The study site is a closed municipal landfill occupying about 12 hectares on the Canadian River floodplain south of the town of Norman in central Oklahoma [3]. The alluvium consists of fluvial sediments 10-12m thick with a water table that is typically 1.5 to 2.5 m below land surface. Solid municipal waste was deposited at the site beginning in 1922 and continued unrestricted until 1985 when the landfill was closed and covered with local clay and silt. The landfill contains no liner or leachate collection devices. As a result, leachate emanating from the refuse comprises a complex waste stream that contaminates the local aquifer to at least 1.5 km from the base of the mound [7]. The aquifer is uniformly anoxic ($O_2$<5 μM) and iron reduction, sulfate

reduction and methanogenesis are important microbially catalyzed processes occurring at the site [3,8,12]. Sulfate reduction was examined at two locations (identified as site 35 and site 47 in figure 1). The upgradient site near the landfill (35) is characterized by high DOC, and low sulfate while the downgradient site (47) contains lower levels of DOC and higher sulfate concentrations (Table 1). Each location has a series of wells located along a transect that is perpendicular to the direction of groundwater flow. This arrangement allowed us to conduct simultaneous push-pull tests in separate wells that intercepted zones of comparable groundwater geochemistry. The wells at each location had a single 30 cm long screen located 3.7 m (site 35) and 1.6 m (site 47) below land surface.

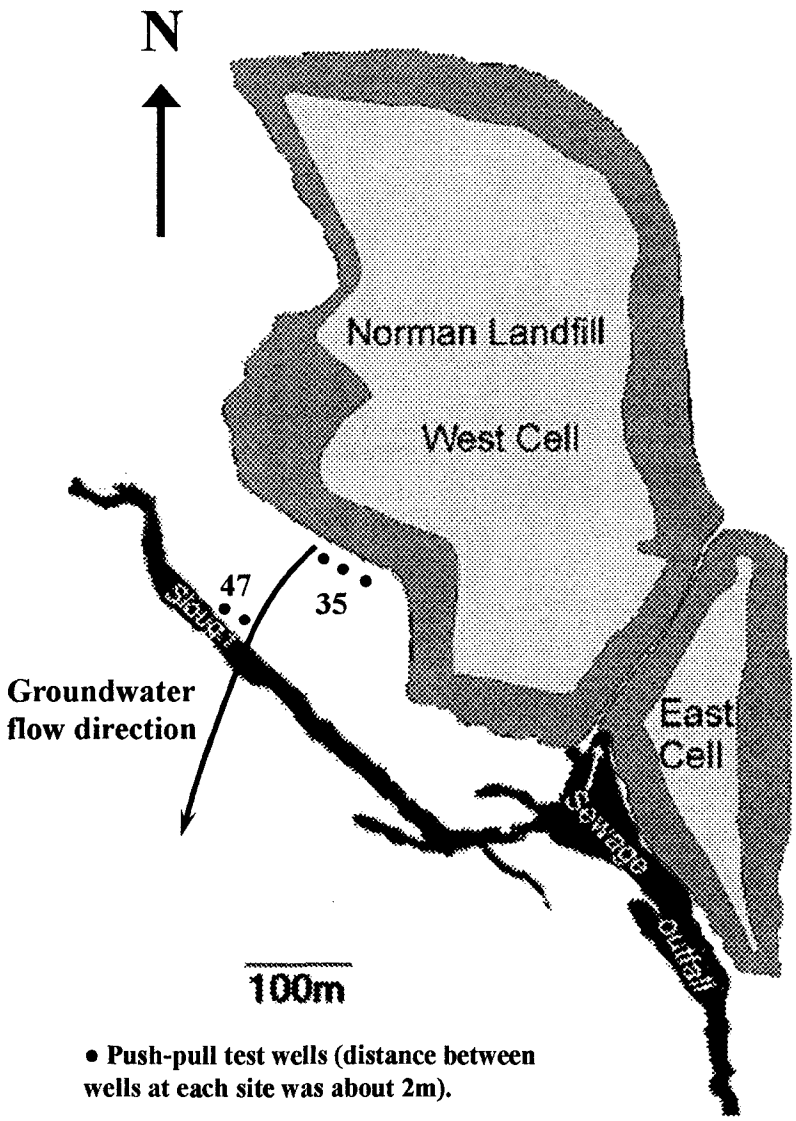


Figure 1. Map of the study area. Numbers refer to well sites along the groundwater flowpath. Site characteristics can be found at http://csdokokl.cr.usgs.gov/norlan/.

**Push-pull tests.** Sulfate reduction rates were estimated using the push-pull test procedure [13]. This procedure involves injection of a test solution containing a reactant and conservative tracer into the aquifer. The solution is extracted while samples are taken for determination of reactant and tracer loss. Ratios of extracted/injected concentrations ($C/C_0$) are used to interpret reactant loss relative to that of the tracer, thereby correcting for dilution losses due solely to groundwater flow and to estimate *in situ* microbial activity. In this study, test solutions were prepared using 50 L of groundwater amended with sodium sulfate (0.3 mM at site 35; 70 μCi carrier-free $Na_2{}^{35}SO_4$ at site 47) and sodium bromide (1.2 mM at both sites) as reactant and tracer, respectively. The solution was extracted from the test well into a plastic carboy and sparged with $N_2/CO_2$ (4/1) for 15 min prior to the start of each test. To start the tests, the test solution was injected into the aquifer using a peristaltic pump. Once the injection phase was complete, the solution was extracted from the same well periodically over a period of 23 days. In addition, some test solutions included added formate (20 mM) as a potential electron donor. During extraction, liquid samples (5 ml) were taken at discrete time intervals and analyzed by high-performance liquid chromatography (Dionex, Sunnyvale, CA) for sulfate, bromide, and formate.

We anticipated difficulty detecting sulfate reduction against the high background levels of sulfate at the downgradient location (Table 1). Therefore, we included 70 μCi $Na_2{}^{35}S$-sulfate in the test solutions to provide a more sensitive means of assessing *in situ* microbial activity. The radiotracer allowed us to monitor the reduction of both injected $^{35}S$-sulfate and $^{32}S$-sulfate. Furthermore, any $^{35}S$-sulfate reduced during the test, would precipitate in the aquifer as stable iron sulfides and be subsequently quantified in the

laboratory via autoradiography (InstantImager, Packard Instrument Co., Downers Grove, IL ) of intact cores obtained from the area impacted by the push-pull tests. The distribution of $^{35}$S-sulfate and $^{35}$S-sulfide was determined in unwashed samples. The unreacted $^{35}$S-sulfate was then removed by an anoxic water wash to allow the determination of precipitated $^{35}$S-sulfide in the sediment.

**Sediment core collection.** Sediment cores were collected with a Geoprobe sampling device, (Geotech, Inc., Salina, KS). Cores were flushed with $N_2$ immediately after collection and transported to the laboratory where the samples were processed in an anaerobic glove bag.

| constituent | well designation[a] upgradient site 35 | downgradient site 47 |
|---|---|---|
| DOC (mM) | >8 | 3.3 |
| specific conductance ($\mu s*cm^{-1}$) | 4990 | 5940 |
| methane ($\mu M$) | 396 | 45 |
| sulfate (mM) | 0.038 | 7.1 |
| chloride (mM) | 9.7 | 13.6 |
| hydrogen (nM) | 1.6 | ND[b] |
| pH | 7.0 | 6.9 |
| oxygen ($\mu M$) | <10 | <10 |

[a]DOC and specific conductance for site 35 and 47 are from [6] and Isabelle Cozarrelli, personal communication, respectively.
[b]ND, not determined

Table 1. Values of selected chemical and physical parameters from the well adjacent to the landfill (35) and the well located 90 meters downgradient (47).

**Sulfate reduction activity in sediment.** Filter-sterilized groundwater from the respective sites was used to supply soluble organic carbon to serve as electron donors for sulfate reduction in sediment samples. Serum bottle (160ml) incubations containing 50g of sediment as the inoculum and 75ml filter-sterilized groundwater were amended with sulfate (where necessary) to an initial concentration of 7mM. Sediment from near and distal sites were used in all possible combinations with filter-sterilized groundwater from the various locations. The bottles were sealed with butyl rubber stoppers and incubated under a $N_2/CO_2$ (4/1, 1atm.) headspace at 20°C in the dark. Sulfate depletion in slurries was determined by HPLC.

**Electron donor amendments to cores.** Sulfate reduction as a function of electron donor amendment was examined in sediment cores. Cores were transported within two hours of extraction and placed inside a $N_2$-flushed glove bag where they were sectioned to produce segments (20 x 5 x 0.5cm) to be used in radioisotope experiments. Sulfate reduction was assessed by monitoring the conversion of $^{35}$S-sulfate to $^{35}$S-sulfide on the surface of the core segments. The incubation was started by uniformly applying an anoxic sterile solution of 100 μCi of $Na_2{}^{35}SO_4$ in 15 ml water to the face of each core segment. The segments were incubated in gas tight containers in the dark at 20°C under a headspace of $N_2/CO_2$ (4/1) for 14 to 90 days. Once the incubation was complete, the core segments were washed with anoxic water to remove unreacted $^{35}$S-sulfate while leaving the precipitated $^{35}$S-sulfide unaltered. After the segments were washed, the distribution of $^{35}$S-sulfide was visualized by autoradiography. To investigate the effect of various amendments on sulfate reduction, core segments were prepared as above and subdivided into three sections of similar area. The first third was amended with lactate

by adding 5ml of a sterile lactate solution (10 mM) containing 33 μCi $^{35}$S-sulfate. Amendments that included washed preparations of *Desulfovibrio* G11 were prepared by centrifuging log-phase cells at 15,000 x g for 20 min. The cell pellet was resuspended in sterile anoxic water and centrifuged again. The cycle was repeated three times with fresh water to thoroughly wash media components from the cells. The final cell pellet was resuspended in 10 ml anoxic water and divided into two aliquots. The first aliquot was used as a live cell preparation; the second was boiled for 20 min to heat-inactivate the cells. Radiolabeled sulfate was added to each of these aliquots to a final activity of 33 μCi. Then, 5 ml of each cell suspension (4.5 mg protein * $ml^{-1}$) was applied to the appropriate third of the core section. All amendments and cell manipulations were done in a $N_2$-flushed anaerobic glove bag.

## Results

***In situ* field sulfate reduction rates.** Measured sulfate consumption rates in push-pull tests conducted at site 35, adjacent to the landfill (Figure 1) were ~ 3 μmole $SO_4^{-2}$*L $sediment^{-1}$*$day^{-1}$. Previous work indicated that sulfate reduction was an active microbial respiratory process occurring in the area [8,12,29]. The steady state dissolved hydrogen concentration in wells at this site was consistently 1.6-2.0 nM supporting the contention that sulfate reduction in this location was a dominant terminal electron accepting process [8]. The estimated rate determined in the push-pull test was similar to that observed in unamended laboratory incubations of intact core material obtained from the same depth (Figure 3). When two subsequent push-pull tests were conducted with 20 mM added formate, sulfate consumption rates increased by a factor of about four to ~ 14 μmole $SO_4^{-2}$*L $sediment^{-1}$*$day^{-1}$ (estimated over the first 15 days of the tests). The

increased rate due to the presence of formate was comparable to that measured in laboratory incubations of material taken from near the water table (Figure 3).

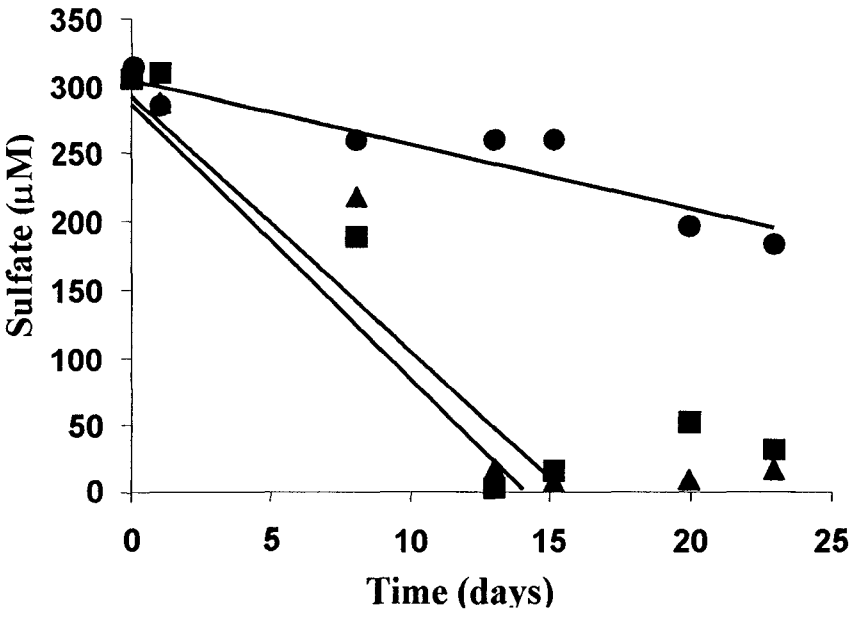


Figure 2. Microbial sulfate consumption at site 35 in push-pull tests amended with sulfate only (●) and in the presence of added sulfate and formate (▲ and ■). Sulfate data have been corrected for dilution via sodium bromide values.

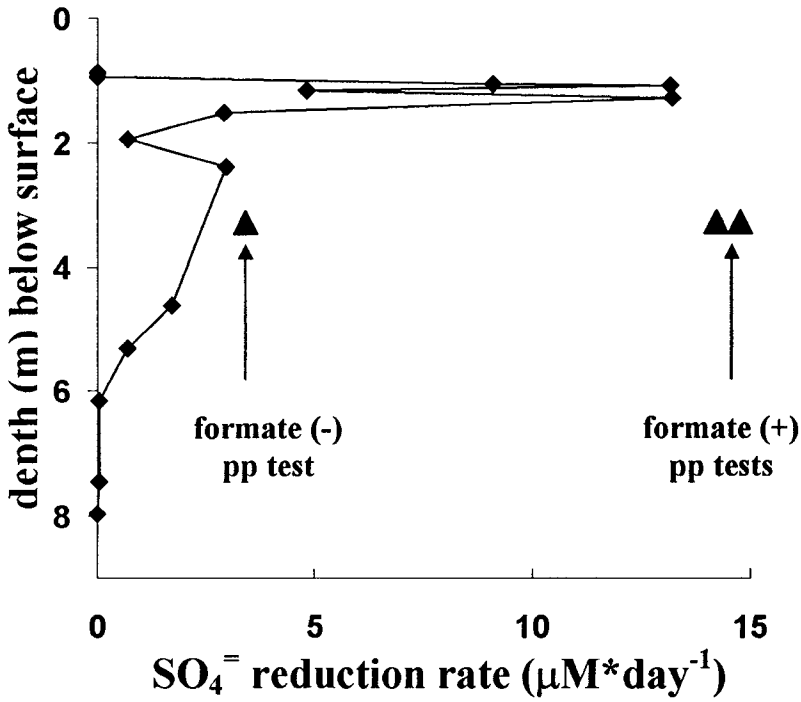


Figure 3. Comparison of sulfate reduction rates in intact cores (♦) determined from a previous study [6] to those estimated from push-pull tests (▲) in this study. The y-axis values for push-pull test rates correspond to the depth where tests were done.

In contrast, measured rates of sulfate reduction in push-pull tests conducted at site 47, located downgradient of the source (Figure 1) were not detectable. Breakthough curves for $^{35}$S-sulfate and bromide were identical indicating that observed decreases in sulfate concentration were due simply to dilution as the injected test solution gradually drifted from the well (Figure 4A). Recoveries of $^{35}$S-sulfate and bromide were also nearly identical at 68.4% and 63.4%, respectively. Further, the addition of 20 mM formate did not stimulate sulfate reduction at this site even though this potential electron donor was consumed within 5d after injection (Figure 4B). In the formate amended test, recoveries of $^{35}$S-sulfate (79.2%) and bromide (80.7%) were almost identical. Sulfate reduction was also not detected in laboratory incubations. Although the residual radioactive signal was uniformly distributed in samples of cored material (data not shown) indicating that injected $^{35}$S-sulfate from the push-pull test contacted the portion of the aquifer sampled. There was no evidence of the accumulation of $^{35}$S-sulfide. These findings confirm that little or no sulfate reduction occurred at the site distal from the landfill despite ample concentrations of sulfate and DOC (Table 1).

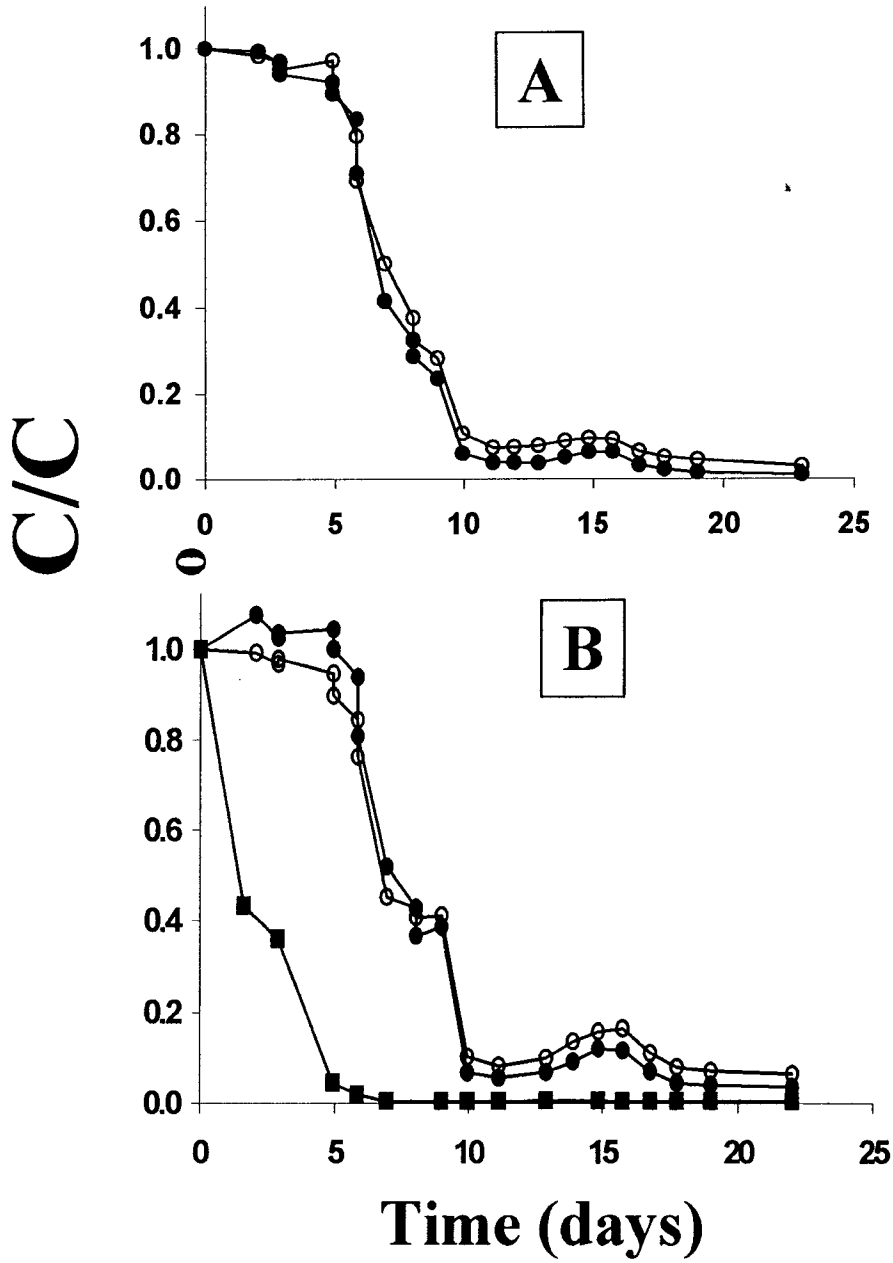


Figure 4. Breakthrough curves of sulfate (●), bromide (○), and formate (■) in an unamended (A) and formate-amended (B) push pull test at the downgradient location (site47.)

**Sulfate reduction activity in cores.** Possible explanations for the lack of sulfate reduction at the downgradient site include the lack of organisms with the necessary metabolic potential, the presence of an inhibitory substance, and the lack of suitable electron donors. To explore these possibilities in more detail, laboratory incubations were conducted using sediment cores collected from this site. Results showed only a sparse distribution of sulfate reduction activity in the core segments despite incubations of up to seven weeks (data not shown). For example, a core taken from the downgradient site and incubated for 90d in the presence of $^{35}$S-sulfate showed little overall sulfate reduction (Figure 5). The small amount of activity that was noted was spatially localized (Figure 5). The same core was subsequently divided into three subsections and supplemented with lactate (10 mM), an inoculum of *Desulfovibrio* G11 (22.5 mg protein), or a heat-killed treatment of the same organism. After a 17d incubation, the core segments were assayed again (Figure 5). The presence of a suitable inoculum was ensured by the addition of live *Desulfovibrio* to the core segment and this treatment resulted in a 9-fold increase in sulfate reduction. However, the heat-killed preparation as well as the lactate amendment stimulated sulfate reduction to a comparable degree (Figure 5). The stimulation in sulfate reduction by both the live and heat-killed cell treatments suggested that the former served largely as an equivalent nutritional augment. We questioned if the live inoculum was capable of sulfate reduction in the core or if microbial activity was affected by an unknown inhibitor. The ability of the cells to reduce sulfate was confirmed in incubations of twice-autoclaved sediment (5 g) with live inoculum (1 ml of a washed cell suspension, 4.5 mg protein/ml). Sulfate was consumed (>2 mM) in these incubations and the sediment turned black in a few hours (data not

shown). The addition of heat-killed *Desulfovibrio* G11 (1 ml of the same cell suspension, boiled) to twice-autoclaved slurries did not result in sulfate depletion or a black precipitate.

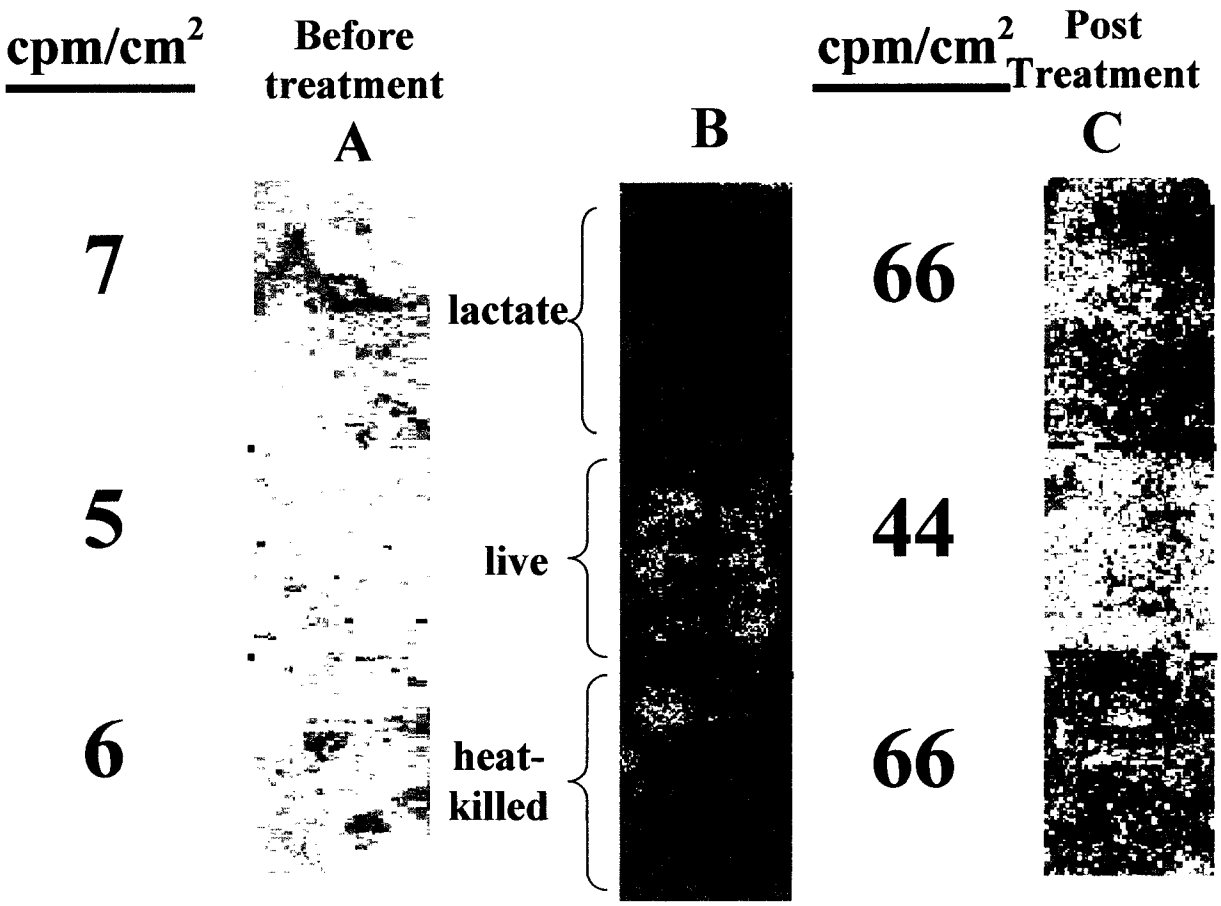


Figure 5. Sulfate reduction activity distributions in a core segment incubated with $^{35}$S-sulfate and amendments of lactate and *Desulfovibrio* preparations. Image A represents sparse distribution of $^{35}$S-sulfide in an unamended core segment incubated for 90 days in the presence of radiolabelled sulfate. Image B is the same segment analyzed immediately after lactate, $^{35}$S-sulfate, and *Desulfovibrio* amendments showing uniform distribution of the radiotracer. Image C is the same segment after 17 days of incubation and represents precipitated $^{35}$S-sulfide remaining after unreacted $^{35}$S-sulfate was removed by washing.

**Effect of groundwater quality on sulfate reduction.** We examined the ability of filter-sterilized groundwater from either the upgradient or downgradient site to supply electron donors for sulfate reduction in an additional series of laboratory incubations. Combinations of sediment and groundwater from site 35 consumed sulfate at the fastest rates, designated for comparative purposes as 100% (Figure 6). The activity was diminished to only 18% when groundwater from the distal site was used as the source of electron donor. The diminished rate was similar to the 19% value observed in incubations prepared using sediment and groundwater from the distal location. Groundwater from near the landfill was able to enhance the sulfate reduction rate by the organisms in the downgradient sediments to about 59%.

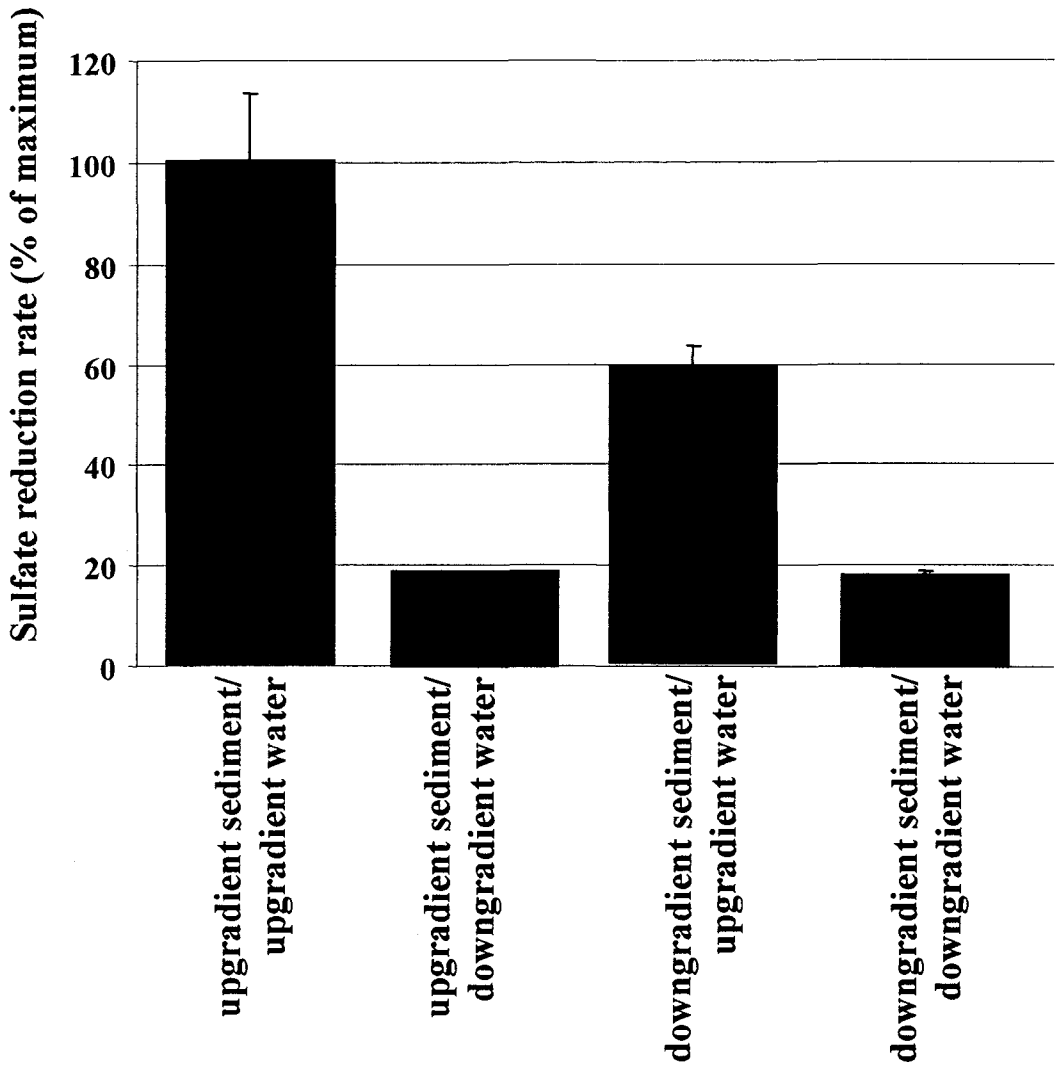


Figure 6. Sulfate reduction rates in sediment slurries at saturating (5mM) sulfate concentrations and in the presence of different groundwaters as potential electron donor sources. Slurries containing sediment and groundwater from the upgradient site consumed sulfate at the highest rate (156nmole $SO_4^{=}$*g wet wt.$^{-1}$*day$^{-1}$) and were designated as 100%. Rates for the other treatments are relative to 100%. The values are the means of triplicate incubations +/- standard error.

We considered whether the presence of an unknown inhibitory substance in downgradient groundwater reduced the level of activity in the samples. However, this did not appear to be the case. If sediment from near the landfill was incubated with no addition of groundwater, we would predict a sulfate reduction rate of only about 8% of the maximum observed in Table 1 (based on the residual amount of water in the sediment). However, addition of downgradient groundwater resulted in a rate of about 18% , more than twice the expected level in absence of water from the distal site. Therefore, the presence of an inhibitor could not explain the reduced rate observed when groundwater from the distal site was used.

We examined the ability of hydrogen and formate to serve as potential electron donors for sulfate reduction in lab incubations (data not shown). Sulfate reduction was not stimulated by either potential electron donor in incubations using sediment from the upgradient site. In contrast, sulfate reduction in sediment from the distal site was stimulated by a factor of five in the presence of added hydrogen; and by a factor of two in the presence of added formate. In the presence of added formate, a small amount of methane was produced in slurries from the downgradient site. However, sulfate consumption, methane, and acetate production accounted for <10% of the formate that was consumed, suggesting an alternate fate for formate exists at this site, a result that was consistent with the field observations (Figure 2).

## Discussion

Endogenous electron donors in the sediment/groundwater closest to the landfill supported measurable *in situ* rates of sulfate reduction (Figure 2). However, these rates could be increased by the addition of a labile electron donor like formate. Presumably,

the stimulated effect observed in field tests was due to the proliferation of formate utilizing sulfate-reducing bacteria. This rate is comparable to those obtained in laboratory incubations using sediments from near the water table (1.5 m depth, Figure 3) where the increased rates are supported by higher sulfate concentrations that result from seasonal oxidation of iron sulfides [29].

Sulfate reduction was not detected in field tests conducted at the downgradient site regardless of formate amendment [Figure 4]. Dissolved oxygen concentrations were uniformly low throughout the tests, indicating that aerobic conditions were not the reason for the lack of sulfate consumption. In addition, the lack of activity was not due to sulfate limitation, as the concentration of this anion remained nonlimiting during the course of the push-pull tests. One explanation for the lack of sulfate reduction in push-pull tests at the downgradient site was competition for formate by microorganisms other than sulfate reducers. Although sulfate consumption was not detected, added formate was rapidly degraded over the first 5d of the test indicating the presence of an active microbial community capable of metabolizing this compound. Similar to field results, added formate was rapidly consumed in slurries from the downgradient site but resulted in only a slight increase in the sulfate reduction rate (data not shown). After determining an electron balance in the slurries, less than 10% of the consumed formate was accounted for by sulfate reduction, methanogenesis, and acetogenesis further suggesting an alternative fate for formate exists at this site.

It is unlikely that it is merely the concentration of DOC that limits sulfate reduction at the downgradient site. The level of DOC near the landfill mound is relatively high (>8 mM) and at least as high as that measured in other contaminated

aquifers including those polluted with landfill leachate [2,5,22,24], and at least an order of magnitude higher than that typically found in aquifers upgradient from landfills [5,27,29]. In slurries from the Grindsted landfill, microbial iron reduction could not be stimulated by additions of amorphous iron hydroxides alone, despite the presence of comparably high DOC levels in the leachate [21]. However, iron reduction was stimulated in the presence of acetate. These results are similar to those obtained in this study suggesting that the relatively recalcitrant nature rather than the quantity of electron donor is the primary factor limiting the rate of sulfate respiration. Dissolved organic matter emanating from the Norman landfill has been fractionated and examined previously [24]. The hydrophobic fraction was found to contain primarily highly branched, cyclic aliphatic compounds that likely represent sizing agents released during the biodegradation of cellulose from paper. Less refractory organic matter such as polysaccharides, cellulose, and proteins were either not detected or present at very low levels. Presumably, these compounds are present in the refuse deposited in the landfill but are degraded rapidly, leaving the more recalcitrant molecules to migrate downgradient to the sampled area. Thus, the high degree of aliphaticity of the leachate organic matter along with the lack of more labile carbon structures is consistent with the inability of the DOC fraction to support maximum rates of sulfate reduction. Moreover, DOC at the downgradient location (3.3 mM) is still 13 times higher than background concentrations [29]. If dilution were a significant factor in attenuating DOC levels along the flowpath, we would expect the concentration of other dissolved constituents to approach those found in background water. However, chloride and specific conductance determinations at the downgradient site remain three-times higher than background levels

[29] and are not diminished relative to the upgradient site (Table 1), indicating that dilution alone cannot account for the decreased DOC concentrations along the 90m flowpath. These results suggest that microbial activity is responsible for decreasing organic matter concentrations along the flowpath. Indeed, several microbial processes have been detected in the aquifer that can contribute to the degradation of DOC along the groundwater flowpath [8]. Nevertheless, substantial amounts of DOC persist even at a distance of 90m from the landfill. We hypothesize that microbial degradation along the flowpath results in a diminished biodegradability of the DOC such that sulfate reduction is limited by electron donor at the distal site.

To further elucidate factors limiting sulfate consumption downgradient from the landfill, radiotracer experiments were done in cores from the distal site (Figure 5). The ability of lactate, as well as a heat-killed preparation of *Desulfovibrio* to stimulate sulfate reduction indicated the lack of a suitable inoculum was not the reason for the lack of activity in the core. Active populations of sulfate reducing bacteria are clearly present in the sediment, but their activity could only be realized if they were supplied with a more labile form of electron donor. Moreover, this electron donor limitation could be supplied by lactate or a heat-killed cell preparation.

To further explore the lack of activity at the distal site, the ability of filter-sterilized groundwaters to support microbial sulfate consumption was examined in slurries that were replete with this anion. These experiments demonstrated the presence of active sulfate reducing microorganisms in the sediment from both sites sampled when groundwater from near the landfill supported relatively rapid rates of sulfate consumption whether the inoculum source was sediment from either site [Figure 6]. Thus, despite the

obvious presence of a capable sulfate reducing community in these sediments, their activity was diminished to similar levels as the result of the inferior biodegradability of electron donor supplied by groundwater from the distal site.

These results are especially interesting in the context of using bioaugmentation to stimulate in situ bioremediation in contaminated aquifers. Several studies have examined microbial inoculation as a strategy to remediate contaminated aquifers [9,25,30]. However, in addition to acting as a catalytic entity, the microbial inoculant can also serve as a labile source of electron donor. Indeed, microbial inoculation experiments demonstrate various degrees of success, in part because of the lack of survival of the injected microorganisms [31]. The inactivation and subsequent lysis of inoculated cells would provide a rich source of electron donor in the form of cell debris. This electron donor then becomes available to the native microbial community driving the catalysis of various processes that may include the very transformation the original inoculation was intended to produce. This is illustrated by the control treatment in Figure 5 where the heat-killed preparation of *Desulfovibrio* is included. A similar control containing an inactivated cell preparation is also necessary in field studies where microbial inoculation is employed as a remediative strategy. However, this type of treatment is seldom carried out and thus, the true nature of the contribution made by the microbial inoculant is not clear.

In summary, the lack of sulfate reduction at the distal site was not due to a lack of a suitable inoculum, sulfate limitation, the presence of an unknown inhibitory substance or the DOC quantity. Rather the results are more consistent with a limitation in DOC biodegradability.

## References


1. Aeckersberg F (1998) Growth, natural relationships, cellular fatty acids and metabolic adaptation of sulfate-reducing bacteria that utilize long-chain alkanes under anoxic conditions. Arch. Microbiol. 170:361-369.

2. Amirbahman A, Schönenberger R, Johnson CA, Sigg L (1998) Aqueous- and solid-phase biogeochemistry of a calcareous aquifer system downgradient from a municipal solid waste landfill (Winterthur, Switzerland). Environ. Sci. Technol. 32:1933-1940.

3. Beeman RE, Suflita JM (1987) Microbial ecology of a shallow unconfined ground water aquifer polluted by municipal landfill leachate. Microb. Ecol. 14:39-54.

4. Bjerg PL, Rügge K, Pedersen JK, Christensen TH (1995) Distribution of redox-sensitive groundwater quality parameters downgradient of a landfill (Grindsted, Denmark). Environ. Sci. Technol. 29:1387-1394.

5. van Breukelen BM, Röling WFM, Groen J, Griffioen J, van Verseveld HW (2003) Biogeochemistry and isotope geochemistry of a landfill leachate plume. J. Cont. Hydrol. 65:245-268.

6. Chapelle FH, Bradley PM (1997) Chapter 61. Alteration of aquifer geochemistry by microorganisms. In: Hurst CJ, Knudsen GR, McInerney MJ, Stetzenbach LD, Walter MV (eds.), Manual of Environmental Microbiology. ASM Press, Washington, D.C., pp.558-564.

7. Christenson S, Scholl MA, Schlottmann JL, Becker CJ (1999) Ground-water and surface-water hydrology of the Norman landfill research site. U.S. Geological Survey Water Resources Investigations Report 99-4018C, U.S. Geological Survey, West Trenton, NJ; 501-507.

8. Cozzarelli IM, Suflita JM, Ulrich GA, Harris SH, Scholl MA, Schlottmann JL, and Christenson S (2000) Geochemical and microbiological methods for evaluating anaerobic processes in an aquifer contaminated by landfill leachate. Environ. Sci. Technol. 34, 4025-4033.

9. ElFantroussi S, Belkacemi M, Top EM, Mahillon J, Naveau H, Agathos SN (1999) Bioaugmentation of a soil bioreactor designed for pilot-scale anaerobic bioremediation studies. Environ. Sci. Technol. 33:2992-3001.

10. Ensley BD, Suflita JM (1995) Metabolism of environmental contaminants by mixed and pure cultures of sulfate-reducing bacteria, p. 293-332. *In* L.L. Barton (ed.), Sulfate-reducing bacteria. Plenum Press, New York, N. Y.

11. Fauque GD (1995) Ecology of sulfate-reducing bacteria, p. 217-241. *In* L.L. Barton (ed.), Sulfate-reducing bacteria. Plenum Press, New York, N. Y.

12. Harris SH, Ulrich GA, Suflita JM (1999) Dominant terminal electron accepting processes occurring at a landfill leachate plume-impacted site as indicated by field and laboratory measurements. U.S. Geological Survey Water Resources Investigations Report 99-4018C, U.S. Geological Survey, West Trenton, NJ; 541-548.

13. Istok JD, Humphrey MD, Schroth MH, Hyman MR, O'Reilly KT (1997) Single-well "push-pull" tests for in situ determination of microbial activities. Groundwater 35:619-631.

14. Jakobsen R, Postma D (1994) In situ rates of sulfate reduction in an aquifer (Rømø, Denmark) and implications for the reactivity of organic matter. Geology 22:1103-1106.

15. Jørgensen BB (1982) Mineralization of organic matter in the sea bed-the role of sulphate reduction. Nature 296:643-645.

16. Kleikemper J, Pelz O, Schroth MH, Zeyer J (2002) Sulfate-reducing bacterial community response to carbon source amendments in contaminated aquifer microcosms. FEMS Microbiol. Ecol. 42:109-118.

17. Krumholz LR, McKinley JP, Ulrich GA, Suflita JM (1997) Confined subsurface microbial communities in Cretaceous rock. Nature 386:64-66.

18. Kuever J, Kulmer J, Jannsen S, Fischer U, Blotevogel K (1993) Isolation and characterization of a new spore-forming sulfate-reducing bacterium growing by complete oxidation of catechol. Arch. Microbiol. 159: 282-288.

19. Lovley DR, Klug MJ (1985) Model for the distribution of sulfate reduction and methanogenesis in freshwater sediments. Geochchim. Cosmochim. Acta 50:11-18.

20. Lovley DR, Phillips EJP (1987) Competitive Mechanisms for inhibition of sulfate reduction and methane production in the zone of ferric iron reduction in sediments. Appl. Environ. Microbiol. 53:2636-2641.

21. Ludvigsen L, Albrechtsen H-J, Heron G, Bjerg PL, Christensen TH (1998) Anaerobic microbial redox processes in a landfill leachate contaminated aquifer (Grindsted, Denmark). J. Cont. Hydrol. 33:273-291.

22. Ludvigsen L, Albrechtsen H-J, Ringelberg DB, Ekelund F, Christensen TH (1999) Distribution and composition of microbial populations in a landfill leachate contaminated aquifer (Grindsted, Denmark). Microb. Ecol. 37:197-207.

23. McMahon PB, Chapelle FH (1991) Microbial production of organic acids in aquitard sediments and its role in aquifer geochemistry. Nature 349:233-235.

24. Nanny MA, Ratusuk N (2002) Characterization and comparison of hydrophic neutral and hydrophobic acid dissolved organic carbon isolated from three municipal landfill leachates. Water Res. 36:1572-1584.

25. Newcombe DA, Crowley DE (1999) Bioremediation of atrazine-contaminated soil by repeated application of atrazine-degrading bacteria. Appl. Microbiol. Biotechnol. 51:877-882.

26. Parkin TB (1990) Characterizing the variability of soil denitrification. FEMS Symposium 56(Denitrif. Soil Sediment):213-228.

27. Rügge K, Bjerg PL, Christensen TH (1995) Distribution of organic compounds from municipal solid waste in the groundwater downgradient of a landfill (Grindsted, Denmark). Environ. Sci. Technol. 29:1395-1400.

28. So CM, Young LY (1999) Isolation and characterization of a sulfate-reducing bacterium that anaerobically degrades alkanes. Appl. Environ. Microbiol. 65:2969-2976.

29. Ulrich GA, Breit GN, Cozzarelli IM, Suflita JM (2003) Sources of sulfate supporting anaerobic metabolism in a contaminated aquifer. Environ. Sci. Technol. 37:1093-1099.

30. Weiner JM, Lovley DR (1998) Anaerobic benzene degradation in petroleum-contaminated aquifer sediments after inoculation with a benzene-oxidizing enrichment. Appl. Environ. Microbiol. 64:775-778.

31. Wagner-Döbler I (2003) Chapter 10. Microbial inoculants-snake oil or panacea? In : Head IM, Singleton I, Milner MG (eds.), Bioremediation: A Critical Review, Horizon Scientific Press, Norfolk, England, pp 259-289.

32. Winfrey MR, Zeikus JG (1977) Effect of sulfate on carbon and energy flow during microbial methanogenesis in freshwater sediments. Appl. Environ. Microbiol. 33:275-281.

33. Zhang X, Young LY (1997) Carboxylation as an initial reaction in the anaerobic metabolism of naphthalene and phenanthrene by sulfidogenic consortia. Appl. Environ. Microbiol. 63,4759-4764.

# Chapter 2

*In situ* hydrogen consumption kinetics as a potential measure of subsurface microbial activity


## Abstract

Rates of microbial hydrogen consumption were estimated from field tests conducted in two contaminated aquifers (Norman, OK and Cape Cod, MA) under various electron-accepting conditions using injection/withdrawal tests amended with hydrogen and a conservative tracer. *In situ* rates determined from first order constants varied by over three orders of magnitude from 0.002 $nM*hr^{-1}$ for an aerobic interval to 2.5 $nM*hr^{-1}$ for a sulfate-reducing interval. Despite this range, the method could easily be adjusted to accommodate the variation in rates that existed between the sites. Comparable determinations in sediment slurries exhibited hydrogen consumption kinetics that differed from field estimates. Thus, microbial activities measured in the laboratory may be influenced by factors not present *in situ*. In a denitrifying zone the rate of hydrogen oxidation was 0.02 $nM*hr^{-1}$. However, the presence of air or an antibiotic mixture immediately abolished hydrogen consumption in this zone, suggesting that these measurements may be useful to gauge the effect of environmental insults on field microbial activities. These results reflect the relative ability of the resident microorganisms to process hydrogen coupled to several different electron acceptors. Anaerobic degradation of organic compounds relies on rapid consumption of hydrogen and subsequent maintenance at low levels. Thus, *in situ* measures of hydrogen turnover

potentially reflect the rate the microbial food chain is functioning, including the rate of organic matter degradation.

## Introduction

Hydrogen is an important intermediate being both produced and consumed by a wide variety of microorganisms during the decomposition of organic matter. In anaerobic environments, the thermodynamics associated with many bioconversions is regulated by the concentration of hydrogen [1]. For the same reasons, the transport and fate of many contaminants in the environment is also influenced by the partial pressure of hydrogen. Organisms dominating the consumption of hydrogen influence the redox status of the environment, which in turn influences the rate and extent of organic matter degradation. Thus, the rate of hydrogen turnover in the environment reflects the rate the microbial food chain is functioning. Furthermore, field measures of hydrogen turnover can assess the impact of contaminant chemicals on the normal functioning of microbial communities. Since hydrogen is a crucial intermediate that can be turned over rapidly and likely serves as the primary electron donor in many environments [2-5], a great deal of effort has been expended to appreciate the factors governing the bacterial consumption of hydrogen in the environment.

Most attempts at understanding hydrogen metabolism in nature are based on consumption kinetics exhibited by pure cultures of hydrogenotrophic bacteria cultivated in the laboratory [6-9]. Such studies have successfully described the competition for hydrogen as an electron donor supporting the metabolism of various hydrogenotrophs [10-12]. Sophisticated models employing Michaelis-Menten or Monod growth

parameters, threshold considerations, and thermodynamic constraints have all been proposed [13-16] to describe hydrogen consumption between defined mixed cultures under various redox conditions. While such studies have provided insight on hydrogen consumption by pure or defined mixed cultures of bacteria, they are often of restricted utility when applied to more complex environments. For instance, a strict competition for a limiting resource is rarely the only microbial interaction influencing the hydrogen status in complex environments. Similarly, various hydrogenotrophs exhibit threshold concentrations below which hydrogen consumption, while thermodynamically feasible, ceases [7,8,11,17,18]. Unlike pure culture studies, hydrogen is typically consumed to a steady state concentration in the environment that reflects the predominant terminal electron accepting process. Under these conditions hydrogen production is balanced by consumption, although the absolute level of hydrogen is kinetically controlled [19]. To our knowledge the prospect of a true threshold, as defined by Conrad, 1994 has not been observed in any environmental sample.

The study of hydrogen consumption by microbial assemblages has revealed several phenomena that would not otherwise be evident with pure culture investigations. For instance, thermodynamic constraints associated with hydrogen consumption under different redox conditions help to restrict the distribution of specific microorganisms to areas where they can harness biologically useful energy [21-23]. A study of hydrogen kinetics in soil slurries led to the postulation of a role for abiontic hydrogenases that exhibit kinetic parameters far different from any known pure culture hydrogenotroph [24-25]. As noted, a steady state hydrogen concentration is readily observed in environmental samples [20,22]. Although the assumption of steady state may not always

be the case *in situ* [21], such measures have proven to be a better indicator of the predominant electron accepting conditions than more traditional redox determinations [19,26].

Similarly, it might be expected that an examination of hydrogen consumption in the field would more accurately reflect *in situ* microbial activities that would otherwise be difficult to discern through laboratory investigations. While the steady state hydrogen concentration is consistently measured in field investigations and interpreted relative to the dominant terminal electron accepting conditions in an environment (19,21,26-30, this study], such determinations are independent of the rate of hydrogen production and consumption and therefore do not assess the dynamics of microbial activity. Based on the central nature of hydrogen as a metabolic intermediate, field measures of hydrogen turnover have the potential to assess *in situ* microbial activity and thereby serve as an indicator of total community metabolism. *In situ* hydrogen consumption determinations have the advantage of capturing the dynamics of the microbial food chain, thus providing a valuable augmentation to current assessments of field microbial activities.

In this study *in situ* hydrogen consumption rates were measured using single well injection tests under several terminal electron-accepting conditions in two contaminated aquifers. Microbial hydrogen consumption was observed under aerobic, as well as nitrate-, iron-, and sulfate-reducing conditions and in the presence of different types of contamination. *In situ* rates calculated from the first order constants and corresponding steady state hydrogen values varied by over three orders of magnitude suggesting that such determinations have a needed degree of sensitivity to assess total microbial activity in the field. Quantitative descriptions of subsurface microbial activity to process a key

metabolic intermediate like hydrogen will help assess the influence of contaminating materials on the functioning of these ecosystems and gauge the potential impact of remedial efforts.

## Materials and Methods

**Site descriptions.** The Norman landfill and Cape Cod sites are described in detail elsewhere [31-33]. The Norman site is a closed municipal landfill occupying approximately 12 hectares on the Canadian River alluvium in central Oklahoma, USA. The alluvium is 10-12 meters thick with a water table that is typically 2 meters below land surface. Solid waste was deposited in the landfill beginning in 1922 and continued until 1985 when the site was closed and covered with local clay and silt. There were no restrictions on the material deposited in the landfill and no liner or leachate collection devices were used. As a result, the leachate emanating from the refuse comprises a complex waste stream that permeates the thickness of the aquifer to approximately 1.5 km from the mound. Recent geochemical surveys of the groundwater show uniformly low levels of $O_2$ (<5 μM) throughout the plume [32]. The interval examined in this study intercepts a zone where microbial sulfate reduction is an important redox process and contains some of the highest levels of dissolved organic carbon (DOC), ferrous iron, ammonia, and chloride measured at the site [31,32].

The Cape Cod site is a freshwater sand and gravel aquifer, located near Falmouth, Massachusetts that has been contaminated by the disposal of treated sewage onto rapid infiltration sand beds for more than 60 years. This has resulted in a groundwater contaminant plume that is more than 5 km long, 1 km wide and 30 m deep [33]. The

contaminant plume, which is characterized by steep vertical concentration gradients [34], contains high concentrations of nitrate (>1 mM) and moderate concentrations of dissolved organic carbon (50-400 μM), most of which is relatively refractory [35]. Denitrification and iron reduction are the dominant electron accepting reactions known to occur at the site [36,37]. In 1995, sewage disposal at the Cape Cod site was discontinued. Concentrations of nitrate, DOC and other constituents have decreased, but remain elevated, while oxygen gradients remain essentially unchanged, even at the infiltration beds where the plume originates.

***In situ* hydrogen consumption determinations.** *In situ* hydrogen consumption rates were estimated by injecting hydrogen dissolved in local groundwater and interpreting its loss relative to a conservative tracer, sodium bromide. At Norman, rates were estimated using the push-pull test procedure [38]. This procedure involves preparation of an injectate solution by constantly flushing a reservoir of groundwater with a compressed gas mixture containing 10% $CO_2$ and a ratio of $H_2/N_2$ that was adjusted depending on the desired dissolved hydrogen concentration. The reservoir was fitted with a vented cap and commercial aquarium stones were used to allow for continuous sparging of groundwater and dissolution of gases and bromide in the injectate. The injectate contained either 2.5 or 150 μM dissolved hydrogen and 1.2 mM sodium bromide as required.

At Cape Cod, the injectate was prepared by pumping groundwater into a gas-impermeable bladder (100 L) that had been fitted with ports through which injections of gaseous as well as dissolved components were made. The bladder was flushed with $N_2$ and purged seven times before addition of 15 L $N_2$ and 15 mL $H_2$. Sodium bromide (10.3

g) was then added from an anoxic stock solution. In the denitrifying zone at Cape Cod, efforts were made to assess the impact of stressors by adding the antibiotics streptomycin (20 g) and ampicillin (10 g) or an air headspace to the injectate. The bladder was taken to the field site and filled with 80 L of groundwater. The gases in the headspace were allowed to equilibrate with groundwater in the bladder by gentle mixing. Then, the headspace was vented and the solution was injected directly into the well from which it was extracted.

Upon incubation in the aquifer, the tracer clouds were periodically sampled from the same well. Samples were collected by peristaltic pump and placed in He-flushed vials where hydrogen was allowed to equilibrate between gaseous and liquid phases. At Norman, hydrogen in the vial headspace was measured in the field within a few minutes of sampling, although the levels did not change if the vials were stored on ice for up to 24 hr, which was the procedure for bromide determinations. In the Cape Cod tests the vials were placed on ice and analyzed for hydrogen within 24 hr. Bromide was determined with a high pressure liquid chromatograph equipped with a conductivity detector (Dionex Corporation, Sunnyvale, CA). Hydrogen was determined on a gas chromatograph equipped with a mercury vapor detector (Trace Analytical, Sparks, MD). Apparent *in situ* rates were estimated from breakthrough curves of hydrogen and bromide. Decreasing bromide concentrations during extraction were attributed to abiotic processes such as dilution and dispersion. Thus, in tests where bromide concentrations decreased during extraction, such values were used to correct hydrogen levels for abiotic loss and generate apparent rates of microbial hydrogen consumption. In tests where bromide values were unchanged throughout the extraction (no abiotic loss), *in situ* rates were

estimated directly from hydrogen loss data. Steady state dissolved hydrogen concentrations were determined by the gas stripping method [39] and combined with first order rate estimates to gauge *in situ* hydrogen turnover.

First order rates from *in situ* tests were normalized to the volume of aquifer so comparisons to laboratory measurements could be made (see Discussion). These calculations were done based on the porosity of each aquifer (0.40 at Norman, 0.39 at Cape Cod).

**Laboratory experiments.** Slurries of sediment and groundwater were constructed to compare hydrogen consumption in the laboratory to results obtained in the field. Sediment was obtained from the same areas as the field tests and incubated at *in situ* temperatures (15°C for Cape Cod and 19°C for Norman). Sediment (100 g) and groundwater (80 mL) from Cape Cod were incubated in 150 mL Erlenmeyer flasks while the same materials from Norman (50 g, 75 mL) were incubated in 160 mL serum bottles. The incubations contained 1atm. $N_2/CO_2$ (4/1) in the headspace, to which 0.01 to 3 mL of hydrogen was added at the start of the assay

**Analysis of hydrogen turnover.** At low initial hydrogen concentrations, first order rates were determined from the *in situ* hydrogen depletion curves. At high initial hydrogen concentrations, hydrogen depletion exhibited zero, mixed, and first order decay. Such curves are amenable to nonlinear regression analysis for the estimation of apparent kinetic constants as well as rate determinations [40]. These parameters were estimated from progress curve data by nonlinear least squares analysis using a computer model based on the Michaelis-Menten equation [41].

## Results

***In situ* microbial hydrogen consumption.** *In situ* hydrogen consumption rates were estimated in two aquifers where either oxygen, nitrate, $iron_{(III)}$, or sulfate served as the predominant electron acceptor. Within a sulfate-reducing zone at the Norman, OK site, substrate loss at saturating concentrations of hydrogen (150 μM), occurred at a rate that was faster than that of sodium bromide (Figure 1A). This is indicative of biological hydrogen consumption. Hydrogen data were corrected for dilution via sodium bromide values to reveal an *in situ* consumption rate that was constant over the first 0.5 hr of the test, consistent with a zero order rate process (Figure 1B). As hydrogen was depleted, the rate began to decrease and eventually transitioned to a first order process. Estimates of the kinetic constants derived from the entire progress curve suggested an apparent $K_m$ and $V_{max}$ of 3.48 μM [± 5.24] and 182 μmol*L $sediment^{-1}$*$hr^{-1}$ [±24], respectively. However, nonlinear regression analysis suggested the first order rate deviated from that predicted by Michaelis-Menten kinetic theory. Rather, there was an alternate first order rate constant (1.3 $hr^{-1}$) that was slower than model predictions and persisted until the end of the incubation (Figure 1C). This first order estimate was comparable to the value calculated from a replicate test at this site using lower initial hydrogen concentrations (1.2 $hr^{-1}$; Figure 1C, Table 1).

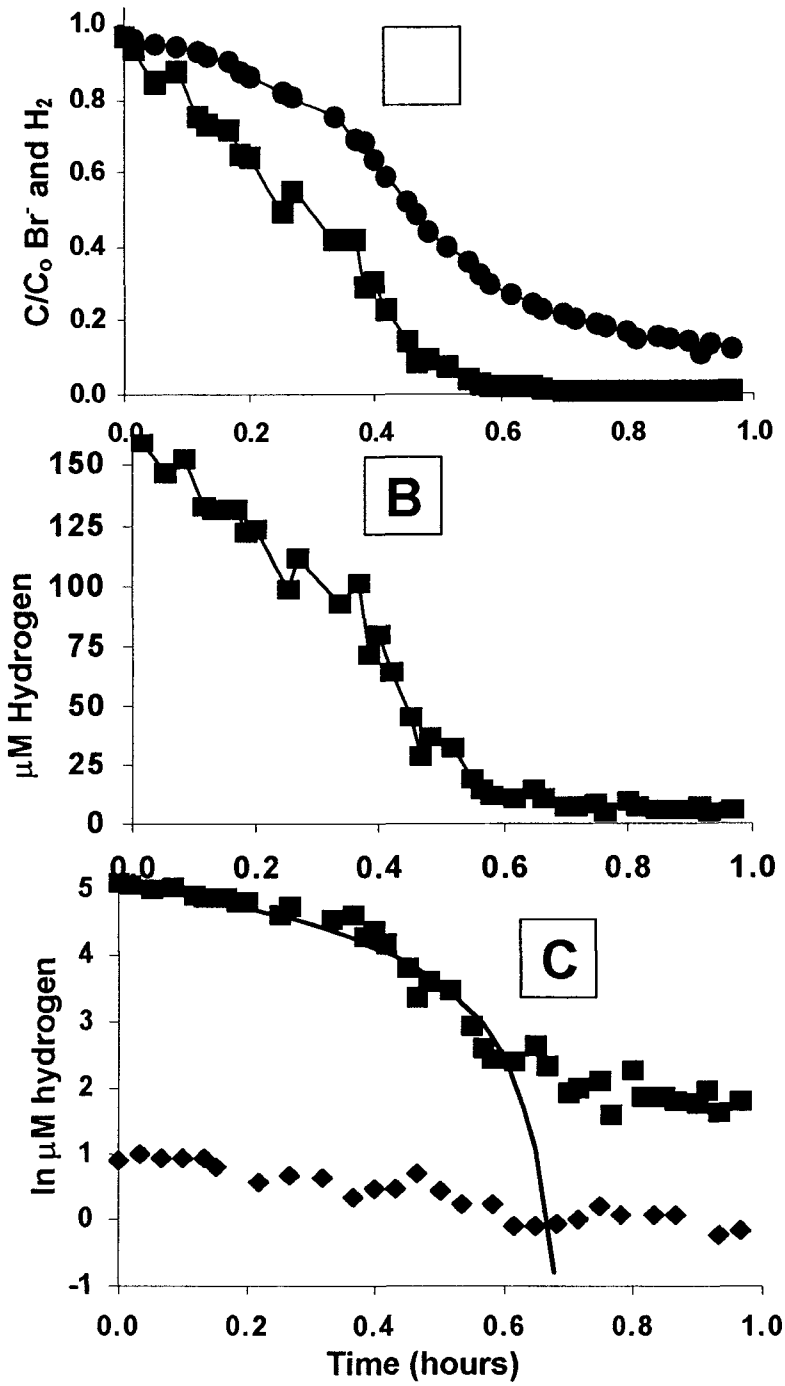


Figure 1. A: Breakthrough curves of sodium bromide (•) and hydrogen (■) during an *in situ* test under sulfate reducing conditions at the Norman landfill site. B: zero, mixed, and first order hydrogen consumption after correcting data in plot A for abiotic loss via sodium bromide values. Plot C: Ln-transformed hydrogen values (■) from plot B illustrating deviation from model predictions (—) in the first order region of the progress curve and results from a replicate test (♦) begun with a lower initial hydrogen concentration.

Hydrogen consumption at the Cape Cod site was slow relative to Norman and occurred with little or no abiotic loss, as evidenced by consistent bromide concentrations throughout a test in the iron reducing zone (Figure 2A). Hydrogen was consumed over a 10 hr period in two different iron reducing zones at Cape Cod. Although the areas interrogated by these tests were separated by 120 m, the first order rate constant for both tests were comparable (0.18 $hr^{-1}$; Figure 2B). The iron reducing interval at Cape Cod is spatially distinct from another zone in which nitrate reduction is the dominant redox process. The first order rate constant derived under denitrifying conditions at Cape Cod was 0.05 $hr^{-1}$ (Figure 2C). In a shallower, less contaminated aerobic zone, the first order rate constant was only 0.01 $hr^{-1}$ (Figure 2D).

These first order rate constants were combined with measured steady state hydrogen concentrations to estimate *in situ* rates of hydrogen turnover. Rates determined in this way ranged from 0.002-0.02 $nM*hr^{-1}$ at Cape Cod and 2.52 $nM*hr^{-1}$ at Norman (Table 1).

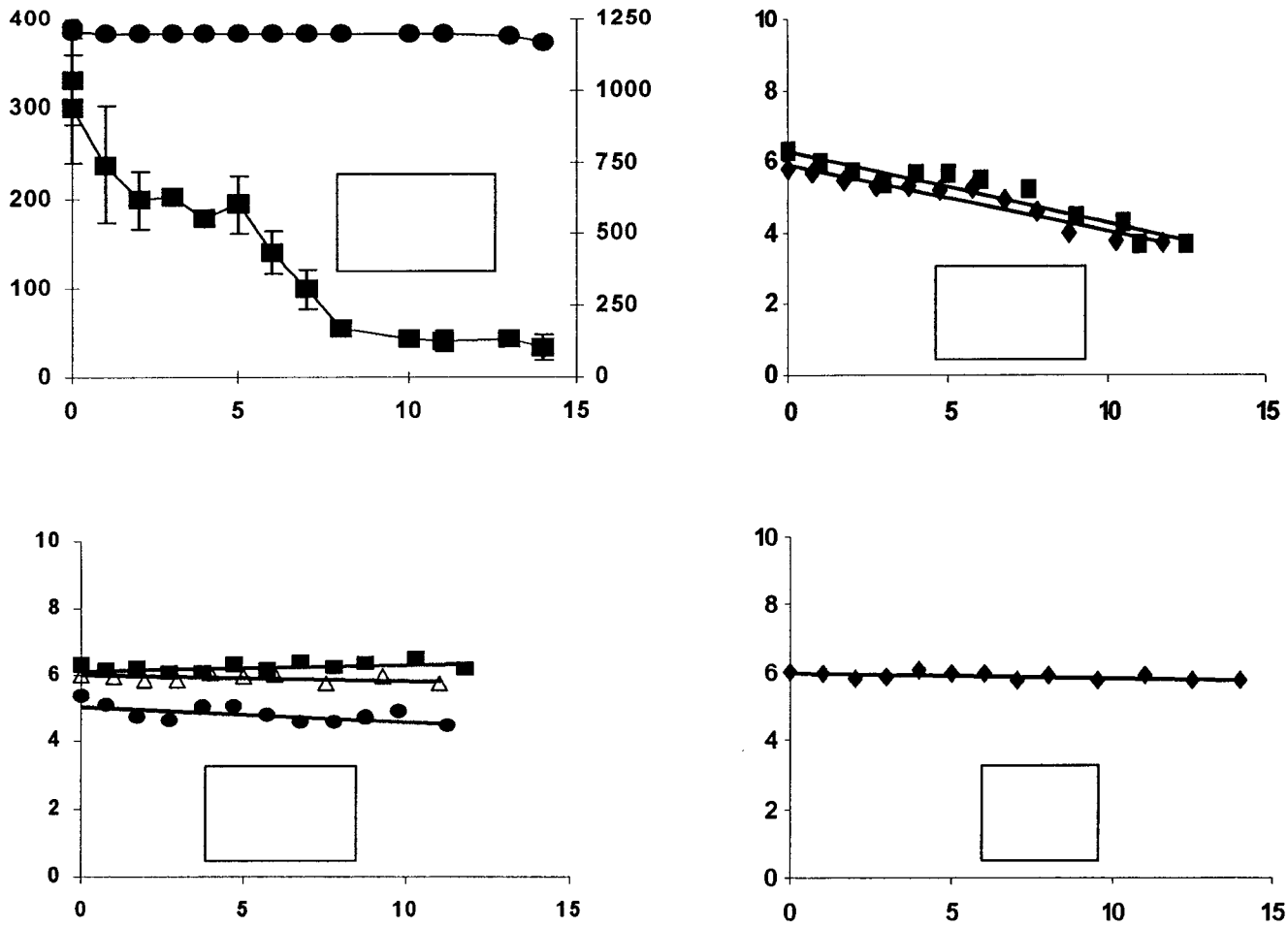


Figure 2. Hydrogen consumption curves from *in situ* tests illustrating apparent first order rates under the various electron-accepting conditions. A: Bromide (•) and hydrogen (■) breakthrough curves in an iron-reducing interval. B: ln-transformed hydrogen depletion data from replicate tests in two iron reducing zones separated by 120m. C: ln-transformed hydrogen depletion data from tests conducted in a nitrate reducing zone and amended with $H_2$ only (•), $H_2$ in air (Δ), or with $H_2$ and streptomycin/ampicillin mixture (■). D: ln-transformed hydrogen depletion in an aerobic zone.

| | Cape Cod | | | Norman |
|---|---|---|---|---|
| e- acceptor | $O_2$ | $NO_3^-$ | $Fe^{+3}$ | $SO_4^=$ |
| DOC (mM) | 0.1 | 0.2 | 0.05 | >8 |
| specific conductivity ($\mu S*cm^{-1}$) | 55-100 | 146 | 150-260 | 4990 |
| $k_1$ ($hr^{-1}$) | 0.01 | 0.05 | 0.18 | 1.2 |
| steady state $H_2$ (nM) | 0.2[a] | 0.4[a] | 0.1[a] | 2.1 |
| in situ rate ($nM*hr^{-1}$) | 0.002 | 0.020 | 0.018 | 2.52 |
| $\Delta G^{o'}$ (kJ/mol $H_2$)[b] | -237 | -224 | -50 | -38 |

[a]from R. Jakobsen, unpublished data
[b]from Lovley and Goodwin, 1988 and references therein

Table 1. Summary of hydrogen consumption rates, geochemical parameters and thermodynamics as a function of the predominant electron-accepting processes active within the groundwater zones examined in this study.

**Impact of stressors on *in situ* hydrogen turnover.** We hypothesized that the *in situ* hydrogen consumption rate was a sensitive measure of microbial community activity. To test this hypothesis, the influence of various amendments were examined in the denitrifying zone at the Cape Cod site (Figure 2C). A mixture of the antibiotics, streptomycin (0.25 $g*L^{-1}$) and ampicillin (0.13 $g*L^{-1}$) effectively eliminated hydrogen consuming activity in the nitrate reducing zone. Furthermore, the addition of oxygen to the test solution also abolished hydrogen consumption in this area of the aquifer.

**Hydrogen consumption in laboratory incubations.** We compared the *in situ* observations of hydrogen consumption with laboratory incubations of sediment and groundwater from Norman. Unlike the field determinations, samples from the Cape Cod site did not consume hydrogen over 48 hr incubation. Although hydrogen consumption was observed in slurries from Norman, the kinetics were very different from the field results (Figure 3). Analysis of the laboratory progress curves yielded a much lower $K_m$ of 0.16 μM [±0.04]and a $V_{max}$ estimate of 16.18 $\mu mol*L\ sediment^{-1}*hr^{-1}$ [±1.03]. First order rates in these slurries ranged from 84-126 $hr^{-1}*L\ sediment^{-1}$. Unlike the *in situ* determinations, the laboratory incubations also did not exhibit a detectable steady state or threshold hydrogen concentration. Rather, hydrogen was consumed according to Michaelis-Menten kinetics to below the detection limit (0.01 nM) and remained there for at least 14 days.

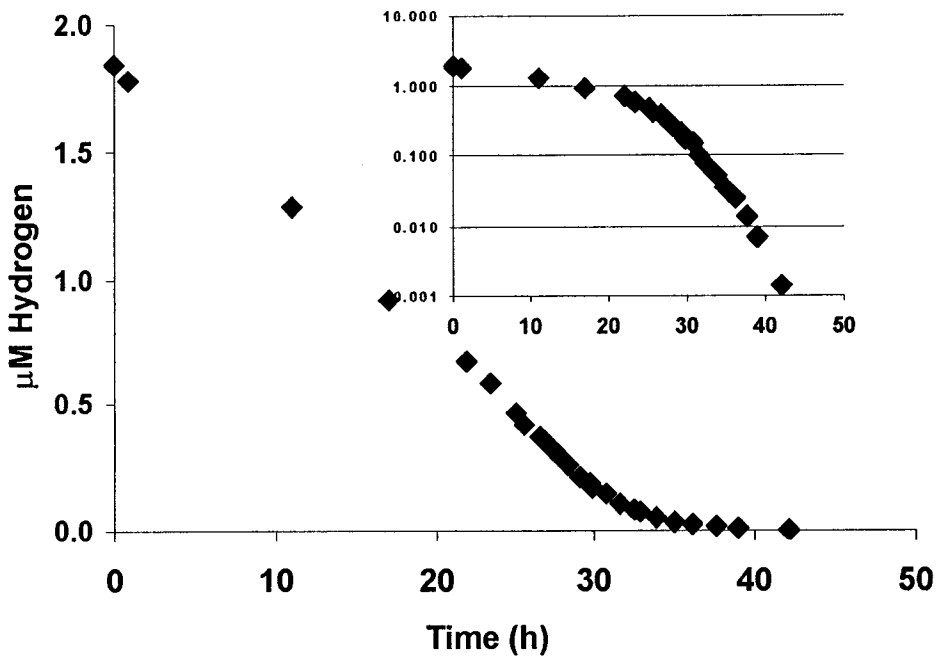


Figure 3. Hydrogen consumption in a sediment slurry from the Norman landfill site. The inset shows the corresponding semi-logarithmic plot.

## Discussion

The purpose of this investigation was to develop and test an *in situ* method of assessing total microbial community metabolism in a groundwater environment. Field hydrogen consumption measurements provide first order rate constants, which in combination with steady state determinations produce estimates of *in situ* microbial hydrogen consumption rates. Such measurements capture the dynamics associated with the flux of hydrogen, a critical metabolic intermediate. Furthermore, in environments where hydrogen flux is at or near steady state, *in situ* hydrogen consumption reflects the rate of organic matter oxidation. Thus, the terminal electron accepting process can be identified (via steady state determinations) in addition to the rate that the microbial food chain is functioning.

*In situ* microbial hydrogen consumption kinetics were examined in two contaminated aquifers under several electron-accepting conditions. Hydrogen consumption was 10-1000 times faster at Norman relative to Cape Cod (Table 1). Because of the large rate difference, it was necessary to use slightly different approaches at the two sites. The push-pull test procedure [38] was a useful technique for estimating the relatively rapid hydrogen consumption rates at Norman. At Cape Cod however, hydrogen consumption was much slower and required a different approach illustrated by the natural gradient tests. Nevertheless, in all cases we were able to estimate first order rate constants and use those values to calculate *in situ* rates (Table 1). Thus, by adjusting

the methodology to match the conditions at the different sites, we were able to quantify hydrogen consumption rates that differed by more than three orders of magnitude.

The Michaelis-Menten equation predicts a constant rate of decrease in the overall reaction rate as substrate concentrations become limiting. However, *in situ* hydrogen consumption demonstrated a deviation from Michaelian behavior during the latter portion of one of the *in situ* tests at Norman (Figure 1B). I*n situ* hydrogen production may be responsible for this deviation. Fermentative hydrogen production would not be favorable at the higher concentrations used in this test. However, as this substrate is consumed, hydrogen production from the oxidation of dissolved organic matter would become thermodynamically favorable and result in a net decrease in the overall hydrogen consumption rate. The hydrophobic fraction of DOC at Norman has been examined previously and found to consist primarily of highly branched, cyclic, aliphatic compounds resulting from the degradation of cellulose from paper [42]. Figure 4 illustrates the thermodynamics associated with the initial oxidative (hydrogen-producing) step in the degradation of cyclohexane carboxylate, a relatively simple representative of such a class of compounds. Compared to less refractory fermentation intermediates such as ethanol and benzoate, cyclohexane carboxylate oxidation is thermodynamically unfavorable unless hydrogen levels are below 10 μM, similar to the concentration at which the deviation from the model occurs in Figure 2. Thus, hydrogen production from electron donors like cyclohexane carboxylate may be responsible for the net decrease in the apparent first order rate observed during *in situ* tests. This observation underscores the necessity of using rate-limiting concentrations (<5μM) of hydrogen in these tests. Dissolved hydrogen concentrations that are below saturating levels result in first order

consumption and provide apparent first order rate constants that can be used to determine *in situ* rates. In addition to hydrogen production, the rate deviation may result from the presence of various hydrogen consuming populations that exhibit different kinetics. As hydrogen becomes depleted, organisms that exhibit a higher $K_m$ become unsaturated, and their rate of hydrogen consumption slows. Microorganisms that exhibit a lower $K_m$, such as that determined in sediment slurries (Figure 3), continue to consume hydrogen at the maximum rate. Thus, the first order rate may not be constant when hydrogen consumption is examined *in situ*.

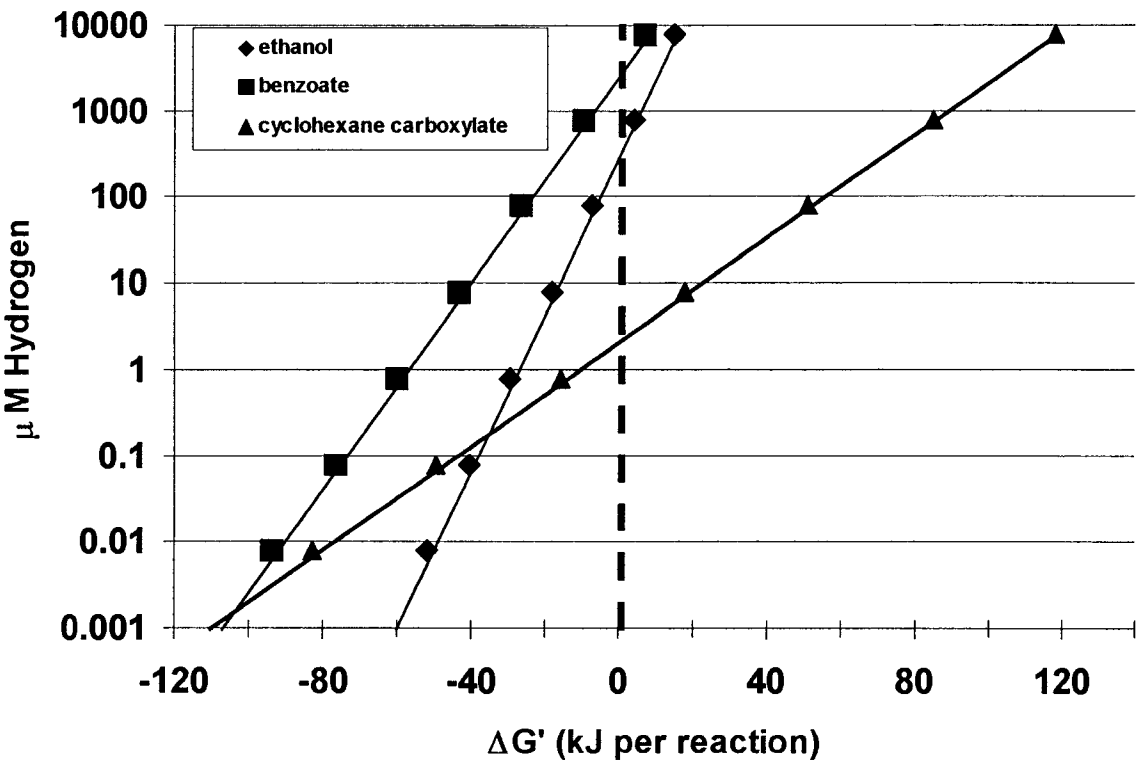


Figure 4. Theoretical energy yield as a function of hydrogen concentration for selected fermentation intermediates. Reaction stoichiometry and thermodynamic yield for ethanol oxidation are from [1]. The same parameters for benzoate and cyclohexane carboxylate are from [52].

In addition, the steady state hydrogen concentration, while consistently measured by many investigators in the field [19,21,26,28,29 this study], was difficult for us to reproduce in the laboratory. Despite measured hydrogen concentrations in the field of 1 to 2 nM, we consistently observed hydrogen depletion below these levels in slurries from the Norman landfill site (Figure 3). Furthermore, hydrogen was not consumed by slurries from Cape Cod over a 48 hr incubation despite our observation of active hydrogen depletion during *in situ* tests conducted at the site. These results suggest that microbial activities measured in the laboratory can be influenced by factors not present in the microorganisms' natural habitat. Consequently, information from laboratory analyses may be insufficient for understanding the dynamics of microbial activity as it occurs in the environment. I*n situ* tests are more sensitive by design in that a large volume of aquifer can be interrogated while using a small amount of hydrogen, all of which is dissolved in the groundwater and therefore in contact with the resident microorganisms. Indeed, the complexity associated with field studies as well as the limitations inherent in applying laboratory-based findings to natural settings, especially in the case of contaminated aquifers, are issues that have been addressed previously [43-45].

These tests were useful for determining hydrogen oxidation rates under both nitrate reducing and aerobic conditions (Figure 2). Relative to sulfate reduction and methanogenesis, little is known about hydrogen consumption under denitrifying conditions. Hydrogen oxidizing denitrifying bacteria appear to be common constituents of the Cape Cod aquifer, several of which have been isolated and characterized according to their hydrogen consuming capacity [46]. Many of these isolates exhibited kinetic

parameters that were comparable to *Paracoccus denitrificans*, a well-characterized hydrogen oxidizing denitrifying bacterium. Although the relative extent to which hydrogen serves as an electron donor in the presence of nitrate is not clear, the presence of organisms capable of catalyzing this process suggests that whatever hydrogen might be produced would be readily consumed via denitrification in the environment. *In situ* hydrogen consumption tests could be a useful means of assessing the importance of this electron donor coupled to denitrification in environments where nitrate is available.

The importance of hydrogen metabolism to the overall functioning of a subsurface habitat suggests that perturbations that negatively impact ecosystem health may be manifested in the ability of the microbial communities to process hydrogen. A fairly simple test of this hypothesis was conducted by including two treatments designed to affect hydrogen metabolism in the denitrifying zone at Cape Cod where *in situ* hydrogen consumption was already shown to occur (Figure 2). Addition of air to test solutions resulted in the elimination of hydrogen consumption *in situ*. Although denitrifying bacteria generally prefer oxygen as an electron acceptor, this molecule does not simply replace nitrate in these bacteria; specific enzymes are produced depending on the availability of either electron acceptor [47]. Moreover, the enzymes involved in the reduction of nitrate to nitrogen are known to be inhibited by oxygen. Given these conditions, it is not unexpected that a relatively subtle stressor such as oxygen imposes a negative impact on hydrogen consumption in a denitrifying environment in the short-term. We would expect hydrogen to be consumed eventually by the organisms at this site even in the presence of air. It would likely require more time than the 15 hr test interval for the hydrogen consuming community to modify their metabolism from denitrification

to aerobic respiration. This point further illustrates the utility of these tests for estimating field rates of microbial activity. Since these tests can be completed in a few hours, hydrogen consuming microorganisms have little time to adapt. In addition, dissolved hydrogen concentrations can be kept low enough (<1 μM) to preclude microbial growth in response to the added substrate. Thus, the results obtained from such tests are reflective of *in situ* activity in the sampled area.

In addition to air, the presence of the antibiotics streptomycin and ampicillin effectively eliminated hydrogen consumption (Figure 2C). Although these compounds would be expected to have a negative impact on microbial hydrogen metabolism, the complete abolition of hydrogen turnover may not be expected because the enzymes and organisms capable of hydrogen oxidation are already present and active in the aquifer as evidenced by the earlier test (Figure 2C). Nevertheless, the hydrogen consuming community was abruptly affected by the presence of the antibiotics. It thus seems likely that *in situ* hydrogen consumption measurements would be sensitive to other insults that affect the process of organic matter degradation in aquifers. A contamination episode may be such an insult that would be manifested by an alteration in the apparent *in situ* hydrogen consumption rate. Thus, the degree of insult to the microbial population may be gauged by *in situ* hydrogen consumption tests in addition to the progress of remediation in contaminated aquifers. Moreover, tests such as these may indicate when the progress of remediation has returned a polluted environment to its original condition.

Given the different geochemical conditions between and within the two sites, we are cautious about drawing conclusions concerning the relationship between field microbial hydrogen consumption rates and the predominant electron accepting

conditions. Nevertheless, we noted that *in situ* rates were proportional to the electron accepting regime as well as to DOC concentrations in the tested areas (Table 1). Thus, field rates of microbial hydrogen consumption may be influenced by not only the electron accepting process, but by the quality of electron donor. The faster rates sustained under sulfate-reducing conditions may reflect the relative importance of interspecies hydrogen transfer under those conditions. In anaerobic environments, organic matter is oxidized by several, metabolically different groups of microorganisms [48]. This process involves fermentative or syntrophic hydrogen production followed by consumption by terminal microorganisms such as sulfate reducers or methanogens [1,49]. These terminal microorganisms maintain hydrogen at low partial pressures allowing organic matter oxidation to be thermodynamically favorable. It follows that in environments where interspecies hydrogen transfer is required for organic matter degradation, hydrogen turnover would necessarily be an efficient process. However, microorganisms that utilize oxygen or nitrate as electron acceptor are more likely to mineralize organic matter without producing hydrogen as a free intermediate [50]. Thus, hydrogen utilization under these conditions could be of lesser total importance, and may explain the faster rate observed under sulfate reducing conditions.

The value of conducting *in situ* experiments lies in the ability to capture the complexity of microbial interactions within their biotic and abiotic surroundings that would not otherwise be observed in laboratory assessments. We normalized first order rates from this and other studies by volume to compare hydrogen consumption rates from *in situ* tests to laboratory measures in this and other studies. In the laboratory, first order rates in slurries from the Norman site were comparable to similar incubations of aerobic

soil (36-108 $hr^{-1}*L^{-1}$ [6], assuming 100 g wet soil=50 mL volume), but slower than slurries from a eutrophic lake (517 $hr^{-1}*L^{-1}$ [51]). However, when estimates from *in situ* tests were normalized by volume, the resulting rates were several orders of magnitude slower (0.006 to 0.8 $hr^{-1}*L^{-1}$) than most laboratory measures including those from Norman. This disparity between field and laboratory measures does not necessarily argue for a preference of one approach over another, especially given the limited number of sites and conditions examined in this study. However, the ability to incorporate the complex interactions of regulating microbial communities with their biotic and abiotic surroundings is an attractive feature of *in situ* tests. Such features indicate field measurements will serve as a valuable augmentation to more traditional laboratory investigations for providing accurate descriptions of microbial activities in the environment.

These results should be considered as a baseline study for comparison to *in situ* rates measured at other sites in the future. The large differences in rates observed at Norman and Cape Cod may stem from the substantial differences in organic matter concentrations that exist at the two sites. Thus, a series of similar measurements made within a single site may be a useful approach for characterizing microbial activity rather than comparing the absolute values obtained in this study with those from other locations. Nevertheless, the multiple electron-accepting regimes and diverse geochemical conditions interrogated here should serve as a model to ascertain whether other systems respond accordingly as well as a foundation for the interpretation of future results.

## References


[1] McInerney, M. J. (1999) Anaerobic metabolism and its regulation. In: Biotechnology 2nd Edn. (Rehm, H.-J., and Reed, G. Eds.), pp. 456-478. Weinheim, Germany: Wiley-VCH

[2] Winfrey, M. R., Nelson, D. R., Klevickis, S. C., and Zeikus, J. G. (1977) Association of hydrogen metabolism with methanogenesis in Lake Mendota sediments. Appl. Environ. Microbiol. 33, 312-318.

[3] Abram, J. W., and Nedwell, D. B. (1978) Hydrogen as a substrate for methanogenesis and sulphate reduction in anaerobic saltmarsh sediment. Arch. Microbiol. 117, 93-97.

[4] Winfrey, M. R., and Zeikus, J. G. (1979) Anaerobic metabolism of immediate methane precursors in Lake Mendota. Appl. Environ. Microbiol. 37, 244-253.

[5] Postma, D., and Jakobsen, R. (1996) Redox zonation: equilibrium constraints on the $Fe_{III}/SO_4$-reduction interface. Geochim. Cosmochim. Acta 60, 3169-3175.

[6] Conrad, R., and Seiler, W. (1979) The role of hydrogen bacteria during the decomposition of hydrogen by soil. FEMS Microbiol. Lett. 6, 143-145.

[7] Conrad, R., Aragno, M., and Seiler, W. (1983) The inability of hydrogen bacteria to utilize atmospheric hydrogen is due to threshold and affinity for hydrogen. FEMS Lett. 18, 207-210.

[8] Lovely, D.R. (1985) Minimum threshold for hydrogen metabolism in methanogenic bacteria. Appl. Environ. Microbiol. 49, 1530-1531.

[9] Robinson, J. A., and Tiedje, J. M. (1984) Competition between sulfate-reducing and methanogenic bacteria for $H_2$ under resting and growing conditions. Arch. Microbiol. 137, 26-32.

[10] Lupton, F. S., and Zeikus, J. G. (1984) Physiological basis for sulfate-dependent hydrogen competition between sulfidogens and methanogens. Curr. Microbiol. 11, 7-12.

[11] Cord-Ruwisch, R., Seitz, H., and Conrad, R. (1988) The capacity of hydrogenotrophic anaerobic bacteria to compete for traces of hydrogen depends on the redox potential of the terminal electron acceptor. Arch. Microbiol. 149, 350-357.

[12] Peters, V, Janssen, P. H., and Conrad, R. (1998) Efficiency of hydrogen utilization during unitrophic and mixotrophic growth of *Acetobacterium woodii* on hydrogen and lactate in the chemostat. FEMS Microbiol. Ecol. 26, 317-324.

[13] Hoh, C.-Y., and Cord-Ruwisch, R. (1996) A practical kinetic model that considers endproduct inhibition in anaerobic digestion processes by including the equilibrium constant. Biotech. Bioeng. 51, 597-604.

[14] Hoh, C.-Y., and Cord-Ruwisch, R. (1997) Experimental evidence for the need of thermodynamic considerations in modeling of anaerobic environmental bioprocesses. Water Sci. Technol. 36, 109-115.

[15] Jin, Q., and Bethke, C. M. (2003) A new rate law describing microbial respiration. Appl. Environ. Microbiol. 69, 2340-2348.

[16] Watson, I. A., Oswald, S. E., Mayer, K. U., Wu, Y., and Banwart, S. A. (2003) Modeling kinetic processes controlling hydrogen and acetate concentrations in an aquifer-derived microcosm. Environ. Sci. Technol. 37, 3910-3919.

[17] Conrad, R., and Wetter, B. (1990) Influence of temperature on energetics of hydogen metabolism in homoacetogenic, methanogenic, and other anaerobic bacteria. Arch. Microbiol. 155, 94-98.

[18] Sonne-Hansen, J., Westermann, P., and Ahring, B. K. (1999) Kinetics of sulfate and hydrogen uptake by the thermophilic sulfate-reducing bacteria *Thermodesulfobacterium* sp. strain JSP and *Thermodesulfovibrio* sp. strain R1Ha3. Appl. Environ. Microbiol. 65, 1304-1307.

[19] Lovely, D. R., and Goodwin, S. (1988) Hydrogen concentrations as an indicator of the predominant terminal electron-accepting reactions in aquatic sediments. Geochim. Cosmochim. Acta 52, 2993-3003.

[20] Conrad, R. (1994) Compensation concentration as critical variable for regulating the flux of trace gases between soil and atmosphere. Biogeochem. 27, 155-170.

[21] Jakobsen, R., Albrechtsen, H.-J., Rasmussen, M., Bay, H., Bjerg, P. L., and Christensen, T. H. (1998) $H_2$ concentrations in a landfill leachate plume (Grindsted, Denmark): *In situ* energetics of terminal electron acceptor processes. Environ. Sci. Technol. 32, 2142-2148.

[22] Hoehler, T. M., Alperin, M. J., Albert, D. B., and Martens, C. S. (1998) Thermodynamic control on hydrogen concentrations in anoxic sediments. Geochim. et Cosmochim. Acta 62, 1745-1756.

[23] Hoehler, T. M., Alperin, M. J., Albert, D. B., and Martens, C. S. (2001) Apparent minimum free energy requirements for methanogenic archaea and sulfate-

reducing bacteria in an anoxic marine sediment. FEMS Microbiol. Ecol. 38, 33-41.

[24] Häring, V., and Conrad, R. (1994a) Demonstration of two different $H_2$-oxidizing activities in soil using an $H_2$ consumption and tritium exchange assay. Biol. Fertil. Soils 17, 125-128.

[25] Häring, V., Kluber, D. and Conrad, R. (1994b) Localization of atmospheric $H_2$-oxidizing soil hydrogenases in different particle fractions of soil. Biol. Fertil. Soils 18, 109-114.

[26] Chapelle, F. H., Haack, S. K., Adriaens, P., Henry, M. A., and Bradley, P. M. (1996) Comparison of Eh and $H_2$ measruements for delineating redox processes in a contaminated aquifer. Environ. Sci. Technol. 30, 3565-3569.

[27] Stevens, T. O., and McKinley, J. P. (1995) Lithoautotrophic microbial ecosystems in deep basalt aquifers. Science 270, 450-454.

[28] Geig, L. M., Kolhatkar, R. V., McInerney, M. J., Tanner, R. S., Harris, S. H., Sublette, K.L., and Suflita, J.M. (1999) Intrinsic bioremediation of petroleum hydrocarbons in a gas condensate-contaminated aquifer. Environ. Sci. Technol. 33, 2550-2560.

[29] Harris S. H. , Ulrich G.A., Suflita J.M. (1999) Dominant terminal electron accepting processes occurring at a landfill leachate plume-impacted site as indicated by field and laboratory measurements. U.S. Geological Survey Water Resources Investigations Report 99-4018C, U.S. Geological Survey, West Trenton, NJ; 541-548.

[30] Stevens, T. O., and McKinley, J. P. (2000) Abiotic controls on $H_2$ production from basalt-water reactions and implications for aquifer biogeochemistry. Environ. Sci. Technol. 34, 826-831.

[31] Beeman, R. E, and Suflita, J. M. (1987) Microbial ecology of a shallow unconfined ground water aquifer polluted by municipal landfill leachate. Microb. Ecol. 14, 39-54.

[32] Cozzarelli, I. M., Suflita, J. M., Ulrich, G. A., Harris, S. H., Scholl, M. A., Schlottmann, J. L., and Christenson, S. (2000) Geochemical and microbiological methods for evaluating anaerobic processes in an aquifer contaminated by landfill leachate. Environ. Sci. Technol. 34, 4025-4033.

[33] LeBlanc, D.R.. (1984) Sewage plume in a sand and gravel aquifer, Cape Cod, Massachusetts, USGS Water Supply Paper 2218, US Government Printing Office, Washington, D.C.

[34] Smith, R.L., Harvey, R.W., and LeBlanc, D.R. (1991a) Importance of closely spaced vertical sampling in delineating chemical and microbiological gradients in groundwater studies, J. Contam. Hydrol. 7:285-300.

[35] Harvey, R.W., and Barber, L.B., II. (1992) Associations of free-living bacteria and dissolved organic compounds in a plume of contaminated groundwater, J. Contam. Hydrol. 9, 91-103.

[36] Smith, R.L., Howes, B.L., and Duff, J.H. (1991b) Denitrification in nitrate-contaminated groundwater: Occurrence in steep vertical geochemical gradients, Geochim. Cosmochim. Acta 55:1815-1825.

[37] Kent, D.B., Davis, J.A., Anderson, L.C.D., Rea, B.A., and Waite, T.D. (1994) Transport of chromium and selenium in the suboxic zone of a shallow aquifer: Influence of redox and adsorption reactions, Water Resour. Res. 30:1099-1114.

[38] Istok J.D., Humphrey M.D., Schroth M.H., Hyman M.R., O'Reilly K.T. (1997) Single-well "push-pull" tests for in situ determination of microbial activities, Groundwater 35:619-631.

[39] Chapelle, F.H., Vroblesky, D.A., Woodward, J.C., and Lovley, D.R. (1997) Practical considerations for measuring hydrogen concentrations in groundwater. Environ. Sci. Technol. 31, 2873-2877.

[40] Robinson, J. A. (1985) Determining microbial kinetic parameters using nonlinear regression analysis. Adv. Microb. Ecol. 8, 61-114.

[41] Goudar, C. T., and Devlin, J. F. (2001) Nonlinear estimation of microbial and enzyme kinetic parameters from progress curve data. Water Environ. Res. 73, 260-265.

[42] Nanny, M. A., and Ratasuk, N. (2002) Characterization and comparison of hydrophobic neutral and hydrophobic acid dissolved organic carbon isolated from three municipal landfill leachates. Water Res. 36, 1572-1584.

[43] Madsen, E. (1991) Determining *in situ* biodegradation. Environ. Sci. Technol. 25, 1663-1673.

[44] Smith, R. L., Garabedian, S. P., and Brooks, M. H. (1996) Comparison of dentitrification activity measurements in groundwater using cores and natural-gradient tracer tests. Environ. Sci. Technol. 30, 3448-3456.

[45] Madsen, E. (1998) Epistemology of Microbiology. Environ. Sci. Technol. 32, 429-439.

[46] Smith, R. L., Ceazan, M. L., and Brooks, M. H. (1994) Autotrophic, hydrogen-oxidizing, denitrifying bacteria in groundwater, potential agents for bioremediation of nitrate contamination. Appl. Environ. Microbiol. 60, 1949-1955.

[47] Stouthamer (1982) The bioenergetics of denitrification. Anton. van Leeuwen. 48, 545-553.

[48] Conrad, R. (1999) Contribution of hydrogen to methane production and control of hydrogen concentrations in methanogenic soils and sediments. FEMS Microbiol. Ecol. 28, 193-202.

[49] Schink, B. (1997) Energetics of syntrophic cooperation in methanogenic degradation. Microbiol. Mol. Biol. Rev. 61, 262-280.

[50] Zehnder, A. J. B., and Stumm, W. (1988) Geochemistry and biogeochemistry of anaerobic habitats, In: Biology of Anaerobic Microorganisms, (Zehnder, A. J. B., ed.), pp. 1-38. New York: John Wiley and Sons.

[51] Conrad, R., Bonjour, F., and Aragno, M. (1985) Aerobic and anaerobic microbial consumption of hydrogen in geothermal spring water. FEMS Microbiol. Lett. 29, 201-205.

[52] Elshahed, M. S., and McInerney, M. J. (2001) Benzoate fermentation by the anaerobic bacterium *Syntrophus aciditrophicus* in the absence of hydrogen-using microorganisms. Appl. Environ. Microbiol. 67, 5520-5525.

# Chapter 3

Examination of the rate, fate and threshold associated with hydrogen consumption by anaerobic bacteria: a basis for an amensalism between acetogens and methanogens

## Abstract

Hydrogen consumption kinetics and thresholds were examined in resting cultures of various hydrogenotrophs. The acetogens *Acetobacterium woodii, Eubacterium limosum* and strain SS1 whole cells exhibited apparent hydrogen $K_m$ values (4.6-5.0 μM) that were similar to the methanogen *Methanospirillum hungatei* JF1 (5.0 μM) but higher than that observed for *Desulfovibrio* G11 (1.1 μM). In addition, hydrogen threshold values (409-519 nM) were typically 100 to 500 times higher in acetogens, similar to previous findings. The threshold in the acetogens was not controlled by a thermodynamic equilibrium as the ΔG' values remained more negative than –68 kJ $mol^{-1}$ at the cessation of hydrogen consumption. Hydrogenase activity in cell free extracts of *A. woodii* did not exhibit a threshold and kinetic parameter estimates for hydrogen consumption were different than comparable measures in whole cells. Thus, a higher level of regulation likely exists in whole cells that is not evident in enzyme preparations. At high hydrogen concentrations, a model based on a two term Michaelis-Menten equation was used to predict hydrogen consumption by resting cocultures of *A. woodii* and *M. hungatei*. The model accurately predicted the rate of hydrogen oxidation but not its fate. The presence of the acetogen had a stimulatory effect on the rate of methane production by *M. hungatei* resulting in a greater than expected proportion of hydrogen

consumed by the latter organism. These results suggest that cell-cell interactions influence the fate of hydrogen in defined cocultures and environmental fate processes are likely to be at least as complex.

## Introduction

Hydrogen is a central intermediate that is both produced and consumed during the oxidation of organic matter in anaerobic environments. In the absence of alternate electron acceptors, hydrogen oxidation must occur via carbon dioxide reduction, a process catalyzed by acetogenic bacteria and methanogenic archaea. It is therefore reasonable to expect intense competition between these organisms for hydrogen in electron acceptor limited environments. In non-marine environments, methanogenesis is typically the primary electron sink based in part, on the greater energy yield of methane production relative to acetogenesis [12] as well as the ability of methanogens to consume hydrogen below the threshold exhibited by acetogenic bacteria [8,9,48]. Nevertheless, acetogens successfully coexist with methanogens, often in comparable cell numbers in many anaerobic ecosystems [26,27,30,51] and even dominate electron flow in the gastrointestinal tract of many eucaryotic organisms [2,5,37,55]. While the ability of acetogens to grow mixotrophically is known [5,25,31], and yields more energy per mol hydrogen consumed than autotrophy, defined coculture studies give little indication that this mode of metabolism provides acetogens with a distinct advantage over other hydrogen consuming cells [4,29,42]. Other studies have suggested that acidic, low temperature, and carbon-limited environments favor acetogenesis over other microbial processes [7,23,27,41,43]. While these studies have advanced the understanding of the preferred modes of existence of acetogens and methanogens, we decided to examine the

kinetics of competition for hydrogen by these organisms with particular attention to the reasons for the relatively high thresholds exhibited by acetogenic bacteria.

Competition for hydrogen by cocultures can be described by the sum of the consumption kinetics [34,45] exhibited by the organisms as well as the respective substrate thresholds [28]. Once the substrate is depleted below an organism's threshold, the bacterium with the lower threshold dominates competition [35]. Hydrogen consumption in cultures of two competing microorganisms can be approximated using a two-term Michaelis-Menten equation containing the $K_m$ and $V_{max}$ exhibited by both species [34]. This model accurately described hydrogen consumption and fate in defined mixtures of sulfate reducing and methanogenic bacteria [45]. At saturating substrate concentrations, organisms exhibiting a higher $V_{max}$ are expected to have an advantage [27] while the ratio $V_{max}/K_m$ is a better assessment of competitive fitness when the substrate concentration is much lower [18]. The lower $K_m$, higher $V_{max}$, and lower threshold exhibited by sulfate reducing bacteria have been used to explain their ability to outcompete methanogens for hydrogen [8,9,28,35,45,49]. Recently, these same parameters were used to predict the outcome of hydrogen competition between psychrophilic acetogens and methanogens as a function of temperature and hydrogen concentration [27].

We measured the hydrogen consumption kinetic parameters and thresholds for a number of anaerobes and used these values to model hydrogen competition between *Acetobacterium woodii* and *Methanospirillum hungatei* JF1. We then compared model predictions to experimental findings. Similar to results in a previous study [45], a two-term Michaelis-Menten equation accurately depicted hydrogen consumption by

nongrowing cocultures at saturating hydrogen concentration. However, the actual fate of hydrogen was consistently in favor of the methanogen, despite model predictions of an equal partitioning of the electron donor between the two bacteria. That is, the presence of whole acetogen cells, cell extracts, or membrane preparations stimulated hydrogen consumption by the methanogen, but heat-inctivated preparations did not. Thus, at high hydrogen concentration there is likely an interkingdom amensalistic interaction between the organisms that influences the outcome of competition.

At low hydrogen concentrations, the threshold of the acetogens *A. woodii, Eubacterium limosum,* and strain SS1 were 2-3 orders of magnitude higher than the values exhibited by *M. hungatei* and *Desulfovibrio* G11, a finding consistent with previous reports [42]. Closer examination of the factors controlling hydrogen threshold in *A. woodii* revealed that they were not due to an analytical insufficiency, a thermodynamic equilibrium, a nutritional limitation, inhibition by endproducts or moribund cells, or the simple balance between production and consumption. These results indicate that interactions besides simple competition and thresholds influence the disposition of hydrogen in anaerobic environments.

## Materials and Methods

**Organisms, and growth conditions.** Cultures of *Acetobacterium woodii* (ATCC 29683), *Eubacterium limosum* (ATCC 8486) and SS1 [31] were grown in a defined medium [52] with syringate (8 mM) as the sole source of organic carbon under a $H_2/CO_2$ (4:1, 202 kPa) headspace. For heterotrophic growth, fructose was used in place of syringate and the headspace was $N_2/CO_2$ (4:1, 101 kPa). *Methanospirillum hungatei* JF-1 was grown in a defined medium [40] containing 10mM acetate and a $H_2/CO_2$ (4:1, 202 kPa) headspace.

*Methanospirillum hungatei* was chosen for use in competition experiments with *A. woodii* because this methanogen does not make methane from acetate, which would complicate hydrogen fate determinations. *Desulfovibrio* G11 was grown with 0.3% lactate in the medium of [40] with a $N_2/CO_2$ (4:1, 101 kPa) headspace. All cultures were grown in 2 L flasks containing 1 L medium at 35°C on a rotary shaker.

**Resting cell suspensions.** Cells were harvested anaerobically during the log phase of growth ($A_{600}$=0.1 to 0.3) by centrifugation (15,000 x g for 15 min at 25°C) and washed in 400 ml anaerobic HEPES buffer (10 mM N-2-hydroxyethylpiperazine-N'-2-ethane-sulfonic acid; pH 7.2), containing 40 mM $NaHCO_3$, 0.4g/L $MgCl_2$, 0.15g/L $CaCl_2$. The final cell pellet was resuspended in 10-20 ml of the same buffer and used for hydrogen consumption assays.

**Kinetic parameter and threshold determinations.** The kinetic parameters $K_m$ and $V_{max}$ as well as hydrogen thresholds were determined from hydrogen consumption progress curves [16]. Washed cells were placed in 2L flasks containing 0.5 L of the wash buffer and a $N_2/CO_2$ (4:1, 101 kPa) headspace. Syringate (8 mM) and sulfate (20 mM) were included in experiments with acetogens and *Desulfovibrio* G11, respectively. The flasks were continuously stirred and biomass levels were adjusted to avoid hydrogen mass transfer limitiations. Progress curve assays were started by injecting hydrogen (70 ml) into the flasks to an intial dissolved concentration of about 30 μM (~4 kPa). Threshold values were also determined in resting cell suspensions after hydrogen decay ceased. The viability of cell preparations was confirmed by reamending the flasks with hydrogen and monitoring substrate loss again. In experiments where the threshold level was examined as a function of endproduct formation, either sodium acetate or sodium gallate was

included in the buffer in concentrations up to 100 mM.

Whole-cell protein was determined by the bicinchoninic acid assay (Pierce, Rockford, IL) with bovine serum albumin as the standard. Samples of whole cells and standards were boiled for 20 min in 0.1 N NaoH to lyse the cells prior to protein determination.

**Energetic calculations.** Once the hydrogen threshold was reached, the pH, temperature, and concentrations of reactants and products were determined. The available Gibb's free energy ($\Delta G'$) for hydrogen oxidation under nonstandard conditions was determined from measured concentrations according to the following equation:

$$\Delta G' = \Delta G^{\circ\prime} + RT \ln \frac{[C_7H_4O_4(OCH_3)^-][CH_3COO^-][H_2O]}{[C_7H_3O_3(OCH_3)_2^-][HCO_3^-][H_2]}$$

where $[H_2]$ is the hydrogen partial pressure (in atmospheres), R is the gas constant (8.31 J $mol^{-1}$ $K^{-1}$), T is the temperature (°K) and the values in brackets are the molar concentrations of reactants and products. The standard free energy change ($\Delta G^{\circ\prime}$) for syringate reduction with hydrogen was determined from the data in [24,31].

**Hydrogenase assays.** Hydrogenase activity was examined in cell-free extracts of *A. woodii* grown mixotrophically with $H_2$/syringate or fermentatively with fructose. Washed cells were lysed via French pressure under strict anaerobic conditions. The crude lysate was centrifuged (27,200 x g for 30 min at 4°C) to remove unbroken cells and larger cell debris. The supernatant was used as a crude cell extract in hydrogenase assays. Hydrogenase kinetics were determined from substrate vs. velocity assays in 80 ml serum vials containing 20 ml of the Tris buffer described by [34], methyl viologen (10 mM) as an artificial electron acceptor, and hydrogen (0.2-3.0 ml) as the substrate. Bottles

were equilibrated to 30°C prior to addition of the extract (1.5-2.5 ml) to start the reaction. Initial rates were estimated when less than 7% of the hydrogen pool had been oxidized (<3 min). Kinetic parameters for hydrogenase were estimated via nonlinear regression analysis [46].

**Hydrogen competition experiments.** Hydrogen consumption by a non-growing coculture was described by a two-term Michaelis-Menten equation having the form:

$$-dS/dt = V_{max1}S/(K_{m1} + S) + V_{max2}S/(K_{m2} + S)$$

where $V_{max1}$ and $V_{max2}$ are the maximum substrate consumption rates and $K_{m1}$ and $K_{m2}$ are the half-saturation constants for the competing organisms [34]. Hydrogen kinetic parameters for individual *A. woodii* and *M. hungatei* preparations were used to simulate hydrogen consumption and fate by defined cocultures [16]. Most competition experiments contained *A. woodii* at a 1.4-fold biomass advantage (based on total protein) because simulations indicated this would result in a nearly equal partitioning of hydrogen between the two organisms. The experimental procedure used for the coculture competition assays was the same as that used for the kinetic parameter estimation. Competiton experiments consisted of duplicate coculture incubations as well as control monoculture preparations of *A. woodii* or *M. hungatei* at the same cell density. The fate of hydrogen consumed by the methanogen and acetogen was determined by measuring methane production and syringate consumption, respectively.

**Hydrogen, methane and syringate determination.** Hydrogen and methane were measured from headspace samples by gas chromatography using instruments equipped with a mercury vapor [39] or flame ionization detector [1], respectively. Culture fluids were centrifuged (15,800 x g for 4 min) prior to analysis by high-performance liquid

chromatography for aromatic compounds [10] while acetate concentrations were determined by gas chromatography [21].

**Influence of *A. woodii* on *M. hungatei*.** *Acetobacterium woodii* preparations were examined for the ability to stimulate hydrogen consumption by resting cells of *M. hungatei*. Assays were done in 160 ml serum bottles containing 50ml of the anaerobic buffer and 10 ml hydrogen as the substrate. Whole cells and crude cell extracts of *A. woodii* were incubated with a washed preparation of *M. hungatei*. Crude extracts were ultracentrifuged (100,000 x g for 60 min at 4°C) to remove the membrane fraction. The pellet and supernatant from the ultracentrifugation were used as membrane and cell-free extract preparations, respectively. Spent buffer (0.5 L) was obtained by allowing *A. woodii* (40-50 μg protein $ml^{-1}$) to consume 2 mmol hydrogen over 6 h and filter-sterilizing the resulting preparation and using it to suspend resting cells of *M. hungatei*. Heat-inactivated *A. woodii* preparations were made by placing washed cells in a boiling water bath for 15 min. Hydrogen consumption and methane production were monitored over 3 h of incubation. Hydrogen consumption by *M. hungatei* was determined based on methane production rates assuming 4 mol hydrogen consumed per mol methane produced.

## Results

**Kinetics of hydrogen consumption in whole cells.** Hydrogen depletion progress curves by resting cell suspensions were used to estimate $K_m$, and $V_{max}$ for the selected anaerobes (Table 1). The three acetogens examined in this study displayed similar $K_m$ values for hydrogen of about 4.6-5.0 μM. These values were comparable to the $K_m$ estimate for *M. hungatei* as well as for another acetogen, *Sporomusa termitida* [4].

*Desulfovibrio* G11 exhibited a $K_m$ that was significantly lower at 1.1 μM, a value that is identical to the estimate reported by [45] for the same organism. The mean $V_{max}$ estimates were generally lower in the acetogens than the other organisms. Further, the first order decay constant was determined from hydrogen depletion data for each hydrogenotroph (Table 1). First order hydrogen consumption was statistically slower in the acetogens. Similar values were obtained when the same parameter was calculated by the ratio of $V_{max}/K_m$ (data not shown).

| Organism | $V_{max}$[a] | $K_m$ (μM) | $k_1$[b] ($min^{-1}$*mg $protein^{-1}$) | Threshold (nM) |
|---|---|---|---|---|
| *A. woodii* | 970 ± 87 | 4.6 ± 0.2 | 0.085 ± 0.008 | 409 ± 16 |
| *E. limosum* | 259 ± 18 | 4.6 ± 0.6 | 0.021 ± 0.004 | 457 ± 30 |
| SS1 | 966 ± 39 | 5.0 ± 0.4 | 0.072 ± 0.010 | 519 ± 62 |
| *Sporomusa termitida*[c] | 380 | 6.0 | ND[d] | 640 |
| *M. hungatei* JF1 | 1350 ± 63 | 5.0 ± 0.5 | 0.110 ± 0.009 | 5.8 ± 0.4 |
| *Desulfovibrio* G11 | 1128 ± 27 | 1.1 ± 0.2 | 0.390 ± 0.041 | 0.9 ± 0.4 |

[a]units are nmole*$min^{-1}$*mg $protein^{-1}$
[b]determined from slope of ln $H_2$ vs. time
[c]from [3,4]
[d]ND, not determined

Table 1. Hydrogen kinetic and threshold estimates in whole cells and cell free extracts of selected hydrogenotrophs.

Hydrogen thresholds in pure cultures [9] as well as mixed assemblages of microorganisms [19,20,22] are postulated as being the result of a thermodynamic limitation. Factors that affect the Gibbs free energy from hydrogen oxidation should therefore influence the hydrogen threshold. However, *in situ* $\Delta G'$ values determined once the cultures reached the hydrogen threshold revealed an available energy yield of at least –68 kJ/mol hydrogen (Table 2). In addition, inhibition by the endproducts acetate and methyl-gallate cannot explain these results as the threshold values were not significantly different at concentrations from 0-100 mM endproduct (Figure 1). We questioned whether the viability of the cells was the reason for cessation of hydrogen consumption in these incubations. However, consumption resumed without a lag upon hydrogen reamendment and the same threshold value was attained after each addition of substrate (Figure 2). Toxicity from the undissociated form of acetate could not explain the threshold in *A. woodii*, as concentrations of this form of acetate ranged from 9.8 to 476 μM with no apparent affect on hydrogen threshold (Table 2). Finally, the threshold was not due to an equilibrium in hydrogen flux because no hydrogen production or consumption was observed in washed cells of *A. woodii* when initial hydrogen concentrations were below the threshold level (Figure 2). However, consumption occurred when hydrogen was added to the flask and resulted in a threshold similar to other incubations of *A. woodii.*

| $T_0$ acetate (mM) | $T_f$ undissociated acetic acid (μM)[a] | $T_f$ *in situ* ΔG' (kJ/mol $H_2$)[b] | $T_f$ *in situ* ΔG' (kJ/mol $H_2$)[c] |
|---|---|---|---|
| 0 | 9.8 | -80.1±0.0 | -7.3±0.1 |
| 10 | 56.1 | -74.6±0.1 | -5.9±0.1 |
| 20 | 101.5 | -73.0±0.1 | -5.4±0.1 |
| 50 | 242.8 | -70.0±0.4 | -4.6±0.2 |
| 100 | 476.2 | -68.5±0.2 | -4.3±0.0 |

[a]parameters used in these calculations were as follows: pH=7.1, pKa=4.76, and time final ($T_f$) acetate concentrations, which were typically 2 mM higher than time zero ($T_0$) concentrations.
[b,c]calculated from measured concentrations of reactants and products according to the following reaction stoichiometry:
[b]$C_7H_3O_3(OCH_3)_2^- + HCO_3^- + H_2 \leftrightarrow C_7H_4O_4(OCH_3^-) + CH_3COO^- + H_2O$
[c]$4H_2 + 2HCO_3^- + H^+ \leftrightarrow CH_3COO^- + 4H_2O$
from [30], and $\Delta Gf^o$ values in [23].

Table 2. Time final ($T_f$) determinations of undissociated acetic acid concentrations and in situ ΔG' values calculated as a function of acetate concentrations once resting cells of *A. woodii* reached the hydrogen threshold.

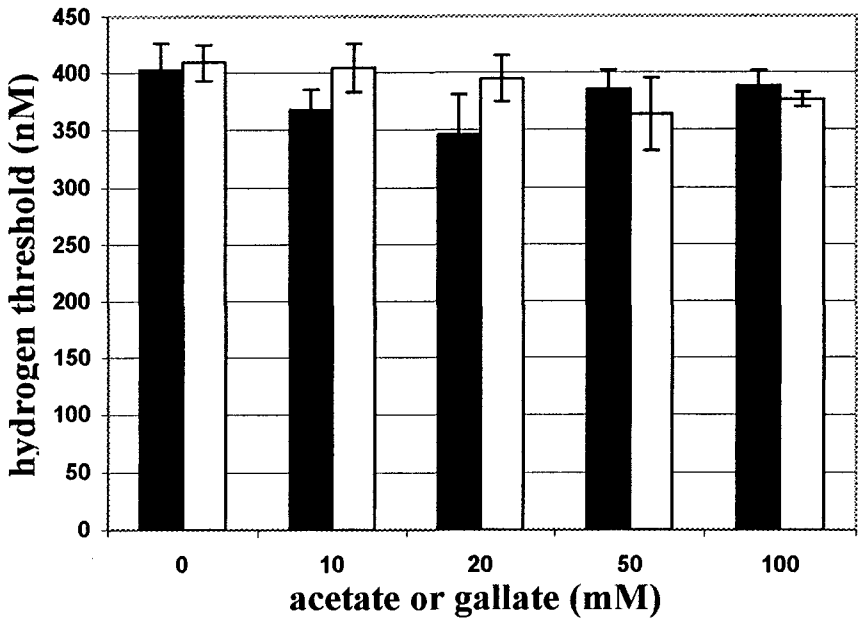


Figure 1. Hydrogen thresholds in resting cells of *A. woodii* as a function of gallate (solid bars) and acetate (open bars) concentration[a].

[a]Mean of triplicate determinations +/- std. dev.

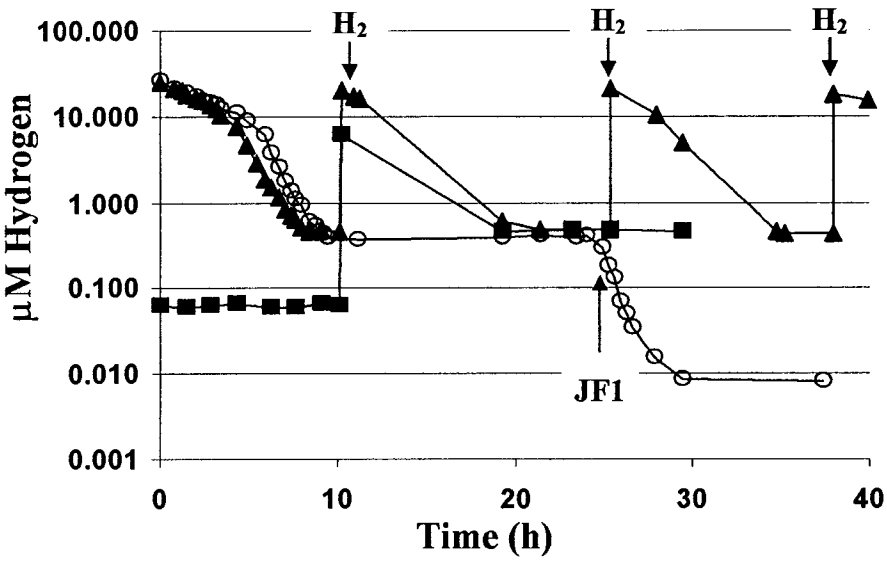


Figure 2. Hydrogen consumption and resulting thresholds in resting cells of *A. woodii* receiving hydrogen reamendment(▲ and ■) or the addition of a washed preparation of *M. hungatei* JF1 (○).

The bioavailability of the hydrogen was also not a factor in the threshold determinations since the addition of *M. hungatei* cells resulted in immediate hydrogen consumption to a rather typical threshold for methanogens of about 6 nM [35], (Figure 2).

**Hydrogenase kinetics.** To determine if the threshold was an inherent property of hydrogenases, hydrogen oxidation in cell free extracts of fructose- and $H_2$/syringate-grown *A. woodii* were estimated by substrate vs. velocity assays (Figure 3). Typically, hydrogenase assays involve measuring the reduction of an artificial electron acceptor (usually a dye). Estimates of $V_{max}$ can be made using these assays but hydrogen $K_m$ and threshold estimates are possible only if the concentration of hydrogen is followed over time. Almost all (>95%) of the hydrogenase activity was located in the soluble fraction of the crude extract (data not shown). Hydrogen threshold determinations were not possible with the cell free extracts because at low substrate concentrations (<1 μM dissolved hydrogen), a net production of hydrogen occurred (data not shown). The $K_m$ estimates for hydrogenase were similar regardless of the substrate on which the cells were grown but the $V_{max}$ estimate was about two times higher when cells were grown with $H_2$/syringate (Figure 3).

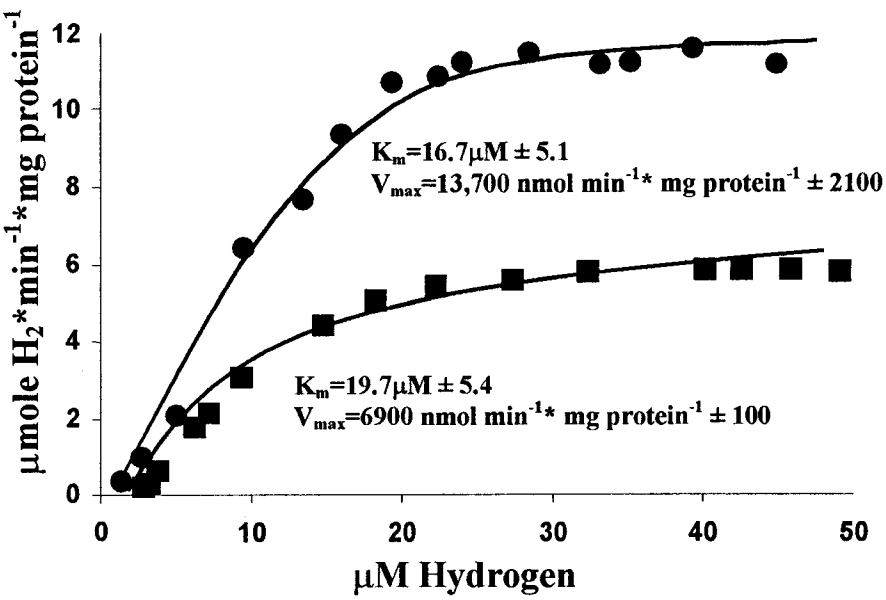


Figure 3. Hydrogen oxidation rate as a function of dissolved hydrogen concentration in cell free extracts of $H_2$/syringate-grown (●) and fructose-grown (■) *A. woodii*.

**Hydrogen competition experiments.** Hydrogen competition by cocultures of *A. woodii* and *M. hungatei* was simulated based on the consumption kinetics exhibited by the individual cultures. Given the relative differences in kinetic parameters, the two-term Michaelis-Menten model predicted roughly equal partitioning of hydrogen between the two bacteria if the acetogen biomass was slightly elevated relative to that of the methanogen. Saturating levels of hydrogen were consumed in precisely the manner predicted by the model (Figure 4A). The two organisms both consumed hydrogen as confirmed by the production of methane and the consumption of syringate. However, control incubations of *M. hungatei* at the same cell density did not consume hydrogen as expected (Figure 4B). In fact, only a low rate of hydrogen consumption (<20% of $V_{max}$) was detected in monocultures of *M. hungatei* at this biomass level. In addition, the methanogen consistently dominated the competition with the acetogen by consuming at least 61% of the available hydrogen (Table 3). When the organisms were included at identical biomass levels, the methanogen consumed 73 to 81% of the hydrogen even though the model predicted that the methanogen would only consume 57% of the substrate (data not shown). Therefore, the model correctly predicted the rate, but not the fate of hydrogen in these experiments.

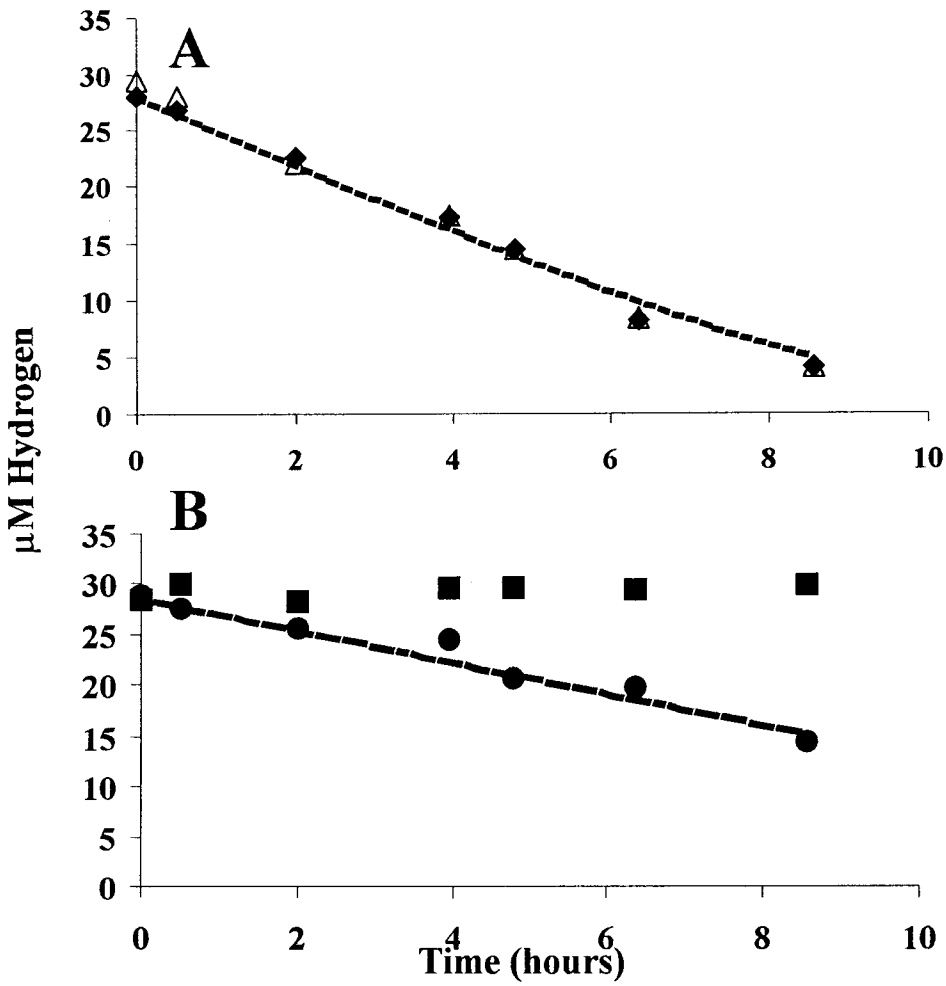


Figure 4. Hydrogen decay in competition experiments. A. Replicate coculture incubations containing *A. woodii* and *M. hungatei* (Δ and ♦) and model prediction (–). B. Monococulture incubations containing *A. woodii* (●) and *M. hungatei* (■) and model prediction (–). *Acetobacterium woodii* and *M. hungatei* were inoculated at a cell densities of 33 and 24 µg protein $ml^{-1}$, respectively.

| Incubation[a] | mmol $H_2$ consumed | mmoles $H_2$ consumed by *M. hungatei*[b] | mmoles $H_2$ consmed by *A. woodii*[c] | $H_2$ recovery (%) |
|---|---|---|---|---|
| Coculture A | 2.54 | 1.68 (66%) | 0.79 (31%) | 97 |
| Coculture B | 2.62 | 1.71 (65%) | 1.16 (44%) | 109 |
| Coculture C | 2.50 | 1.53(61%) | 1.00 (40%) | 101 |
| *A. woodii* | 1.69 | ND[d] | 1.64 (97%) | 97 |
| *M. hungatei* | ND | — | — | — |

[a]Cocultures contained *M. hungatei* and *A. woodii* at 24 and 34 μg protein $ml^{-1}$, respectively. Monocultures contained the same biomass level of each organism as in the cocultures.
[b]Assuming 4mol $H_2$ consumed per mol $CH_4$ produced
[c]Assuming 1mol $H_2$ consumed per mol syringate consumed
[d]ND, not detected

Table 3. Fate of hydrogen in a typical competition experiment between resting cells of *A. woodii* and *M. hungatei*.

We hypothesized that the low rate of hydrogen consumption by *M. hungatei* in control incubations (Figure 4B) was the result of a relatively low cell density. To test this hypothesis, we assessed hydrogen consumption by *M. hungatei* as a function of cell density (Figure 5). Hydrogen consumption rates were not proportional to *M. hungatei* biomass levels in cell suspensions containing less than about 25 μg protein $ml^{-1}$, which was similar to the cell density used in the control incubations. However, at cell densities of about 35-65 μg protein $ml^{-1}$, the rate was similar to the $V_{max}$ determined for this organism. Above this range, hydrogen consumption appeared to be mass transfer limited. Thus, the biomass level in *M. hungatei* controls was below the critical concentration necessary for hydrogen consumption.

Although methanogen biomass concentrations in the controls limited hydrogen consumption, the same cell density of *M. hungatei* in coculture with *A. woodii* always resulted in methane production (Table 2). Furthermore, the methanogen consistently consumed about two-thirds of the available hydrogen in cocultures.

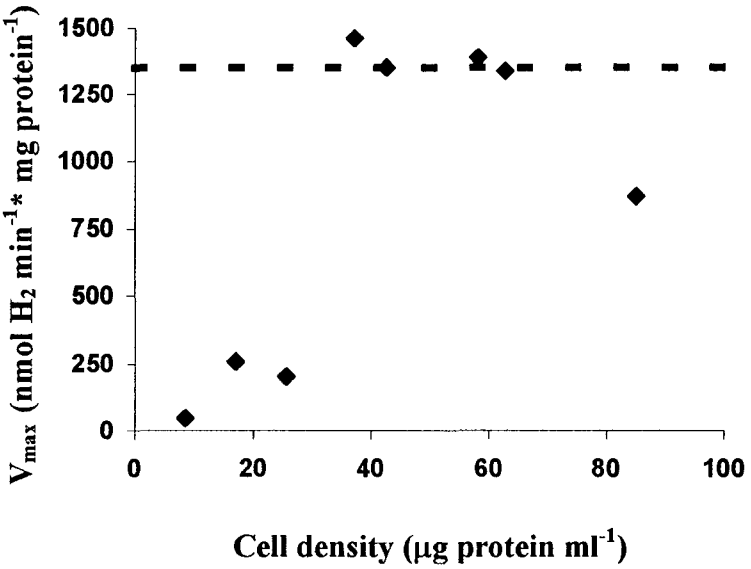


Figure 5. Hydrogen $V_{max}$ estimates in *M. hungatei* as a function of cell density.

The fate of hydrogen in the competition experiments suggested that the presence of the acetogen exerted a positive influence on the hydrogen consuming ability of the methanogen. We hypothesized that higher cell densities in the coculture provided a more reducing environment, thereby protecting *M. hungatei* from traces of oxygen that might have in advertently occurred during the assay. However, increased levels of cysteine-sulfide reductant had little impact on the rate of hydrogen consumption by the methanogen (Table 5). Further, the positive impact of *A. woodii* cells was proportional to the amount of the acetogen in the incubation (Table 5). However, this effect was abolished if *A. woodii* whole cells were boiled. Similarly, no impact was noted if methanogen cells were suspended in spent, filter-sterilized buffer from an acetogenic incubation. Stimulation in hydrogen consumption by *M. hungatei* was noted when cell extracts or membrane fractions of *A. woodii* were included in resting cell incubations of the methanogen. Comparable additions of *Desulfovibrio* G11 had only a slight stimulatory effect while boiled preparations of either the sulfate reducer or the methanogen had a pronounced negative impact on methanogenesis.

| Treatment | relative $H_2$ consumption rate[a] |
|---|---|
| [b]*M. hungatei* JF1 | 1.00 |
| 2X cysteine-sulfide | 1.05 |
| 5X cysteine-sulfide | 1.27 |
| live *A. woodii* (1X)[c] | 6.15 |
| live *A. woodii* (2X) | 7.72 |
| live *A. woodii* (4X) | 10.79 |
| live *A. woodii* (8X) | 13.30 |
| *A. woodii* crude cell extract (4X) | 34.92 |
| *A. woodii* cell-free extract (4X) | 36.63 |
| *A. woodii* membrane preparation (4X) | 20.30 |
| spent *A. woodii* buffer | 1.04 |
| boiled *A. woodii* (1X) | 1.14 |
| boiled *A. woodii* (2X) | 1.08 |
| live *Desulfovibrio* G11 (1X) | 1.96 |
| boiled *Desulfovibrio* G11 (1X) | 0.62 |
| boiled *M. hungatei* JF1 (1X) | 0.08 |

[a]Mean of duplicates; calculated from $CH_4$ production rate over 3 h incubation.
[b]*M. hungatei* was inoculated at a rate-limiting cell density (25μg protein $ml^{-1}$)
[c]Values in parentheses indicate protein concentration of the treatment relative to that of *M. hungatei.*

Table 4. Hydrogen consumption rate by *M. hungatei* as a function of various amendments.

## Discussion

The $V_{max}$ exhibited by the acetogens are lower than those observed for *M. hungatei* and *Desulfovibrio* G11, suggesting that at equivalent biomass, the acetogens would not compete well at high hydrogen concentrations. In an earlier study, acetogens demonstrated a higher $V_{max}$ relative to methanogens isolated from the same low temperature environment [27]. High concentrations of hydrogen may favor acetogenesis over methanogenesis in low temperature environments.

The $K_m$ estimates for the acetogens were similar to those exhibited by *M. hungatei* as well as other methanogens (Table 1; [45]), but first order decay constants were relatively low for the acetogens (Table 1), suggesting these organisms would be less competitive at low hydrogen levels. Furthermore, the high thresholds exhibited by the acetogens indicates they would stop consuming hydrogen at concentrations where *M. hungatei* would continue to metabolize.

Hydrogen thresholds measured in pure cultures of acetogens are typically 100 times higher than for other hydrogen consuming microorganisms [4,9,29,35,42], an observation that has been used to explain the apparent inability of acetogens to compete for trace concentrations of hydrogen. We investigated if the threshold in *A. woodii* was simply due to a loss of activity or a nutritional insufficiency. If true, then resting cells of *A. woodii* should not consume hydrogen upon reamendment, but metabolism repeatedly resumed without a lag and reached the same threshold (Figure 2). We further hypothesized that the hydrogen threshold could be due to endproduct inhibition, either by the accumulation of acetate, methyl gallate or the undissociated form of acetate. To test this, we measured hydrogen thresholds in the presence of up to 100 mM acetate or methyl

gallate. High concentrations these endproducts had no effect on the hydrogen threshold (Figure 1). Moreover, since *A. woodii* consumed hydrogen to the same threshold regardless of the acetate concentration, toxicity from undissociated acetic acid is not responsible for controlling hydrogen thresholds. On the contrary, undissociated acetic acid concentrations reached almost 500 μM without any noticeable affect on the hydrogen threshold (Table 2). In contrast, the methanogenic fermentation of acetate by *Methanosarcina barkeri* was inhibited by only 4-7 μM undissociated acetic acid [13]. Thus, hydrogen thresholds in acetogens appear insensitive to both ionized and undissociated forms of acetic acid. Alternatively, the observation of hydrogen thresholds in pure cultures [9] as well as mixed assemblages of bacteria [20] have been theorized as a thermodynamic limitation. In autotrophically-metabolizing acetogens, the hydrogen threshold was thought to result from a minimum energy requirement of –5 to –7 kJ $mol^{-1}$ required for hydrogen consumption [27,48]. Hydrogen oxidation coupled to the reductive O-demethylation of syringate yields more energy per mol hydrogen than autotrophic metabolism [32]. Thus, if the hydrogen threshold in *A. woodii* is controlled by the thermodynamics of the hydrogen consuming reaction, then the increased energy yield due to the presence of syringate should result in a decreased threshold. We measured hydrogen thresholds in resting cells of *A. woodii* in the presence of syringate and calculated the *in situ* $\Delta G'$ to investigate the energy available when hydrogen consumption stopped. Resting cells of *A. woodii* consumed hydrogen to a threshold that was similar to previous measures for this organism [42,48] as well as other acetogens [4,27]. However, the reaction was far from thermodynamic equilibrium when the threshold was attained (Table 2). Thus, hydrogen thresholds measured in this study

cannot be explained solely on the basis of a thermodynamic limitation. However, when thermodynamic calculations were done without considering the influence of syringate or its endproduct, methyl gallate (Table2), the resulting $\Delta G'$ values were similar to the range (–5 to –7 kJ $mol^{-1}$ hydrogen) found in previous studies [27,48] although less negative than that observed in sediments where acetogenesis was dominant (-18 kJ $mol^{-1}$ hydrogen) [19]. As suggested by [29], the energy yield associated with hydrogen oxidation may be isolated from the energy yield that is released by the reduction of the methyl group of syringate such that the increased thermodynamic yield from O-demethylation is uncoupled from the overall reaction. Thus, hydrogen oxidation, the less energetically favorable of the two processes, may not occur at low hydrogen concentrations despite an apparently large thermodynamic disequilibrium because of the uncoupled nature of the overall reaction.

We questioned if *A. woodii* hydrogenases exhibited a hydrogen threshold. However, even crude preparations with hydrogenase activity did not exhibit a threshold because these preparations exhibited a net production of hydrogen at low (<1 μM) concentrations. Indeed, hydrogenases are known to be reversible enzymes and are often characterized according to the kinetics of hydrogen production [15]. The apparent $K_m$ for hydrogenase in *A. woodii* (18 μM) is about four times greater than that exhibited by the whole cell (5 μM; Table 1). Thus, hydrogen consumption kinetics by whole cells of this organism may reflect a higher level of regulation not observed in hydrogenase preparations. For comparison, the $K_m$ for hydrogen in *A. woodii* hydrogenase was similar to that observed for *Alcaligenes eutrophus* (37 μM) and *Methanobacterium thermoautotrophicum* (10 μM) [33,47].

Hydrogenase preparations exhibited a higher $V_{max}$ when *A. woodii* was grown on $H_2$/syringate relative to fructose-grown cells. These results are analogous to those obtained with another acetogen, *Sporomusa termitida*, in which whole cells pregrown on various organic substrates demonstrated hydrogen dependent acetogenesis but at rates slower (5-85%) than those observed in cells pregrown on $H_2/CO_2$ [4]. One explanation for these rate differences is the production of different hydrogenases. However, it is also possible that *A. woodii* and *S. termitida* produce the same enzymes when growing with different substrates, but simply make more hydrogenase when grown on hydrogen. This explanation is consistent with our findings of a similar $K_m$ when either $H_2$/syringate or fructose was used as growth substrate for *A. woodii* but a higher $V_{max}$ estimate for the former condition (Table 2).

The intracellular location of hydrogenase in these microorganisms may play a role in the outcome of competition. Hydrogenase in *A. woodii* appears to be soluble [43; this study] and therefore located in the periplasm, cytoplasm, or both. Since *A. woodii* is gram positive, it seems likely that the the enzyme is likely located in the cytoplasm. In contrast, hydrogenase from *M. hungatei* is found in the cytoplasmic membrane [50]. If hydrogenase in *A. woodii* is restricted to the cytoplasm, hydrogen must diffuse or be transported from the environment to the interior of the cell before it can be oxidized, whereas this would not be necessary in other hydrogenotrophs expressing periplasmic or membrane-bound hydrogenases. Periplasmic hydrogenases are a universal feature of the genus *Desulfovibrio* [53] and many sulfate reducing bacteria express this enzyme in both the periplasm and cytoplasmic membrane [6,38]. The localization of hydrogenase in the cytoplasm of *A. woodii* may serve as a mechanism regulating consumption at low

hydrogen concentrations, thereby influencing kinetics, thresholds, and ultimately the interaction with other organisms.

Although the two-term Michaelis-Menten model accurately described hydrogen decay by cocultures (Figure 3A) we questioned why the methanogen consumed hydrogen at a relatively slow rate in the controls (Figure 3B). Control incubations contained the respective organisms at a low cell density (~ 30 μg protein $ml^{-1}$) in order to avoid mass transfer limitation when the same cell densities were combined in coculture. Thus, we suspected the low rate of hydrogen consumption by *M. hungatei* in controls was due to a cell density limitation. A minimum cell density of at least 35 μg protein $ml^{-1}$ was necessary to produce consistent $V_{max}$ estimates for this organism (Figure 5). Lower cell densities supported rates that were less than $V_{max}$ while higher densities were likely mass transfer limited. Thus, the rate of hydrogen consumption in *M. hungatei* controls was slower than expected because of the low cell concentrations in those incubations.

However, the same cell density of *M. hungatei* that supported only slow hydrogen decay in controls readily consumed hydrogen (as evidenced by methane production) in coculture with *A. woodii* (data not shown). Moreover, the methanogen consistently dominated hydrogen competition in coculture with the acetogen (Table 3). Thus, the rate of hydrogen consumption by the cocultures was accurately predicted by the model, but the fate of hydrogen was not. Clearly, some interaction other than simple competition influenced the fate of hydrogen even in defined cocultures.

The rate of hydrogen consumption by *M. hungatei* was proportional to the amount of *A. woodii* in the coculture (Table 5), indicating the presence of the acetogen was responsible for the observed increase in methanogenesis. Apparently, the acetogen

supplied some factor that stimulated hydrogen consumption by *M. hungatei* influencing the fate of hydrogen in favor of the latter organism at the expense of the former. Rather than competition, this interaction is best described as an amensalism. Interestingly, a newly isolated *Methanobacterium*-like organism catalyzes the oxidation of metallic iron surfaces during methanogenesis [11]. If the ability to remove electrons from various surfaces is widespread among methanogenic *Archaea*, then *M. hungatei* may be able to use the acetogen cell as a surface from which to scavenge electrons for methane production. This ability would help explain the stimulation of methanogenesis we observe when *M. hungatei* is incubated in the presence of whole cells of *A. woodii*.

Although we did not characterize the stimulating factor to a great extent, the effect appeared to be heat-labile since the stimulation was eliminated by boiling preparations of *A. woodii* prior to adding them to *M. hungatei* resting cells. The presence of *Desulfovibrio* G11 stimulated hydrogen consumption in the methanogen as well, although to a lesser degree. Thus, different combinations of organisms may exhibit a similar interaction. Extracellular signal molecules play a prominent role in cell-cell communication although most of these molecules, such as homoserine lactones are confined to certain bacterial species [14]. Further, a recent study has shown structurally and functionally homologous unsaturated fatty acids responsible for regulating pathogenecity are produced as signal molecules by several bacterial species as well as *Candida albicans* [54]. These compounds may serve as diffusible signals for bacterial and fungal cell-cell communication. These findings suggest that cross-kingdom communication, as would be the case between *A. woodii* and *M. hungatei*, may be a more common phenomenon than currently appreciated. Nevertheless, we suspect a cell-

associated mechanism rather than a diffusible molecule is responsible for the results in the current study since filter-sterilized buffer from *A. woodii* incubations was not stimulatory (Table 5).

These results indicate that factors in addition to kinetics and thresholds exhibited by pure cultures can affect hydrogen consumption rates as well as the fate of this electron donor. If these factors exert an influence in resting cell incubations, less defined systems would be expected to exhibit features that are at least as complex. The finding that *A. woodii* effected a stimulation in methanogenesis by *M. hungatei* was unexpected and contrary to the enigmatic coexistence of acetogens and methanogens. However, it is reasonable to expect that other microbial interactions analogous to the one identified in this study take place in nature. One or more of these interactions may result in the stimulation of acetogenic bacteria and support their persistence in hydrogen-driven ecosystems. In addition, acetogenic bacteria are an extremely versatile physiological group of anaerobic microorganisms. Their ability to metabolize a wide range of substrates is likely an important factor in the persistence of acetogens in the environment.

## References


[1] **Beeman, R. E, and J. M. Suflita.** 1987. Microbial ecology of a shallow unconfined ground water aquifer polluted by municipal landfill leachate. Microb. Ecol. **14**:39-54.

[2] **Breznak, J. A., and J. M. Switzer.** 1986. Acetate synthesis from $H_2$ plus $CO_2$ by termite gut microbes. Appl. Environ. Microbiol. **52**:623-630.

[3] **Breznak, J. A., J. M. Switzer, and H.-J. Seitz.** 1988. *Sporomusa termitida* sp. nov., an $H_2/CO_2$-utilizing acetogen isolated from termites. Arch. Microbiol. **150**:282-288.

[4] **Breznak, J. A., and J. S. Blum.** 1991. Mixotrophy in the termite gut acetogen *Sporomusa termitida*. Arch. Microbiol. **156**:105-110.

[5] **Breznak, J. A..** 1994. Acetogenesis from carbon dioxide in termite hindguts, p. 303-330. *In* Harold Drake (ed.), Acetogenesis. Chapman & Hall, New York.

[6] **Carepo, M., J. F. Baptista, A. Pamplona, G. Fauque, J. J. G. Moura, and M. A. M. Reis.** 2002. Hydrogen metabolism in *Desulfovibrio desulfuricans* strain New Jersey (NCIMB 8313)-comparative study with *D. vulgaris* and *D. gigas* species. Anaerobe **8**: 325-332.

[7] **Conrad, R., F. Bak, H.-J. Seitz, B. Thebrath, H. P. Mayer, and H. Schütz.** 1989. Hydrogen turnover by pshychrotrophic homoacetogenic and mesophilic methanogenic bacteria in anoxic paddy soil and lake sediment. FEMS Microbiol. Ecol. **62**:285-294.

[8] **Conrad, R., and B. Wetter.** 1990. Influence of temperature on energetics of hydrogen metabolism in homoacetogenic, methanogenic, and other anaerobic bacteria. Arch. Microbiol. **155**:94-98.

[9] **Cord-Ruwisch, R., H.-J. Seitz, and R. Conrad.** 1988. The capacity of hydrogenotrophic anaerobic bacteria to compete for traces of hydrogen depends on the redox potential of the terminal electron acceptor. Arch. Microbiol. **149**:350-357.

[10] **DeWeerd, K. A., L. Mandelco, R. S. Tanner, C. R. Woese, and J. M. Suflita.** 1990. *Desulfomonile tiedjei* gen. nov. and sp. nov., a novel anaerobic, dehalogenating, sulfate-reducing bacterium. Arch. Microbiol. **154**:23-30.

[11] **Dinh, H. T., J. Kuever, M. Mußmann, A. W. Hassel, M. Stratmann, and F. Widdel.** 2004. Iron corrosion by novel anaerobic microorganisms. Nature **247**:829-832.

[12] **Dolfing, J.** 1988. Acetogenesis, p. 417-468. *In*: Biology of Anaerobic Microorganisms, A. J. B. Zehnder (ed.), Wiley, New York.

[13] **Fukuzaki, S., N. Nishio, and S. Nagai.** 1990. Kinetics of the methanogenic fermentation of acetate. Appl. Environ. Microbiol. **56**:3158-3163.

[14] **Fuqua, C., M. R. Parsek, and E. P. Greenberg.** 2001. Regulation of gene expression by cell-to-cell communication: Acyl-homoserine lactone quorum sensing. Annu. Rev. Genet. **35**:439-468.

[15] **Friedrich, B., and C. G. Friedrich.** 1990. Hydrogenases in lithoautotrophic bacteria. Advances in Autotrophic Microbiology and One-Carbon Metabolism **1**:55-92.

[16] **Goudar, C. T., and J. F. Devlin.** 2001. Nonlinear estimation of microbial and enzyme kinetic parameters from progress curve data. Water Environ. Res. **73**:260-265.

[17] **Hansen, B., M. Bokranz, . Schönheit, and A. Kröger.** 1988. ATP formation coupled to caffeate reduction by $H_2$ in *Acetobacterium woodii* Nzva16. Arch. Microbiol. **15**:447-451.

[18] **Healey, F. P.** 1980. Slope of the Monod equation as an indicator of advantage in nutrient competition. Microb. Ecol. **5**:281-286.

[19] **Hoehler, T. M., M. J. Alperin, D. B. Albert, and C. S. Martens.** 1998. Thermodynamic control on hydrogen concentrations in anoxic sediments. Geochim. et Cosmochim. Acta **62**, 1745-1756.

[20] **Hoehler, T. M., M. J. Alperin, D. B. Albert, and C. S. Martens.** 2001 Apparent minimum free energy requirements for methanogenic archaea and sulfate-reducing bacteria in an anoxic marine sediment. FEMS Microbiol. Ecol. **38**, 33-41.

[21] **Jackson, B. E., V. K. Bhupathiraju, R. S. Tanner, C. R. Woese, and M. J. McInerney.** 1999. *Syntrophus acidotrophicus* sp. nov., a new anaerobic bacterium that degrades fatty acids and benzoate in syntrophic association with hydrogen-using microorganisms. Arch. Microbiol. **171**, 107-114.

[22] **Jakobsen, R., H.-J. Albrechtsen, M. Rasmussen, H. Bay, P. L. Bjerg, and T. H. Christensen.** 1998. $H_2$ concentrations in a landfill leachate plume (Grindsted, Denmark): *In situ* energetics of terminal electron acceptor processes. Environ. Sci. Technol. **32**, 2142-2148.

[23] **Jones, J. G., and B. M. Simon.** 1985. Interaction of acetogens and methanogens in anaerobic freshwater sediments. Appl. Environ. Microbiol. **49**:944-948.

[24] **Kaiser, J.-P., and K. W. Hanselmann.** 1982. Fermentative metabolism of substituted monoaromatic compounds by a bacterial community from anaerobic sediments. Arch. Microbiol. **133**:185-194.

[25] **Kerby, R., and J. G. Zeikus.** 1987. Anaerobic catabolism of formate to acetate and $CO_2$ by *Butyribacterium methylotrophicum*. J. Bacteriol. **169**:2063-2068.

[26] **Kotsyurbenko, O. R., M. V. Simankova, A. N. Nozhevnikova, T. T. Zhilina, N. P. Bolotina, A. M. Lysenko, and G. A. Osipov.** 1995. New species of psychrophilic acetogens: *Acetobacterium bakii* sp. nov., *A. paludosum* sp. nov., *A. fimetarium* sp. nov. Arch. Microbiol. **163**:29-34.

[27] **Kotsyurbenko, O. R., M. V. Glagolev, A. N. Nozhevnikova, and R. Conrad.** 2001. Competition between homoacetogenic bacteria and methanogenic archaea for hydrogen at low temperature. FEMS Microbiol. Ecol. **38**:153-159.

[28] **Kristjansson, J. K., P. Schonheit and R. K. Thauer.** 1982. Different $K_s$ values for hydrogen of methanogenic bacteria and sulfate reducing bacteria: An explanation for the apparent inhibition of methanogenesis by sulfate. Arch. Microbiol. **131**:278-282.

[29] **Krumholz, L. R., S. H. Harris, S. T. Tay, and J. M. Suflita.** 1999. Characterization of two subsurface $H_2$-utilizing bacteria, *Desulfomicrobium hypogeium* sp. nov. and *Acetobacterium psammolithicum* sp. nov., and their ecological roles. Appl. Environ. Microbiol. **65**:2300-2306.

[30] **LeVan, T. D., J. A. Robinson, J. Ralph, R. C. Greening, W. J. Smolenski, J. A. Z. Leedle, and D. M. Schaefer**. 1998. Assessment of reductive acetogenesis with indigenous ruminal bacterium populations and *Acetitomaculum ruminis*. Appl. Environ. Microbiol. **64**:3429-3436.

[31] **Liu, S., and J. M. Suflita.** 1993. $H_2$-$CO_2$-dependent anaerobic O-demethylation activity in subsurface sediments and by an isolated bacterium. Appl. Environ. Microbiol. **59**, 1325-1331.

[32] **Liu, S., and J. M. Suflita.** 1995. $H_2$ as an energy source for mixotrophic acetogenesis from the reduction of $CO_2$ and syringate by *Acetobacterium woodii* and *Eubacterium limosum* Curr. Microbiol. **31**:245-250.

[33] **Livingston, D. J., J. A. Fox, W. H. Orme-Johnson, and C. T. Walsh.** 1987. 8-Hydroxy-5-deazaflavin-reducing hydrogenase from *Methanobacterium thermoautotrophicum*: 2. Kinetic and hydrogen-transfer studies. Biochem. **26**:4228-4237.

[34] **Lovley, D. R., D. F. Dwyer, and M. J. Klug.** 1982. Kinetic analysis of competition between sulfate reducers and methanogens for hydrogen in sediments. Appl. Environ. Microbiol. **43**:1373-1379.

[35] **Lovley, D. R..** 1985. Minimum threshold for hydrogen metabolism in methanogenic bacteria. Appl. Environ. Microbiol. **49**:1530-1531.

[36] **Lovely, D. R., and S. Goodwin.** 1988 Hydrogen concentrations as an indicator of the predominant terminal electron-accepting reactions in aquatic sediments. Geochim. Cosmochim. Acta **52**, 2993-3003.

[37] **Mackie, R. I., and M. P. Bryant.** 1994. Acetogenesis and the rumen: Syntrophic relationships, p. 331-364 *In* Harold Drake (ed.), Acetogenesis. Chapman & Hall, New York.

[38] **Martin, S. M., B. R. Glick, and W. G. Martin.** 1980. Factors affecting the production of hydrogenase by *Desulfovibrio desulfuricans*. Can. J. Microbiol. **26**:1209-1213.

[39] **Mormile, M. R., K. R. Gurigala, J. A. Robinson, M. J. McInerney, and J. M. Suflita** 1996. The importance of hydrogen in landfill fermentations. Appl. Environ. Microbiol. **62**:1583-1588.

[40] **McInerney, M. J., M. P. Bryant, and N. Pfennig.** 1979. Anaerobic bacterium that degrades fatty acids in syntrophic association with methanogens. Arch. Microbiol. **122**:129-135.

[41] **Nozhevnikova, A. N., O. R. Kotsyurbenko, and M. V. Sinamkova.** 1994. Acetogenesis at low temperature, p. 416-431. *In* Harold Drake (ed.), Acetogenesis. Chapman & Hall, New York.

[42] **Peters, V., P.H. Janssen, and R. Conrad.** 1998. Efficiency of hydrogen utilization during unitrophic and mixotrophic growth of *Acetobacterium woodii* on hydrogen and lactate in the chemostat. FEMS Microbiol. Ecol. **26**:317-324.

[43] **Phelps, T. J., and J. G. Zeikus.** 1984. Influence of pH on terminal carbon metabolism in anoxic sediments from a mildly acidic lake. Appl. Envrion. Microbiol. **48**:1088-1095.

[44] **Ragsdale, S. W., and L. G. Ljungdahl.** 1984. Hydrogenase from *Acetobacterium woodii*. Arch. Microbiol. **139**:361-365.

[45] **Robinson J.A.** 1984. Competition between sulfate-reducing and methanogenic bacteria for $H_2$ under resting and growing conditions. Arch. Microbiol. **137**: 26-32.

[46] **Robinson J.A.** 1985. Determining microbial kinetic parameters using nonlinear regression analysis. Advantages and limitations in microbial ecology. Adv. Microb. Ecol. **8**: 61-114.

[47] **Schneider, K., and H. G. Schlegel.** 1976. Purification and properties of soluble hydrogenase from *Alcaligenes eutrophus* H 16. Biochimi. Biophys. Acta **452**:66-80.

[48] **Seitz, H.-J., B. Schink, N. Pfennig, and R. Conrad.** 1990. Energetics of syntrophic ethanol oxidation in defined chemostat cocultures. Arch. Microbiol. **155**:82-88.

[49] **Sonne-Hansen, J., P. Westermann, and B. K. Ahring.** 1999. Kinetics of sulfate and hydrogen uptake by the thermophilic sulfate-reducing bacteria *Thermodesulfobacterium* sp. strain JSP and *Thermodesulfovibrio* sp. strain R1Ha3. Appl. Environ. Microbiol. **65**:1304-1307.

[50] **Sprott, D. G., K. M. Shaw, and T. J. Beveridge.** 1987. Properties of the particulate enzyme F420-reducing hydrogenase isolated from Methanospirillum hungatei. Can. J. Microbiol. **33**:896-904.

[51] **Stevens, T. O., and J. P. McKinley.** 1995. Lithoautotrophic microbial ecosystems in deep basalt aquifers. Science, **270**:450-454.

[52] **Tanaka, K., and N. Pfennig.** 1988. Fermentation of 2-methoxyethanol by *Acetobacterium malicum* sp. nov. and *Pelobacter venetianus*. Arch. Microbiol. **149**:181-187.

[53] **Voordouw, G.** 1995. The genus *Desulfovibrio*: The centennial. Appl. Environ. Microbiol. **61**:2813-2819.

[54] **Wang, L., Y. He, Y. Gao, J. E. Wu, Y. Dong, C. He, S. X. Wang, L. Weng, J. Xu, L. Tay, R. X. Fang, and L. Zhang.** 2004. A bacterial cell-cell communication signal with cross-kingdom structural analogues. Mol. Microbiol. **511**:903-912.

[55] **Wolin, M. J., and T. L. Miller.** 1994. Acetogenesis from $CO_2$ in the human colonic ecosystem, p.365-385. *In* Harold Drake (ed.), Acetogenesis. Chapman & Hall, New York.

## Appendix 1

Progress Curve Analysis for Enzyme and Microbial Kinetic Reactions using Explicit Solutions based on the Lambert *W* Function


### Abstract

We present a simple method for estimating kinetic parameters from progress curve analysis of biologically catalyzed reactions that reduce to forms analogous to the Michaelis-Menten equation. Specifically, the Lambert *W* function is used to obtain explicit, closed-form solutions to differential rate expressions that describe the dynamics of substrate depletion. The explicit nature of the new solutions greatly simplifies nonlinear estimation of the kinetic parameters since numerical techniques such as the Runge-Kutta and Newton-Raphson methods used to solve the differential and integral forms of the kinetic equations, respectively, are replaced with a simple algebraic expression. The applicability of this approach for estimating $V_{max}$ and $K_m$ in the Michaelis-Menten equation was verified using a combination of simulated and experimental progress curve data. For simulated data, final estimates of $V_{max}$ and $K_m$ were close to the actual values of 1 μM/h and 1 μM, respectively, while the standard errors for these parameter estimates were proportional to the error level in the simulated data sets. The method was also applied to hydrogen depletion experiments by mixed cultures of bacteria in activated sludge resulting in $V_{max}$ and $K_m$ estimates of 6.531 μM/h and 2.136 μM, respectively. The algebraic nature of this solution, coupled with its relatively high accuracy make it an attractive candidate for kinetic parameter estimation from progress curve data.



**Keywords:** kinetics, Lambert *W* function, Michaelis-Menten equation, nonlinear parameter estimation, progress curve analysis

## 1. INTRODUCTION

The Michaelis-Menten equation has been widely used to describe the kinetics of enzyme-catalyzed reactions (Michaelis and Menten, 1913). Applications also include non-growing microbial suspensions where substrate consumption takes place in the absence of active microbial growth (Betlach and Tiedje, 1981; Pauli and Kaitala, 1997; Suflita et al., 1983). A wide variety of data analysis techniques have been developed to obtain the kinetic parameters $V_{max}$ and $K_m$, the maximal rate, and half-saturation constant, respectively, (Atkins and Nimmo, 1975; Duggleby, 1995; Nimmo and Atkins, 1974). The most widely used approach is graphical where the Michaelis-Menten equation is linearized by algebraic manipulation. This linear equation is subsequently plotted as a straight line in rectangular coordinates and the parameters $V_{max}$ and $K_m$ are estimated by linear least squares analysis. Graphical methods of kinetic analysis of substrate-velocity data pairs are well known (Cornish-Bowden, 1995) and include the direct linear plot that does not involve any algebraic manipulations (Cornish-Bowden, 1975; Eisenthal and Cornish-Bowden, 1974). While graphical methods possess the unique advantage of providing a visual representation of experimental data, their parameter estimates can be very inaccurate. This is primarily because a linear transformation of an inherently nonlinear equation, such as the Michaelis-Menten expression, distorts the error in the measured variables and this can subsequently impact estimates of the salient kinetic parameters (Cornish-Bowden, 1995; Duggleby, 1991; Leatherbarrow, 1990; Robinson, 1985).

Some of the limitations described above can be avoided through the coupling of nonlinear parameter estimation techniques and progress curve analysis. This approach involves the use of substrate depletion/product accumulation determinations over time

rather than initial velocity-substrate concentration data pairs to estimate $V_{max}$ and $K_m$ (Duggleby, 1994; Duggleby, 1995; Duggleby and Morrison, 1977; Duggleby and Wood, 1989; Fernley, 1974; Zimmerle and Frieden, 1989). In addition to the potential for obtaining improved parameter estimates, this method is consistent with most experimental designs that typically involve monitoring either substrate or product concentration over time. Despite the obvious advantages of progress curve analyses as described elsewhere (Duggleby, 1995; Robinson, 1985), this method is not commonly used for kinetic parameter estimation. This is because of the computational difficulties associated with progress curve analysis. The integral form of the Michaelis-Menten equation is implicit in the substrate concentration. As a result, numerical approaches such as bisection and Newton-Raphson methods are necessary to compute substrate concentration in the integrated Michaelis-Menten equation (Duggleby, 1995). Alternatively, substrate concentration must be calculated by numerically integrating the differential form of the Michaelis-Menten equation (Duggleby, 1994; Duggleby, 2001; Zimmerle and Frieden, 1989). Kinetic parameter estimation in the Michaelis-Menten equation is a multidimensional approach that involves using one of the numerical techniques described above to solve the Michaelis-Menten equation followed by an iterative estimation of the kinetic parameters $V_{max}$ and $K_m$ using an appropriate nonlinear optimization routine. Implementation of a robust nonlinear kinetic parameter estimation approach can be difficult when there is inadequate experience in numerical techniques and computer programming. We believe a simplification in kinetic parameter estimation from progress curve data can make this approach more appealing to a wider group of experimentalists.

While the implicit nature of the Michaelis-Menten equation presents computational difficulties, the first truly explicit solution of the Michaelis-Menten equation was derived only recently through the use of computer algebra (Schnell and Mendoza, 1997) and we have independently verified that this solution can be used to accurately calculate substrate concentration (Goudar et al., 1999). The availability of this explicit solution of the Michaelis-Menten expression has significant implications for simplifying estimation of $V_{max}$ and $K_m$ through progress curve analysis. Specifically, this approach replaces numerical solution of a differential/nonlinear equation with the evaluation of a simple algebraic expression that provides highly accurate values of the substrate concentration. The algebraic nature of this solution coupled with its relatively high accuracy makes it an attractive candidate for use in nonlinear kinetic parameter estimation from progress curve data.

In the present study, we present a brief derivation of the explicit solution for the Michaelis-Menten equation and illustrate its application for estimating $V_{max}$ and $K_m$ from simulated and experimental substrate concentration data. We also show that this approach is general and can be applied to any kinetic expression that can be reduced to a form analogous to the Michaelis-Menten equation. We have developed a suite of computer programs in MATLAB (The Mathworks, Natick, MA) that use this explicit solution for kinetic parameter estimation and these programs are available free of charge for academic use from the corresponding author.

## 2. THEORY

The Michaelis-Menten equation in the differential form can be used to describe the dynamics of substrate depletion as

$$\frac{dS}{dt} = -\frac{V_{max} S}{K_m + S} \tag{1}$$

where $S$ is the substrate concentration, and $V_{max}$ and $K_m$ are the maximal rate and Michaelis half saturation constant, respectively. Equation (1) can be readily integrated to obtain the integral form of the Michaelis-Menten equation

$$K_m \ln\left(\frac{S_0}{S}\right) + S_0 - S = V_{max} t \tag{2}$$

where $S_0$ is the initial substrate concentration. Equation (2) is nonlinear and clearly implicit with respect to the substrate concentration. Hence, numerical approaches such as bisection and Newton-Raphson methods are necessary to calculate $S$. In order to obtain the explicit form of Eq. (2), we rearrange to form

$$S + K_m \ln(S) = S_0 + K_m \ln(S_0) - V_{max} t \tag{3}$$

Substituting $\phi = S/K_m$ in Eq. (3) results in

$$\phi K_m + K_m \ln(\phi K_m) = S_0 + K_m \ln(S_0) - V_{max} t \tag{4}$$

Dividing Eq. (4) by $K_m$ and rearranging results in

$$\phi + \ln(\phi) = \frac{S_0}{K_m} + \ln\left(\frac{S_0}{K_m}\right) - \frac{V_{max} t}{K_m} \tag{5}$$

The left hand side of Eq. (5) is analogous to the Lambert $W$ function as defined by (Corless et al., 1996)

$$W(x) + \ln\{W(x)\} = \ln(x) \tag{6}$$

where $W$ is the Lambert $W$ function and $x$ the argument of $W$. From equations (5) and (6), an expression for $\phi$ may be obtained as

$$\phi = W\left\{\frac{S_0}{K_m}\exp\left(\frac{S_0 - V_{max}t}{K_m}\right)\right\} \tag{7}$$

As $\phi = S/K_m$, Equation (7) can be written in terms of $S$ as

$$S = K_m W\left\{\frac{S_0}{K_m}\exp\left(\frac{S_0 - V_{max}t}{K_m}\right)\right\} \tag{8}$$

Equation (8), derived from Eq. (2), explicitly relates the substrate concentration to the initial substrate concentration, $S_0$, and the kinetic parameters $V_{max}$ and $K_m$. Substrate concentrations can be readily estimated from Eq. (8) which is a simple algebraic expression.

While the above derivation of the explicit solution has been for the Michaelis-Menten equation, it is equally applicable to several other kinetic models that reduce to forms analogous to the Michaelis-Menten equation. For instance, inhibition reaction mechanisms such as competitive, uncompetitive, non-competitive and mixed inhibition can all be reduced to forms that are analogous to Eq. (1) with different definitions of $V_{max}$ and $K_m$. Hence, they all have explicit closed-form solutions similar to Eq. (8) that can be used for progress curve analysis.

## 3. MATERIALS AND METHODS

### 3.1. Evaluating *W*

There are several methods for computing the value of $W$ as defined by Eq. (6) (Barry et al., 1995a; Barry et al., 1995b; Fritsch et al., 1973). These algorithms are extremely robust and fairly simple to use with one method (Fritsch et al., 1973) converging in a single iteration. The FORTRAN source code implementing the method in Fritsch et al., 1973 is presented in the original publication while that for the method in

Barry et al., 1995a can be obtained from http://www.netlib.org/toms/743. In the present study, we have used the MAPLE® (Waterloo Maple Inc.) implementation of the *W* function as described in Corless et al., 1996.

### 3.2 Substrate Depletion Data

To illustrate the applicability of Eq. (8) for estimating $V_{max}$ and $K_m$ through progress curve analysis, simulated substrate concentration data were generated from Eq. (8) using $S_0$ = 10 μM, $V_{max}$= 1.0 μM/h and $K_m$ = 1.0 μM. For the resulting error-free substrate depletion data to more realistically represent experimental observations, noise of known type and magnitude was introduced. Normally distributed error with a mean of zero and standard deviation ranging from 1 to 4 % of the magnitude of the initial substrate concentration (10 μM) was generated using a pseudo-random number generator. This noise was added to the error-free substrate concentration data obtained from Eq. (8) and the resulting data set was used for estimating $V_{max}$ and $K_m$ using nonlinear least squares.

Experimental hydrogen depletion data were obtained with sewage sludge that was collected from the primary digestor at the municipal treatment plant in Norman, OK. Hydrogen partitioning was mass transfer limited in incubations of undiluted sludge. To overcome this, sludge was centrifuged at 15,000 g for 20 minutes. The resulting supernatant was used as a diluent to make a sludge preparation (10 %) that was not mass transfer limited. Diluted sludge (0.5 L) was transferred to a 2 L Erlenmeyer flask under constant sparging with $N_2/CO_2$ (80%/20%). The flask was stoppered, placed at 37 °C and constantly stirred. Hydrogen (50 mL) was injected into the headspace of the flask to begin the assay. Hydrogen consumption was monitored by periodically removing headspace

samples and analyzing them by gas chromatography (RGA3 Gas Analyzer, Trace Analytical, Sparks, Maryland).

### 3.3. Initial Kinetic Parameter Estimates through Linearization

Given the iterative nature of nonlinear least squares analysis, initial estimates of the parameters are necessary. These initial estimates are typically obtained through linearization of the original nonlinear equation and it is important that they be as accurate as possible since the final solution can be impacted. The integrated Michaelis-Menten can be linearized in three different ways (Robinson and Characklis, 1984)

$$\frac{t}{\ln\left(S/S_0\right)} = \frac{1}{V_m}\frac{(S_0 - S)}{\ln\left(S/S_0\right)} + \frac{K_m}{V_m} \tag{9}$$

$$\frac{(S_0 - S)}{\ln\left(S/S_0\right)} = V_m - \frac{K_m}{t}\ln\left(S/S_0\right) \tag{10}$$

$$\frac{t}{(S_0 - S)} = \frac{K_m}{V_m}\frac{\ln\left(S/S_0\right)}{(S_0 - S)} + \frac{1}{V_m} \tag{11}$$

and standard linear least squares can be used to obtain estimates of $V_{max}$ and $K_m$ from Eqs. (9)–(11). These initial estimates were subsequently used as starting points for estimating $V_{max}$ and $K_m$ through nonlinear least squares analysis as described in the following section.

### 3.4. Nonlinear Kinetic Parameter Estimation

Nonlinear kinetic parameter estimation involves minimizing the residual sum of squares error (RSSE) between experimental and calculated substrate concentration data.

$$\textit{Minimize} \qquad RSSE = \sum_{i=1}^{n}\left[\left(S_{\exp}\right)_i - \left(S_{cal}\right)_i\right]^2 \tag{12}$$

where $(S_{exp})_i$ is the $i^{th}$ experimental substrate concentration and $(S_{cal})_i$ is the $i^{th}$ calculated substrate concentration in a total of $i$ observations. Initial estimates of $V_{max}$ and $K_m$ obtained from Eqs. (9)–(11) were used in Eq. (8) to calculate the first set of substrate concentration data. Subsequently, a comparison was made between the experimental and calculated substrate concentrations and the RSSE was computed from Eq. (12). The kinetic parameters were iteratively updated using the Levenberg-Marquardt method (Marquardt, 1963) until the RSSE in Eq. (12) was minimized.

### 3.5. Computer Implementation

Computer programs have been developed that implement the parameter estimation approach outlined in sections 3.3 and 3.4. Experimental $S$ versus $t$ data are first used to obtain initial estimates of $V_{max}$ and $K_m$ from Eqs. (9)–(11). These initial estimates are subsequently used to obtain final estimates of $V_{max}$ and $K_m$ using nonlinear least squares. The output from this analysis includes detailed statistics regarding quality of the fit and graphical representation of the fit to experimental data along with a plot of the residuals. Finally, three-dimensional visualization of the error surface in the $V_{max}$ and $K_m$ space along with contour plots for the RSSE can be obtained. This visualization allows observation of local minima on the error surface and helps determine if the true global minimum has actually been reached during nonlinear parameter estimation.

## 4. RESULTS

### 4.1. Lambert *W* Function

A plot of the Lambert $W$ function as defined by Eq. (8) is shown in Figure 1 for real values of $W$. From Eq. (8), the argument of the $W$ function, $x$, corresponds to

$\frac{S_0}{K_m}\exp\left(\frac{S_0 - V_{max}t}{K_m}\right)$. The $W$ function has three distinct branches depending upon the values of $x$. For $x > 0$, $W$ is positive and has a unique value (Region 1). For $x$ values in the range of $-1/e < x < 0$, two solutions exist on either side of $W = -1$ (Regions 2 and 3, respectively). An examination of the above expression for $x$ indicates that $x$ is always positive as $K_m$ and $S_0$ are always positive suggesting that unique values of $W$ exist for all $x$ values of interest when applying this solution to the Michaelis-Menten equation.

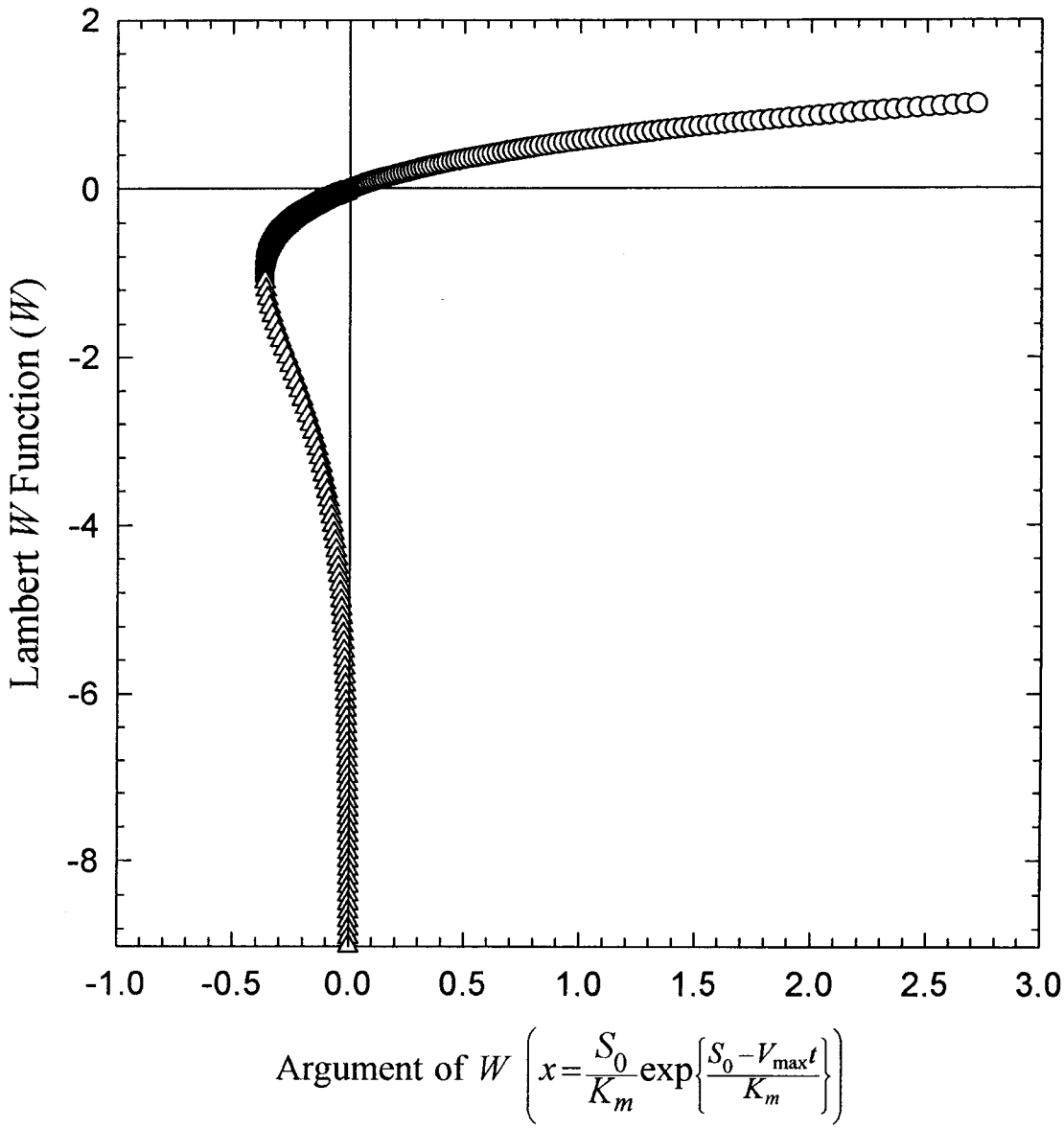


**Figure 1.** The three real branches of the Lambert $W$ function. { (o), x > 0, Region 1; (■), -1/e < x < 0 and 0 > $W$ > -1, Region 2; (Δ), -1/e < x < 0 and $W$ < -1, Region 3}.

## 4.2. Kinetic Parameter Estimation from Simulated Data

Simulated substrate concentration data along with the theoretical predictions corresponding to the best fit kinetic parameters are shown in Figure 2. Significant scatter in simulated substrate depletion curves is seen for errors with standard deviations of 3 and 4 % as might be encountered in actual progress curve experiments Despite the increased scatter, final estimates of $V_{max}$ and $K_m$ were very close to the actual values of 1.0 μM/h and 1.0 μM, respectively. However, the standard errors for both $V_{max}$ and $K_m$ increased with increasing noise levels suggesting that greater uncertainty is associated with the final estimates of the kinetic parameters as error is amplified. The magnitude of the increase in standard errors for $V_{max}$ and $K_m$ was similar to the increase in the standard deviation of the error introduced in the simulated substrate depletion curves.

The standard errors for $K_m$ were approximately six-fold higher than those for $V_{max}$ at all the four noise levels (Figure 2) indicating higher uncertainty in the $K_m$ estimates. Contour plots of the RSSE in the $V_{max}$ and $K_m$ space are shown in Figure 3 where the inner most contours which represent the region of lowest RSSE, extend over a wide range of $K_m$ values and only over a very narrow range of $V_{max}$ values. This suggests substantially lower sensitivity of the RSSE to $K_m$ values and is consistent with the higher standard errors for $K_m$ estimates.

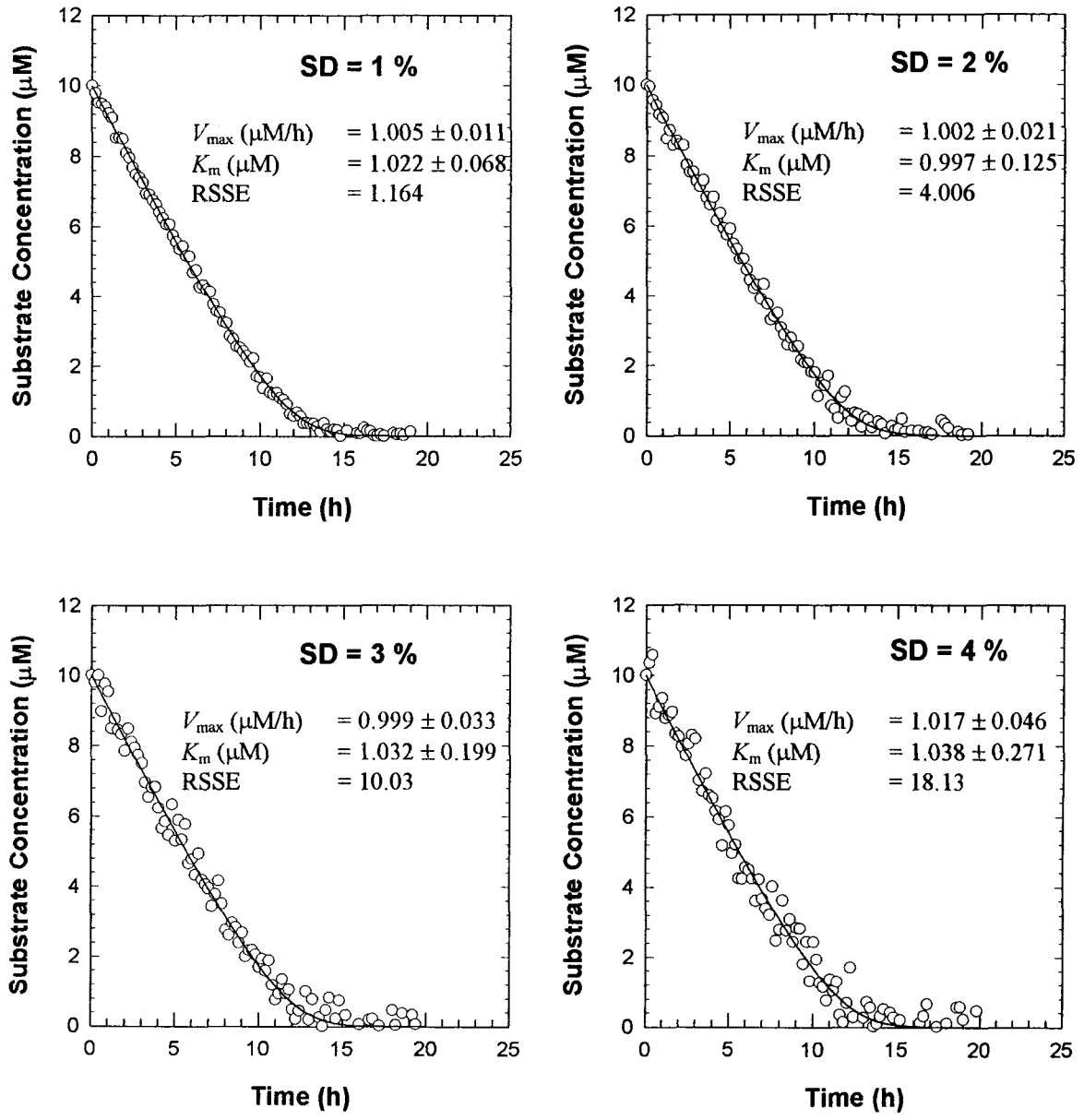


**Figure 2.** Simulated substrate depletion data (points) along with model predictions (solid lines) from Eq. (8) and the best fit kinetic parameters. Simulated substrate depletion data were characterized by normally distributed noise with a mean value of zero and standard deviations of 1, 2, 3 and 4 % of the initial substrate concentration of 10 μM.

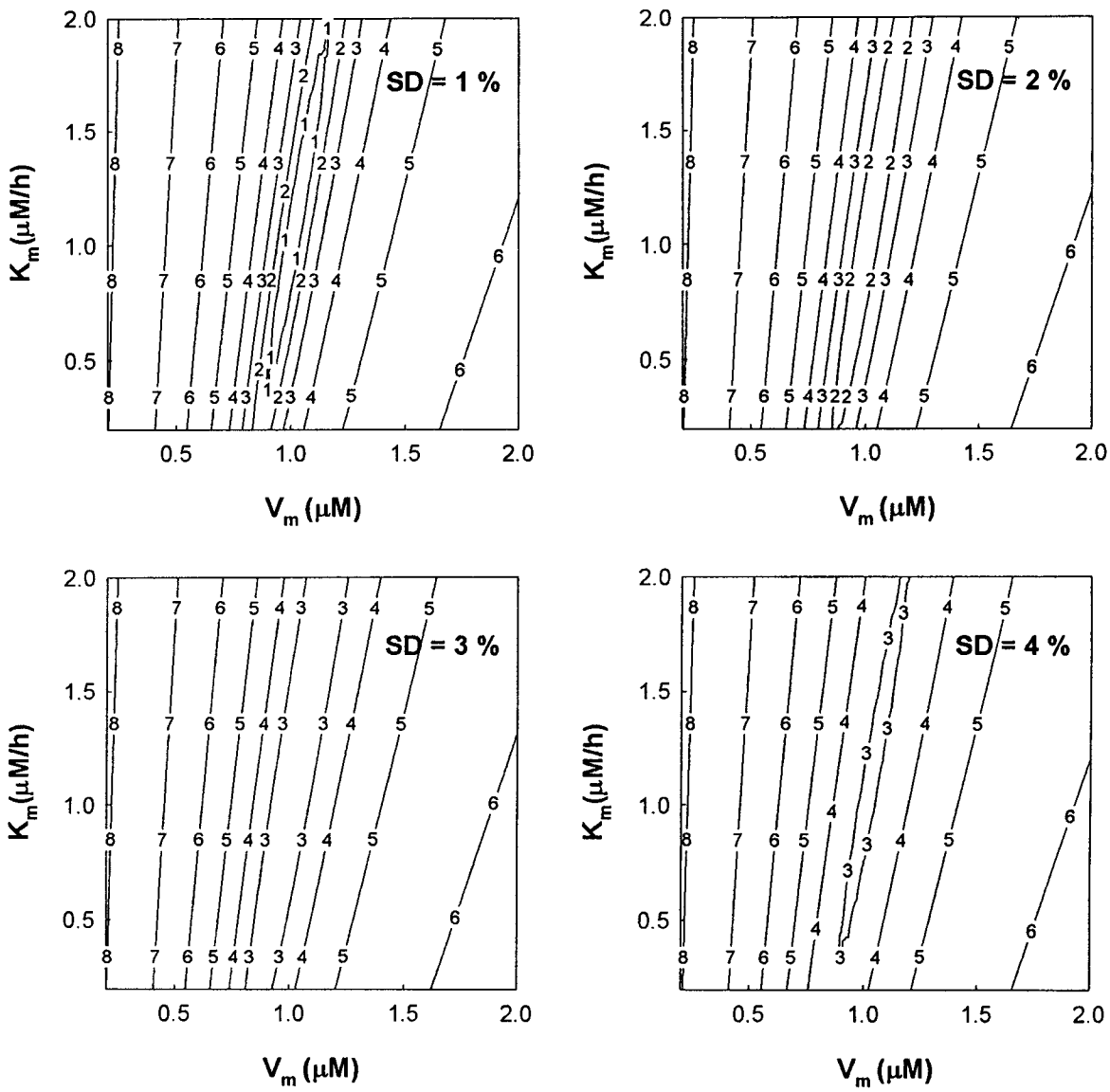


**Figure 3.** Contour plots showing dependence of the RSSE on $V_{max}$ and $K_m$ for the four simulated data sets examined in this study. Final estimates of $V_{max}$ and $K_m$ and the associated standard errors are shown in Figure 2.

High parameter correlation can adversely affect parameter determination and must be taken into account while assessing the quality of model fit to experimental data. The off-diagonal element of the parameter correlation matrix was 0.968 for all cases indicating significant correlation between $V_{max}$ and $K_m$. However, this did not adversely affect final estimates of the kinetic parameters (Figure 2).

### 4.3. Kinetic Parameter Estimation from Experimental Substrate Decay Curves

Hydrogen depletion in activated sludge was used to provide a demonstration of the applicability of this parameter estimation approach. The substrate concentration versus time data were used in Eqs. (9)–(11) to obtain initial estimates of $V_{max}$ and $K_m$. These linearized plots are shown in Figure 4 along with the corresponding estimates of $V_{max}$ and $K_m$. Subsequently, each of these three sets of initial estimates was used to determine the final values of $V_{max}$ and $K_m$ from Eqs. (8) and (12) using nonlinear least squares. This was done to check if the same final $V_{max}$ and $K_m$ determinations would be obtained from the three different initial estimates. While this approach does not solve the problem of the solution converging on a local error minimum, it is a simple way of checking the robustness of the solution. For the hydrogen depletion data set, all starting points converged to the same final solution and a plot of experimental hydrogen depletion data with corresponding model prediction is shown in Figure 5 along with a plot of the residuals. There was good agreement between experimental data and model prediction and the residuals were randomly distributed. The corresponding best fit values of $V_{max}$ and $K_m$ along with their respective standard errors are also shown in Figure 5. The standard errors

for both $V_{max}$ and $K_m$ were low compared to the actual parameter estimates indicative of a robust model fit to experimental data. However, there was significant correlation between $V_{max}$ and $K_m$ as the off-diagonal element of the parameter correlation matrix was 0.967 (a value of 1 indicates complete correlation).

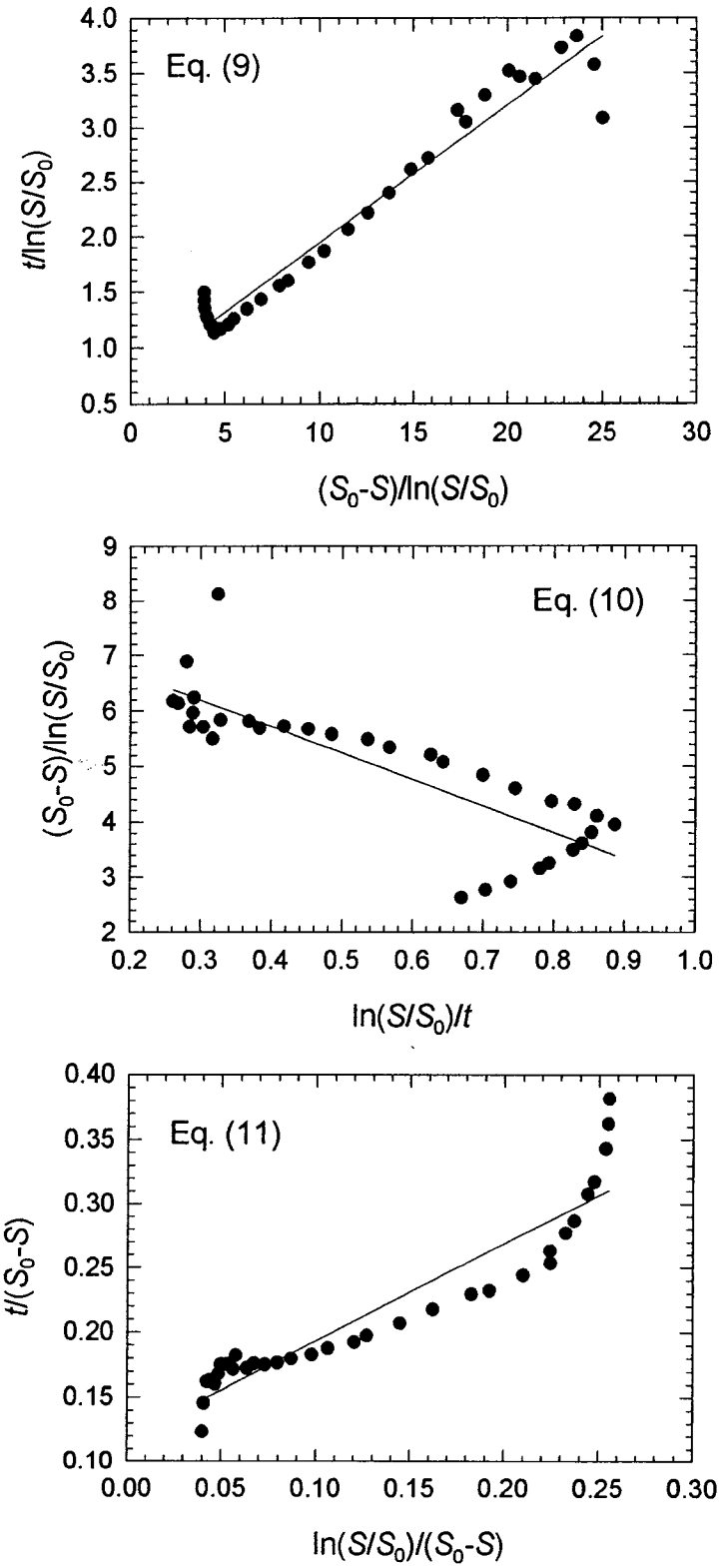


**Figure 4.** The three linearization approaches for obtaining initial estimates of $V_{max}$ and $K_m$ for hydrogen depletion in activated sludge

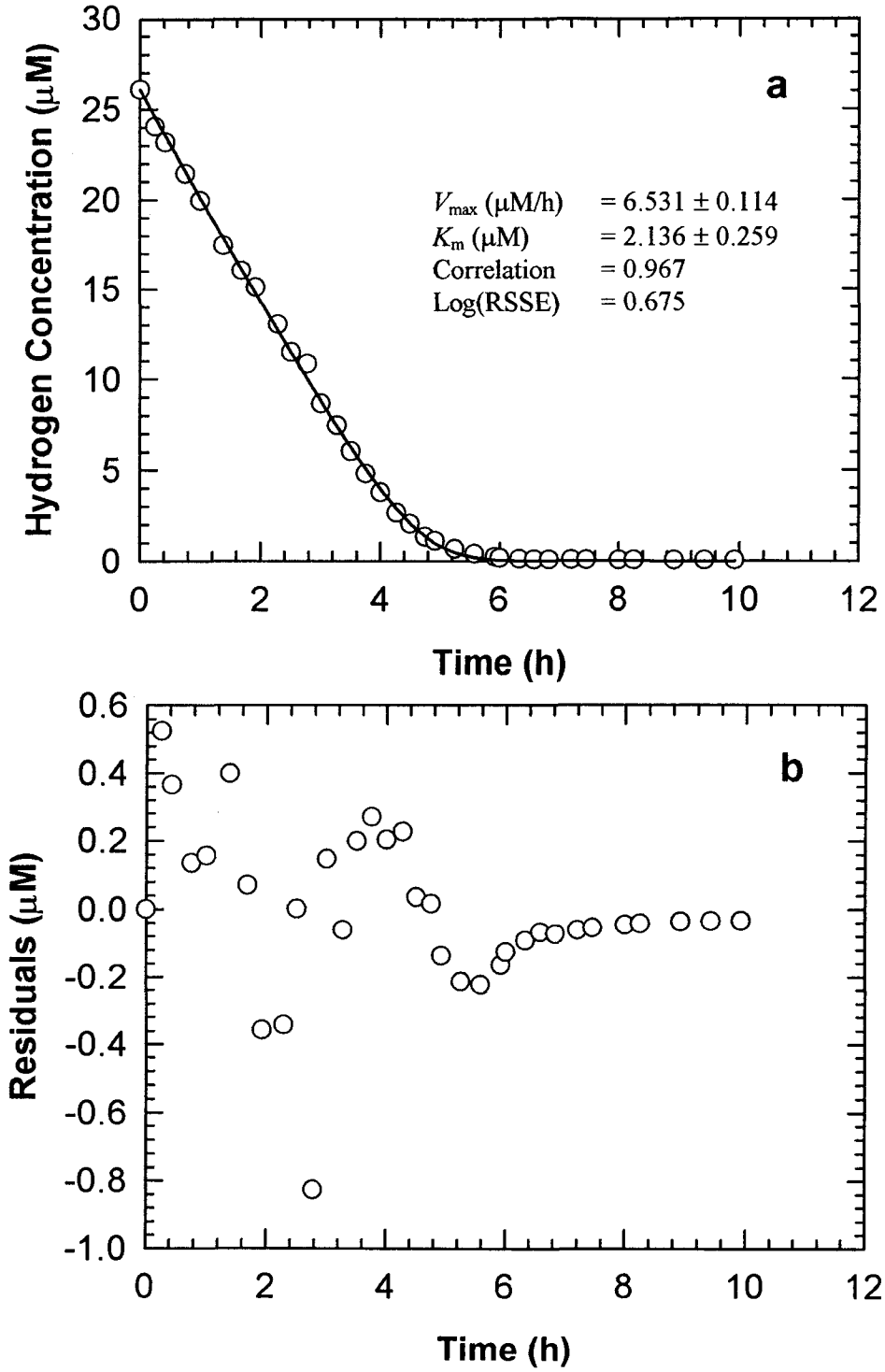


**Figure 5.** Experimental substrate depletion data (points) and model predictions (smooth line) for hydrogen depletion in activated sludge. $V_{max}$ and $K_m$ were estimated from Eqs. (8) and (12) using nonlinear least squares and are presented as parameter ± standard error.

To further characterize the robustness of the fit, RSSE values were generated over a grid of $V_{max}$ and $K_m$ values ($0.2V_{max} < V_{max} < 2V_m$; $0.2K_m < K_m < 2K_m$ ) and a contour plot of the RSSE in the $V_{max}$ and $K_m$ space is shown in Figure 6. The true global minimum corresponded to a Log(RSSE) value of 0.686 which is very close to that obtained from nonlinear parameter estimation (0.675; Figure 5). Whenever possible, a visual examination of the error surface should be made to check for convergence or lack thereof on the true global minimum. Recognizing the value of visual examination of the error surface in the $V_{max}$ and $K_m$ space, this aspect of data analysis has been incorporated in the computer programs developed in this study.

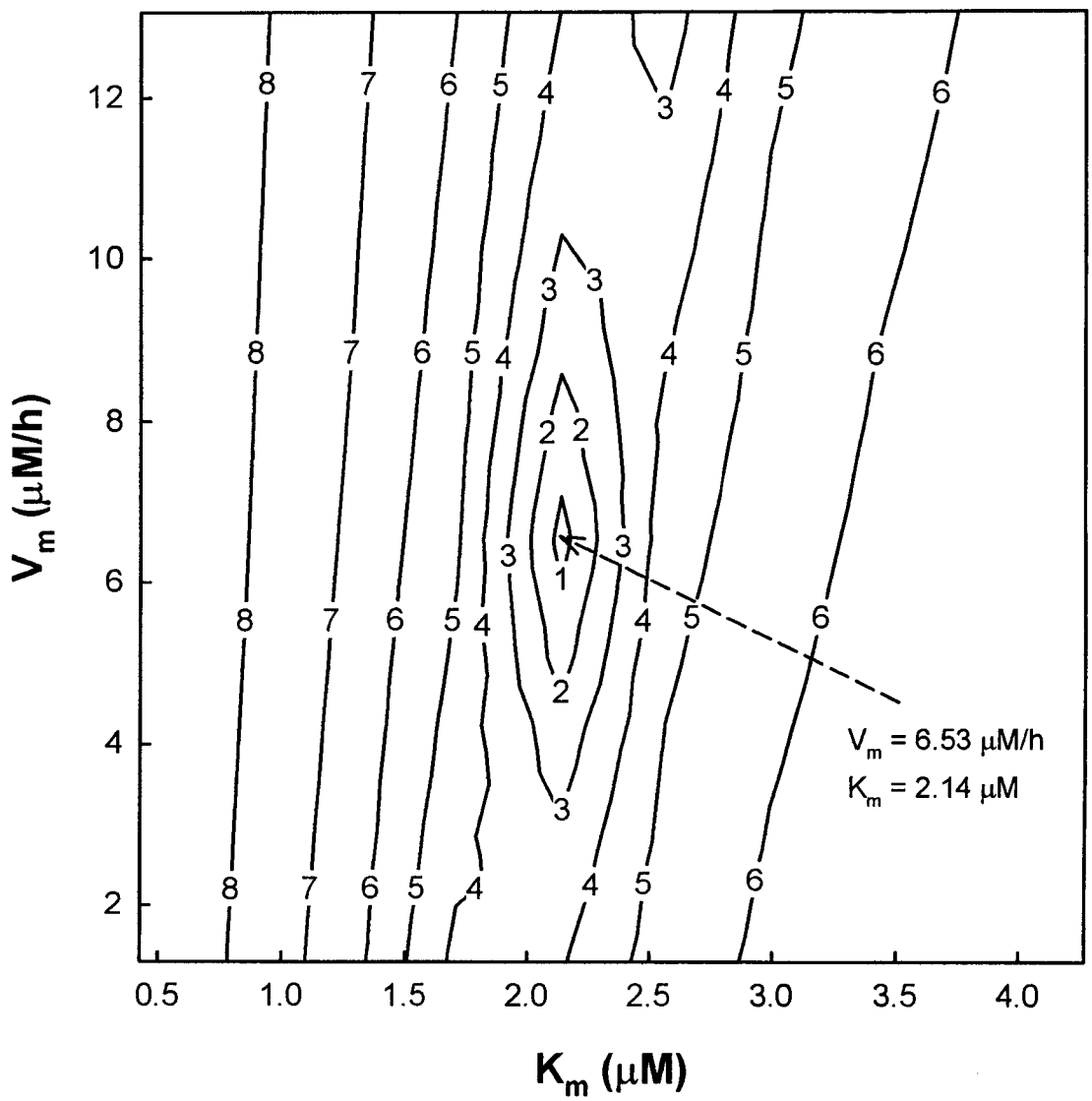


**Figure 6.** Visualization of the error surface {log(RSSE) values} as a two-dimensional contour plot in the $V_{max}$ and $K_m$ space ($0.2V_{max} < V_{max} < 2V_m$; $0.2K_m < K_m < 2K_m$) for hydrogen depletion in activated sludge. The final estimates of $V_{max}$ and $K_m$ from nonlinear parameter estimation were 6.53 μM/h and 2.14 μM, respectively (Figure 5).

## 5. DISCUSSION

An alternate approach for estimating kinetic parameters in enzyme and microbial kinetic progress curves through the use of an explicit closed form solution of the differential rate expressions is presented. Unlike existing solutions that are implicit with respect to the substrate concentration, the new solutions describe substrate concentration as a function of the initial substrate concentration and the kinetic parameters alone and are hence truly explicit. This representation simplifies nonlinear estimation of kinetic parameters from progress curve data as current methods that rely on numerical solutions of the differential/integral rate expressions are replaced with a simple algebraic expression. Moreover, substrate concentrations with accuracy on the order of $10^{-15}$ can be readily obtained using the explicit closed form solution (Goudar et al., 1999). Such accuracies cannot be easily obtained with the standard numerical approaches for solving differential and nonlinear equations.

While we have used the Michaelis-Menten equation to illustrate the applicability of the *W* function based closed form solution, it is important to recognize that this approach is general and can be extended to any enzyme kinetic mechanism that can be reduced to a form analogous to the Michaelis-Menten equation. For instance, the rate expression for competitive inhibition can be written as

$$\frac{dS}{dt} = \frac{V_{max} S}{K_m \left(1 + \frac{i}{K_c}\right) + S} \tag{13}$$

which reduces to Eq. (1) when the substitution $K_m' = K_m\left(1+\frac{i}{K_c}\right)$ is made. Hence the solution presented as Eq. (8) is applicable to Eq. (13) as well as several other reaction schemes involving inhibition mechanisms (Cornish-Bowden, 1995) that reduce to forms analogous to the Michaelis-Menten with different definitions of $V_{max}$ and $K_m$. Progress curve data for these kinetic mechanisms are readily amenable to the parameter estimation approach presented here thereby widening the scope of its applicability.

The computer programs developed in this study allow for comprehensive analysis of experimental substrate depletion versus time data. Three sets of $V_{max}$ and $K_m$ values are first determined through linearization and we recommend that each of these sets be subsequently used to estimate the final values using nonlinear least squares. This will help determine if the same final solution is obtained in all cases and will provide some indication of the robustness of the model fit. After successful parameter estimation, the programs provide detailed statistical information that can be used to asses the quality of the model fit to experimental data. There is also a provision to visualize the error surface in the $V_{max}$ and $K_m$ space which provides very useful information on the presence of multiple minima in the error surface. The computer programs developed in this study are intuitive and extremely easy to use.

## 6. CONCLUSIONS

Solution of both the differential and integral forms of the Michaelis-Menten and analogous equations has traditionally required the use of numerical techniques which adds to the complexity of nonlinear parameter estimation from progress curve data. In the present study, we present a simpler alternate approach to progress curve analysis that uses

explicit, closed-from solutions of the differential rate equations. Applicability of the explicit solutions for progress curve analysis was verified using both simulated and experimental substrate depletion data. The simplicity and accuracy of the Lambert *W* function based solutions should increase the appeal of progress curve analysis for estimating kinetic parameters in the Michaelis-Menten and similar rate expressions. Computer programs have been developed that perform all the analyses presented in this study and are available free of charge for academic use from the corresponding author.

## REFERENCES


Atkins G.L., Nimmo I.A., 1975. A comparison of seven methods for fitting the Michaelis-Menten equation. Biochem. J. 149, 775-777.

Barry D.A., Barry S.J., Culligan-Hensley P.J., 1995a. Algorithm 743: A Fortran routine for calculating real values of the *W*-function. ACM Trans. Math. Softw. 21, 172-181.

Barry D.A., Culligan-Hensley P.J., Barry S.J., 1995b. Real values of the W-function. ACM Trans. Math. Softw. 21, 161-171.

Betlach M.R., Tiedje J.M., 1981. Kinetic explanation for accumulation of nitrite, nitric oxide, and nitrous oxide during bacterial denitrification. Appl. Environ. Microbiol. 42, 1074.

Corless R.M., Gonnet G.H., Hare D.E., Jeffrey D.J., Knuth D.E., 1996. On the Lambert W function. Adv. Comput. Math. 5, 329-359.

Cornish-Bowden A., 1975. The use of the direct linear plot for determining initial velocities. Biochem. J. 149, 305-312.

Cornish-Bowden A., 1995. Fundamentals of Enzyme Kinetics. London: Portland Press Ltd. 343 p.

Duggleby R.G., 1991. Analysis of biochemical data by nonlinear regression, Is it a waste of time. TIBS 16, 51-52.

Duggleby R.G., 1994. Analysis of progress curves for enzyme-catalyzed reactions: application to unstable enzymes, coupled reactions and transient-state kinetics. Biochim. Biophys. Acta 1205, 268-274.

Duggleby R.G., 1995. Analysis of enzyme progress curves by non-linear regression. Methods Enzymol. 249, 61-90.

Duggleby R.G., 2001. Quantitative analysis of the time course of enzyme catalyzed reactions. Methods 24, 168-174.

Duggleby R.G., Morrison J.F., 1977. The analysis of progress curves for enzyme-catalysed reactions by non-linear regression. Biochim. Biophys. Acta 481, 297-312.

Duggleby R.G., Wood C., 1989. Analysis of progress curves for enzyme-catalyzed reactions. Biochem. J. 258, 397-402.

Eisenthal R., Cornish-Bowden A., 1974. The direct linear plot. A new graphical procedure for estimating enzyme kinetic parameters. Biochem. J. 139, 715-720.

Fernley H.N., 1974. Statistical estimation in enzyme kinetics. The integrated Michaelis-Menten equation. Eur. J. Biochem. 43, 377-378.

Fritsch F.N., Shafer R.E., Crowley W.P., 1973. Algorithm 443: Solution of the transcendental equation $we^w = x$. Commun. ACM 16, 123-124.

Goudar C.T., Sonnad J.R., Duggleby R.G., 1999. Parameter estimation using a direct solution of the integrated Michaelis-Menten equation. Biochim. Biophys. Acta 1429, 377-383.

Leatherbarrow R.J., 1990. Using linear and nonlinear regression to fit biochemical data. TIBS 15, 455-458.

Marquardt D.W., 1963. An algorithm for least squares estimation of nonlinear parameters. J. Soc. Ind. Appl. Math. 11, 431-441.

Michaelis L., Menten M.L., 1913. Die kinetik der invertinwirkung. Biochem. Z. 49, 333-369.

Nimmo I.A., Atkins G.L., 1974. A comparison of two methods for fitting the integrated Michaelis-Menten equation. Biochem. J. 141, 913-914.

Pauli A.S., Kaitala S., 1997. Phosphate uptake kinetics by Acinetobacter isolates. Biotechnol. Bioeng. 53, 304-309.

Robinson J.A., 1985. Determining microbial kinetic parameters using nonlinear regression analysis. Advantages and limitations in microbial ecology. Adv. Microb. Ecol. 8, 61-114.

Robinson J.A., Characklis W.G., 1984. Simultaneous estimation of $V_{max}$, $K_m$ and the rate of endogenous substrate production (R) from substrate depletion data. Microb. Ecol. 10, 165-178.

Schnell S., Mendoza C., 1997. Closed form solution for time-dependent enzyme kinetics. J. Theor. Biol. 187, 207-212.

Suflita J.M., Robinson J.A., Tiedje J.M., 1983. Kinetics of microbial dehalogenation of haloaromatic substrates in methanogenic environments. Appl. Environ. Microbiol. 45 (1466).

Zimmerle C.T., Frieden C., 1989. Analysis of progress curves by simulations generated by numerical integration. Biochem. J. 258, 381-387.

## Appendix II

The use of a nonlinear regression routine for estimation of kinetic parameters from progress curves

Nonlinear regression is a technique to fit a curve that defines y as a function of x and one or more parameters. Nonlinear regression analysis requires the use of a microcomputer and involves an iterative approach that is discussed later in this appendix. The CD supplied with this appendix contains the necessary files for estimating $K_m$ and $V_{max}$ from progress curve data via nonlinear regression analysis.

**Steps in using nonlinear regression analysis to estimate $K_m$ and $V_{max}$ from progress curve data.**

The following paragraphs are designed to explain the procedure for using nonlinear regression routines for kinetic analysis of substrate depletion data. A step-by-step procedure for using the programs supplied on the CD is given at the end of this appendix.

**Choosing a mathematical model.** The first step in using nonlinear regression is to choose a mathematical model to be fit to the data. While a computer program can choose a model, the choice should be driven by the scientific context of the experiment. Simply finding an equation that fits the data is not likely to be useful. Enzyme catalyzed reactions can be described by the Michaelis-Menten model. The program discussed in appendix I and provided on the CD that accompanies appendix II uses the Michaelis-

Menten expression to evaluate $K_m$ and $V_{max}$ from progress curve data. Thus, the choice of model has been made when using these files.

**Obtaining initial estimates**. Since nonlinear regression is an iterative routine, initial estimates of $S_0$, $K_m$, and $V_{max}$, are required. Estimates of $S_0$ and $V_{max}$ can be made fairly easily by simply examining the progress curve. However, the $K_m$ can be more difficult to discern in this way. A better approach is to perform linear regression. One of the advantages of the Michaelis-Menten equation is that it is transformably linear. That is, it can be linearized to produce estimates of $S_0$ as well as $K_m$, and $V_{max}$. There are three linearization routines provided on the CD that transform progress curve data using equivalent versions of the Lineweaver-Burk, Hanes-Wolfe, and Eadie-Hofstee transformations. Each transformation generates values of $S_0$, $K_m$, and $V_{max}$ for use in the nonlinear regression routine. Although values obtained from the linearized forms of the Michaelis-Menten equation are less accurate than the results of nonlinear regression, these values are appropriate for use as initial estimates.

It should be noted that the initial values can simply be guesses. If the data clearly define a zero, mixed, and first order decay regions, the estimates do not have to be very accurate for the routine to converge. Generally, the more scatter in the data, the more rigorous one needs to be in determining initial parameters to start the routine. If finding initial estimates is difficult, the program includes a way to simulate a progress curve from kinetic constants provided by the user. Thus, a family of curves can be generated from several possible values of $S_0$, $K_m$ and $V_{max}$ and compared the to the experimental progress

curve. The parameters associated with the simulation that best matches the experimental progress curve should then be used for the initial estimates.

**Assigning constants.** When using nonlinear regression, it is not necessary to fit each parameter in the equation. For example, it may be necessary to subtract a background signal from the data. When following hydrogen depletion by the acetogen *Eubacterium limosum*, a threshold was observed below which hydrogen consumption did not occur (Figure 1). Thresholds are not predicted by Michaelis-Menten kinetics. Thus, the model was adjusted to account for a threshold term ($S_T$) that was experimentally determined and supplied when doing the analysis. A special file is included on the CD that incorporates a threshold term that is useful if a constant should be assigned to a bottom plateau of a curve due to a phenomenon similar to a substrate threshold.

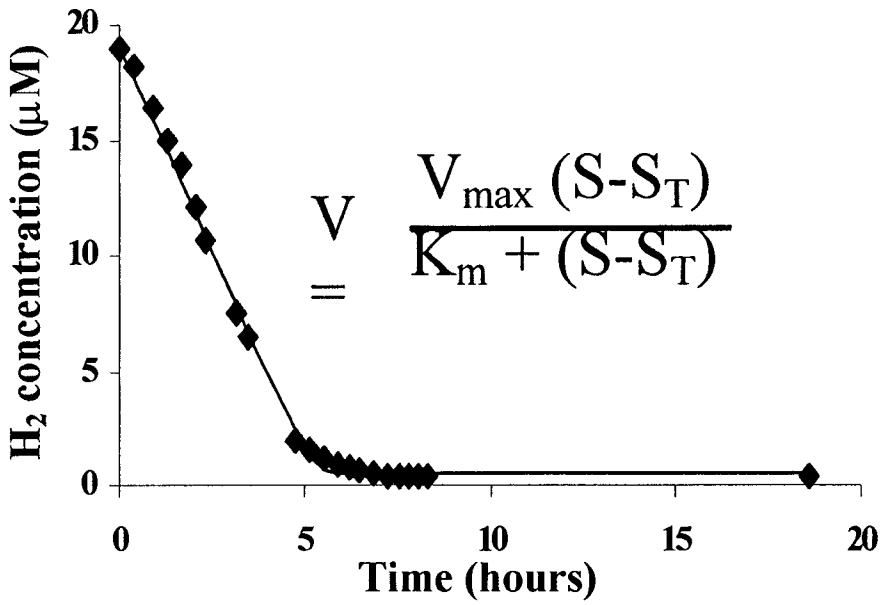


Figure 1. Hydrogen depletion and threshold exhibited by *Eubacterium limosum* (♦) and model fit (solid line). Equation represents modification of the Michaelis-Menten expression to incorporate a substrate threshold ($S_T$).

**Minimizing the sum of the squared error.** Once the data and initial parameters are supplied, the program computes $S_0$, $K_m$, and $V_{max}$ values that fit the data best. It does so by using the initial estimates to draw a curve through the data. The program computes the sum of the squares of the vertical distances between the data points and the curve. The $K_m$ and $V_{max}$ estimates are then adjusted slightly and a second curve is drawn. The routine computes the sum of the squared distances of the second curve and determines which of the two curves is a better fit of the data based on the lower sum of squares. The routine does this many times until further adjustments to the kinetic parameters no longer decrease the sum of squares. It is typical for the algorithm to go through several, even dozens of iterations before estimates of $K_m$ and $V_{max}$ are attained for which the sum of squares has been minimized. The algorithm for adjusting the kinetic parameters to find the lowest sum of squares is the most important part of nonlinear regression routines. Some common algorithms are the method of linear descent and the Gauss-Newton method. These algorithms all differ in the way the initial kinetic estimates are adjusted with each subsequent iteration. More recently, the method of Levenberg and Marquardt has come into use and is comprised of both the linear descent and Gauss-Newton approaches. A more detailed description of these algorithms can be found at www.graphpad.com and in Taylor, 2002. Appendix 2 describes what the authors contend to be an improvement on existing methods for performing nonlinear regression. It is this improved program that is supplied with appendix 1.

**Local minima of error surfaces.** It is possible that the surface of the error function exhibits multiple local minima that may cause the routine to converge on an answer that does not represent the true minimum of the sum of squares. Figure 2 is an adaptation from the GraphPad Software, Inc. website and illustrates a two-dimensional error surface with multiple minima. It is apparent from Figure 2 that the choice of initial parameter estimates is important in order to determine the true best fit. Although this problem is intrinsic to all algorithms that are used for nonlinear regression analysis, there are strategies available to the experimentalist to ensure that local minima are not compromising the accuracy of kinetic parameter estimation. I have had success testing for local minima by running the routine several times (with the same progress curve data) using different initial estimates of $K_m$ and $V_{max}$. If the same final parameter estimates and the same sum of squares are obtained, then local minima are unlikely to be a problem. In fact, I have been able to use initial $K_m$ and $V_{max}$ estimates that are as much as two orders of magnitude larger or smaller than the actual final values without complications of local minima. Figure 2 of appendix 1 illustrates the ability of these programs to estimate the $K_m$ and $V_{max}$ from progress curve data containing various levels of error. Note that while the sum of squares error increases with increasing scatter of the data, the routines are still able to converge on similar parameter estimates. Nevertheless, progress curve data exhibiting little scatter combined with carefully chosen initial estimates are the best tools for avoiding local minima.

It has been my experience that the quality of the progress curve data has a greater influence on the final kinetic estimates and associated standard deviations than do the initial estimates. Attempting to estimate the $K_m$ and $V_{max}$ from a substrate decay curve

that is curvilinear or linear throughout, often results in a $K_m$ that is not physiologically relevant, or a stalled routine. As stated earlier, the best way to use these programs successfully is to start with a good progress curve. By definition, progress curves exhibit zero, followed by mixed, and then first order decay regions. A good approach to obtaining this kind of decay curve is to start at a substate concentration that is 5 to 10-fold greater than the $K_m$ and continue monitoring substrate depletion until the concentration is $1/10^{th}$ of the $K_m$ or less. Figure 5A of appendix 1 is an example of a progress curve that is appropriate for nonlinear regression analysis.

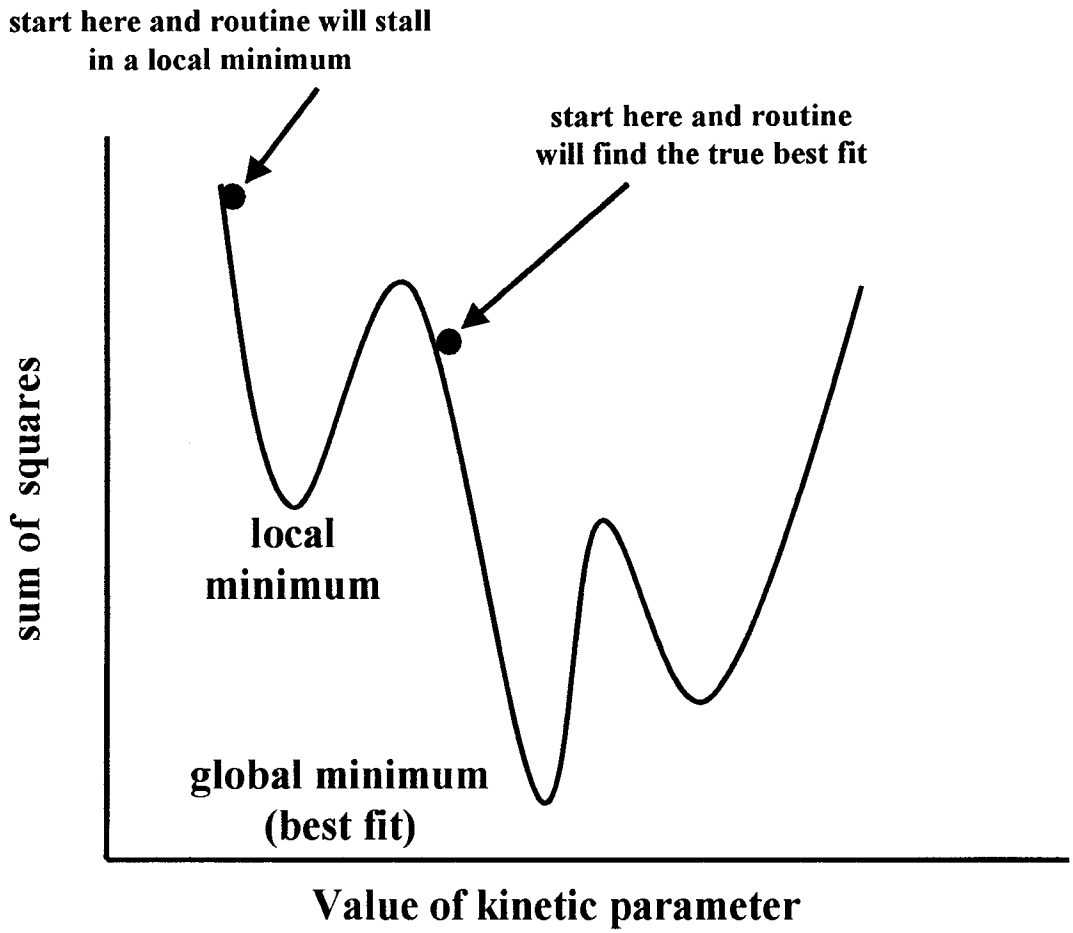


Figure 2. Two-dimensional depiction of a hypothetical error function illustrating the presence of multiple minima adapted from www.graphad.com.

**Installation of programs for kinetic analysis of progress curve data.**

MATLAB requires MS Windows to operate. Once the software is installed, the files can be copied from the CD supplied in this appendix and used for nonlinear regression analysis.

Create a new folder on the hard drive and copy the folders 'kinetics', 'competition', and 'threshold' from the CD to the new folder.

**Obtaining initial estimates of $S_0$, $K_m$, and $V_{max}$ via linear transformations of progress curve data.**

Under the file menu, choose a new m-file.

Copy and paste substrate vs. time data pairs from a spreadsheet program into a new m-file. Make sure the time points are in the left column and substrate concentrations are in the right column. Save the new .m file in the 'kinetics' folder with a filename you will remember.

On the MATLAB main screen, type 'menteninitial' at the EDU prompt to start the program for obtaining initial estimates. When the program menu appears, type in the value for $S_0$ and the name of the file containing the data followed by .m. Press OK.

The initial estimates for $S_0$, $K_m$, and $V_{max}$ will then appear on the dialog screen. In addition, three plots of model and experimental data will be displayed as well as the three linear plots. The three linear plots correspond to the Hanes-Wolfe, Eadie-Hofstee, and Lineweaver-Burk equivalents.

**Estimating $S_0$, $K_m$, and $V_{max}$ via nonlinear regression.**

Type 'mentenfit' at the EDU prompt and press enter. Enter the values for $S_0$, $K_m$, and $V_{max}$ determined from the previous linear transformations. Type the name of the data file followed by .m as before and press OK.

Record the parameter estimates and associated error provided by the program.

Repeat the above procedure with various initial estimates of $K_m$ and $V_{max}$ until you are satisfied that the estimates provided by the program correspond to the lowest possible standard deviations.

**Analysis of hydrogen decay with a threshold.** If a threshold is evident or suspected in the substrate depletion curve, then the analysis should be done with the file specifically designed to account for this phenomenon. The initial estimates must be obtained as explained earlier. Once that has been done, type 'mmthresh' at the EDU prompt on the MATLAB dialog screen. The menu will be similar to that provided by 'mentenfit'

except that an additional cell will be available to supply the experimentally determined threshold value. The rest of the analysis can then be carried out as before.

**Hydrogen decay simulations.** This file is useful for modeling competition between two microorganisms for a single substrate if the following parameters are provided: $S_0$, $K_m$, $V_{max}$, the time course of the incubation, and biomass. Hydrogen consumption can also be simulated by simply providing hypothetical parameters. The resulting simulation can then be used for initial parameter estimation if desired.

Type 'compsolv' at the EDU prompt. Enter the known parameters in the appropriate cells and press OK.

The program will then show a plot of hydrogen depletion for up to two different sets of kinetic estimates as well as a third decay curve that illustrates the result of an additive kinetic effect. It will likely be necessary to obtain the raw data from these simulations. The commands must be entered on the main dialog page of MATLAB at the EDU prompt. The commands are as follows:

| **Command** | **Returns** |
|---|---|
| tspan | time points |
| scala | substrate conc. for parameter set A |
| scalb | substrate conc. for parameter set B |
| scalc | substrate conc. for parameter set C |

Once these data are obtained they can be cut and pasted into any spreadsheet program for further manipulation. Figure 3 shows several simulations for two microorganisms exhibiting different kinetics as well as the decay curve expected for cocultures. The

bacteria exhibit a similar $K_m$ with respect to the substrate but organism 2 has a faster $V_{max}$ as illustrated by the faster decay curve in figure 3A. The results suggest that if organism 1 were included at a 1.3-fold relative biomass advantage (Figure 3B) it would consume the substrate at a comparable rate to organism 2 and would begin to dominate substrate competition at 1.5 times the biomass of organism 2 (Figure 3C). This illustrates how these simulations can be used to predict substrate consumption by cocultures as well as aid in the design of experiments. Figure 4 shows hydrogen consumption by a coculture of *Acetobacterium woodii* and *Methanospirillum hungatei*. The $K_m$ and $V_{max}$ for *A. woodii* were 4.6 μM and 970 nmol $min^{-1}$ mg $protein^{-1}$, respectively. The $K_m$ and $V_{max}$ for *M. hungatei* were 5.0 μM and 1350 nmol $min^{-1}$ mg $protein^{-1}$, respectively. Biomass concentrations for the two microorganisms were adjusted via a biomass term that is provided by the model. The predicted decay curve is the result of a simulation based on the kinetics exhibited by the two microorganisms in pure culture. The agreement suggests that the hydrogen consumption rate by the coculture represents an additive effect of the $V_{max}$ exhibited by the two individual microorganisms.

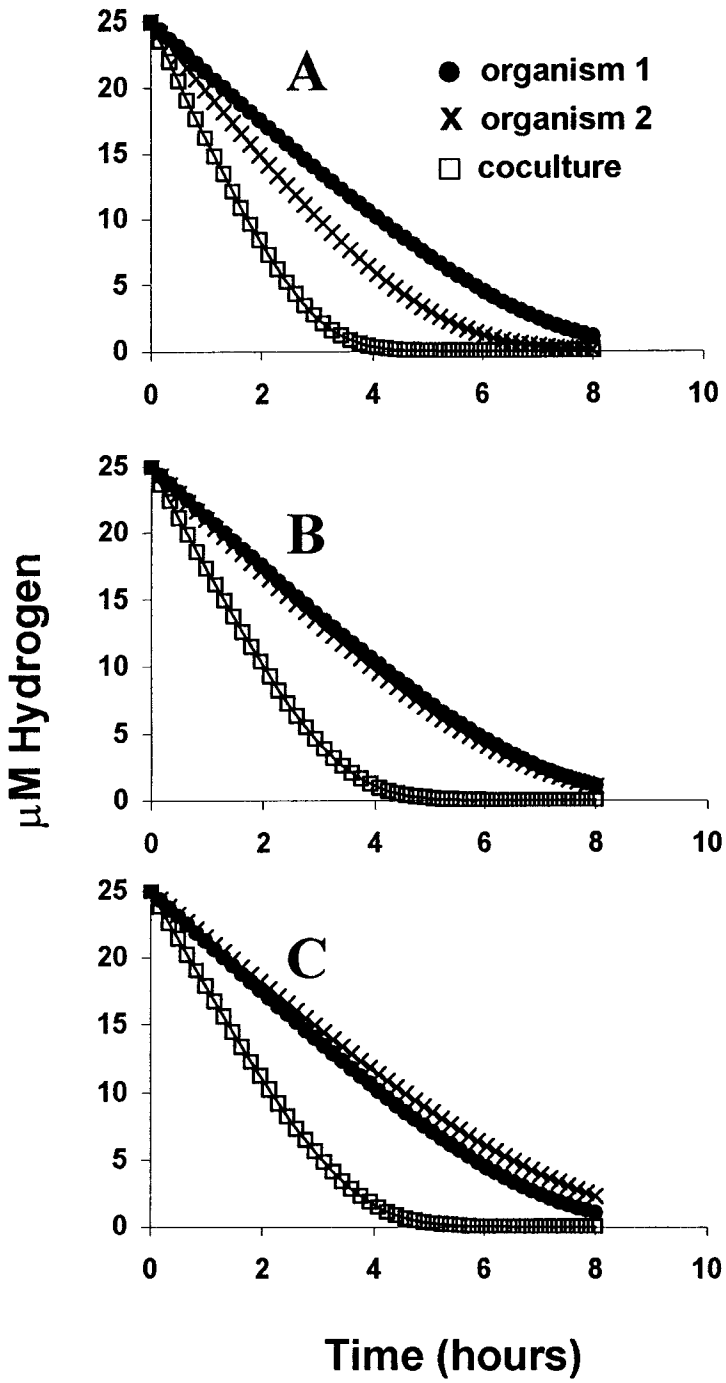


Figure 3. Simulation of hydrogen decay by two organisms in monocultures and in coculture. Organisms included at equal biomass concentrations (A). Organism 1 included at a 1.3-fold (B) and 1.5-fold biomass advantage (C) relative to organism 2.

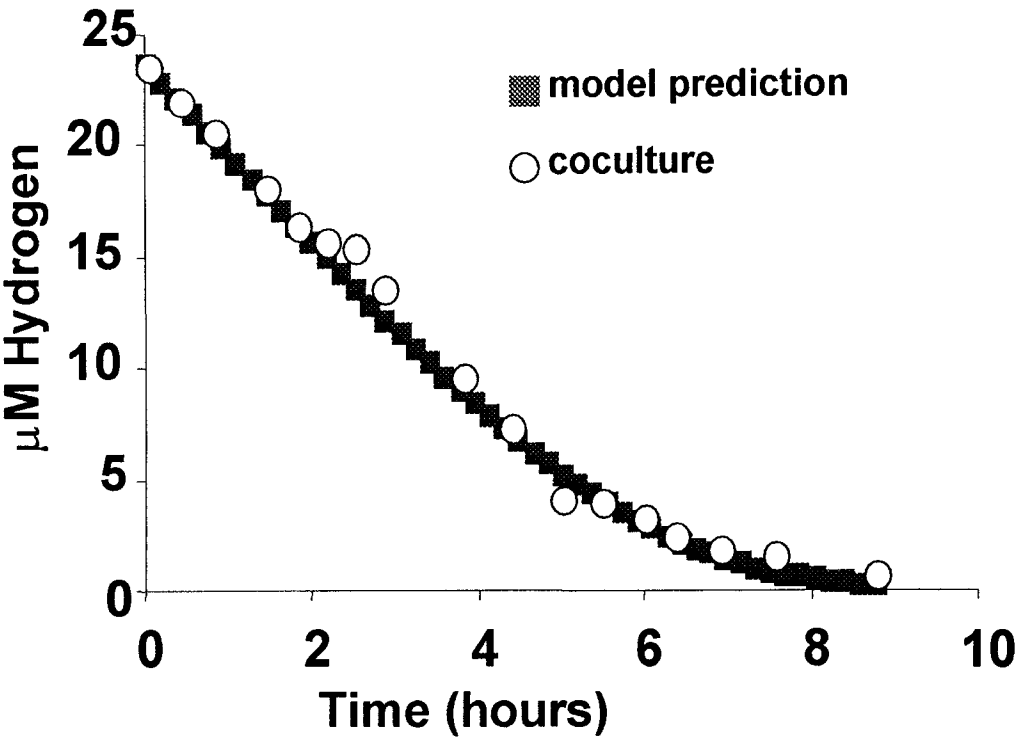


Figure 4. Hydrogen consumption in a coculture of *A. woodii* and *M. hungatei* and the corresponding model prediction based on the kinetics exhibited in pure culture.

## Suggested reading and references

**Cleland, W. W.** 1979. Statistical Analysis of Enzyme Kinetic Data. Methods in Enzymol. 63, 103-138.

**Robinson J.A.** 1985. Determining microbial kinetic parameters using nonlinear regression analysis. Advantages and limitations in microbial ecology. Adv. Microb. Ecol. **8**: 61-114.

**Taylor, K. B.** 2002. Enzyme Kinetics and Mechanisms. Kluwer Academic Publishers, Boston, Mass., USA.

### Websites

GraphPad Software, Inc. www.graphpad.com

The MathWorks, Inc. www.mathworks.com